

arXiv:1809.01669v2 [astro-ph.CO] 6 Sep 2021

Rubin Observatory

**LSST DESC**

# Science Requirements Document

**Version 1.0.2**

Date: Friday 18<sup>th</sup> February, 2022



## Change Record

Version	Date	Description	Owner name
v0.9	03/27/2018	Initial pre-release, for collaboration feedback prior to the 2018 operations review.	Rachel Mandelbaum
v0.99	04/26/2018	Pre-release, for the May 2018 LSST DESC DOE OHEP operations review.	Phil Marshall
v1	09/05/2018	Initial public release. Used internally by the LSST DESC for prioritization of software and dataset development effort, data challenge design, and derivation of performance metrics.	Phil Marshall
v1.0.1	05/01/2019	Fixed a minor issue with an incorrect file in the DESC SRD v1 release, clarified a few details of the signal calculations for the WL and LSS analyses. No changes in the analysis, forecasts, requirements, etc, but data products are now easier to use.	Phil Marshall
v1.0.2	09/06/2021	Updated to reflect observatory renaming, clarified SN forecasting process and degeneracy direction. No change in goals, requirements, or other results.	Rachel Mandelbaum

## Contributors

Contributors to the DESC SRD effort are listed in the table below, with leading contributions shown in bold and affiliations indicated in the notes below the table.

Name	Contribution
David Alonso <sup>1,2</sup>	Forecasting guidance, LSS analysis definition, WL forecast cross-check
Humna Awan <sup>3</sup>	Input on survey definition based on OpSim v3 minion_1016
Rahul Biswas <sup>4</sup>	SN analysis definition, systematics treatment
Jonathan Blazek <sup>5,6</sup>	Forecasting guidance, review of complete draft
Patricia Burchat <sup>7,8</sup>	Initial organization, WL systematic uncertainties list
Elisa Chisari <sup>2</sup>	Forecasting guidance, review of complete draft
<b>Tom Collett</b> <sup>9</sup>	<b>SL forecaster</b> , SL analysis definition
Ian Dell'Antonio <sup>10</sup>	CL analysis definition
Seth Digel <sup>8,11</sup>	Review of complete draft
<b>Tim Eifler</b> <sup>12,13</sup>	<b>Lead forecaster</b> , WL+LSS+CL analysis and systematics definition, joint probe covariance computation
Josh Frieman <sup>14,15</sup>	Review of complete draft
<b>Eric Gawiser</b> <sup>3</sup>	Project management, <b>scientific guidance</b> , text editing
Daniel Goldstein <sup>16,17,18</sup>	SL analysis definition
<b>Renée Hložek</b> <sup>19,20</sup>	<b>SN forecaster</b> , SN analysis definition, systematics treatment
Isobel Hook <sup>21</sup>	Consultation on 4MOST capabilities for SN science case
Željko Ivezić <sup>22</sup>	Review of complete draft, feedback on connection to LSST SRD
Steven Kahn <sup>7,8,11,23</sup>	Review of document and feedback on connection to LSST SRD
Sowmya Kamath <sup>7,8</sup>	WL systematic uncertainties list
David Kirkby <sup>24</sup>	Initial organization, source sample characterization, review of draft
Tom Kitching <sup>25</sup>	WL analysis definition
Elisabeth Krause <sup>12</sup>	Forecasting guidance, Fisher software, CosmoLike infrastructure
Pierre-François Leget <sup>7,8</sup>	WL systematic uncertainties list
<b>Rachel Mandelbaum</b> <sup>26</sup>	<b>Lead author, scientific oversight</b> , project management
Phil Marshall <sup>8,11</sup>	Initial organizational work, scientific guidance, text editing
Josh Meyers <sup>7,8</sup>	WL systematic uncertainties list
Hironao Miyatake <sup>13,27,28</sup>	Cluster mass-observable relation software, CL forecasting guidance
Jeff Newman <sup>29</sup>	Input on WL, LSS, and SN sample definition, review of complete draft
Bob Nichol <sup>9</sup>	Consultation on 4MOST capabilities for SN science case
Eli Rykoff <sup>8,11</sup>	WL, LSS, and CL area definition including dust, depth constraints
F. Javier Sanchez <sup>24</sup>	WL source sample characterization
<b>Daniel Scolnic</b> <sup>15</sup>	<b>SN analysis definition and forecasting</b>
Anže Slosar <sup>30</sup>	LSS analysis definition
Mark Sullivan <sup>31</sup>	Consultation on 4MOST capabilities for SN science case
Michael Troxel <sup>6,32</sup>	Review of complete draft

- <sup>1</sup> School of Physics and Astronomy, Cardiff University
- <sup>2</sup> Department of Physics, University of Oxford
- <sup>3</sup> Department of Physics and Astronomy, Rutgers University
- <sup>4</sup> Oskar Klein Centre, Department of Physics, Stockholm University
- <sup>5</sup> SNSF Ambizione, Laboratory of Astrophysics, École Polytechnique Fédérale de Lausanne (EPFL)
- <sup>6</sup> Center for Cosmology and Astroparticle Physics, Ohio State University
- <sup>7</sup> Department of Physics, Stanford University
- <sup>8</sup> Kavli Institute for Particle Astrophysics and Cosmology (KIPAC), Stanford University
- <sup>9</sup> Institute of Cosmology and Gravitation, University of Portsmouth
- <sup>10</sup> Department of Physics, Brown University
- <sup>11</sup> SLAC National Accelerator Laboratory
- <sup>12</sup> Steward Observatory/Department of Astronomy, University of Arizona
- <sup>13</sup> Jet Propulsion Laboratory, California Institute of Technology
- <sup>14</sup> Fermi National Accelerator Laboratory
- <sup>15</sup> Kavli Institute for Cosmological Physics, University of Chicago
- <sup>16</sup> California Institute of Technology
- <sup>17</sup> Lawrence Berkeley National Laboratory
- <sup>18</sup> Department of Astronomy, University of California, Berkeley
- <sup>19</sup> Department of Astronomy and Astrophysics, University of Toronto
- <sup>20</sup> Dunlap Institute for Astronomy and Astrophysics, University of Toronto
- <sup>21</sup> Department of Physics, Lancaster University
- <sup>22</sup> Department of Astronomy, University of Washington
- <sup>23</sup> Rubin Observatory Project
- <sup>24</sup> Department of Physics and Astronomy, University of California, Irvine
- <sup>25</sup> Mullard Space Science Laboratory, University College London
- <sup>26</sup> McWilliams Center for Cosmology, Department of Physics, Carnegie Mellon University
- <sup>27</sup> Nagoya University
- <sup>28</sup> Kavli Institute for the Physics and Mathematics of the Universe (Kavli IPMU, WPI)
- <sup>29</sup> Department of Physics and Astronomy and PITT PACC, University of Pittsburgh
- <sup>30</sup> Physics Department, Brookhaven National Laboratory
- <sup>31</sup> Department of Physics and Astronomy, University of Southampton
- <sup>32</sup> Department of Physics, The Ohio State University

---

## Contents

Contributors . . . . .	1
Executive Summary and User Guide . . . . .	1
1 Introduction . . . . .	4
2 Definitions . . . . .	5
3 Objectives . . . . .	9
4 High-level requirements . . . . .	10
5 Detailed requirements . . . . .	13
5.1 Large-scale structure . . . . .	16
5.2 Weak lensing ( $3\times 2$ -point) . . . . .	17
5.3 Galaxy clusters . . . . .	20
5.4 Supernovae . . . . .	22
5.5 Strong lensing . . . . .	27
5.6 Combined probes and other requirements . . . . .	28
6 Conclusion and outlook . . . . .	28
Acknowledgments . . . . .	33
References . . . . .	34
Appendices . . . . .	37
A Connections to Rubin Observatory tools and documents . . . . .	37
B Software . . . . .	38
B1 Software packages . . . . .	38
B2 How requirements are set . . . . .	40
B3 Ensuring reproducibility . . . . .	42
C Assumptions . . . . .	43
C1 The LSST observing strategy . . . . .	43
C2 The cosmological parameter space . . . . .	43
C3 Stage III dark energy surveys . . . . .	45
C4 Follow-up observations and ancillary data . . . . .	46
D Baseline analyses . . . . .	47
D1 Large-scale structure . . . . .	47
D2 Weak lensing ( $3\times 2$ -point) . . . . .	53
D3 Galaxy clusters . . . . .	60
D4 Supernovae . . . . .	65
D5 Strong lensing . . . . .	76
E Synthesis of systematic uncertainties across all probes . . . . .	78
E1 Systematic uncertainties in this DESC SRD version . . . . .	78
E2 Systematic uncertainties deferred for future work . . . . .	78
F Defining number densities . . . . .	79
F1 Photometric sample number density . . . . .	79
F2 Source sample number density . . . . .	80

F3	Photometric sample redshift distribution . . . . .	82
F4	Source sample redshift distribution . . . . .	83
G	Forecasting-related plots . . . . .	83

---

## Executive Summary and User Guide

The Dark Energy Science Collaboration (DESC) was formed to design and implement dark energy analysis of the data from the Vera C. Rubin Observatory’s Legacy Survey of Space and Time (LSST) using five dark energy probes: weak and strong gravitational lensing, large-scale structure, galaxy clusters, and supernovae. Assuming the delivery of LSST data by Rubin Observatory according to the design specifications in the LSST Science Requirements Document (LSST SRD), the DESC will carry out further analyses with its own infrastructure (software, simulations, computational resources, theory inputs, and re-analyses of precursor datasets) to produce constraints on dark energy.

The first goal of this document is to quantify the expected dark energy constraining power of all five DESC probes individually and together, with conservative assumptions about analysis methodology and follow-up observational resources (e.g., spectroscopy) based on our current understanding and the expected evolution within the field in the coming years. The second goal is to define requirements on our analysis pipelines which, if met, will enable us to achieve our goal of carrying out dark energy analyses consistent with the Dark Energy Task Force (DETF) definition of a Stage IV dark energy experiment. This is achieved through a forecasting process that includes the flow-down to detailed requirements on multiple sources of systematic uncertainty.

We define two classes of systematic uncertainty: “self-calibrated” ones, for which we will build a physically-motivated model with nuisance parameters over which we marginalize with priors that are either *uninformative* or mildly informative (where justified by other data); and “calibratable” ones, with nuisance parameters that may not be physically meaningful and that relate to some error in the measurement process, for which DESC simulations, theory, other software, or precursor datasets produce *informative* priors. The “total uncertainty” consists of the statistical uncertainty, including the broadening of the posterior due to marginalization over self-calibrated systematic uncertainties, combined with the calibratable systematic uncertainty. Our requirements are set such that these calibratable uncertainties will be a subdominant contributor to the total uncertainty. As our understanding of systematic uncertainties changes, some may switch from calibratable to self-calibrated. We define detailed requirements through a process of error budgeting among different calibratable systematic uncertainties, with forecasts used to check that meeting the detailed requirements will enable us to meet our high-level objectives.

Some of the key outcomes of this process are as follows.

- We have defined high-level objectives that the collaboration hopes to achieve in the next 15 years, including standards for control of systematic uncertainties.
- We have defined a baseline analysis for each probe that is consistent with LSST being a stand-alone Stage IV dark energy experiment, with joint-probe marginalized uncertainties on dark energy equation-of-state parameters  $(w_0, w_a)$  of  $\sigma(w_0) = 0.02$  and  $\sigma(w_a) = 0.14$  (combined  $1\sigma$  statistical and systematic uncertainties), where  $w(a) = w_0 + (1 - a)w_a$ .
- We have defined a set of quantifiable requirements on each probe, including the flow-down to

detailed requirements on the level of systematics control achieved by DESC infrastructure. These can be compared with the current state-of-the-art and future plans in order to prioritize efforts in the coming years. The detailed requirements in this first version of this document are a limited subset of those we expect to define in the end; here we focus on photometric redshift uncertainties, weak lensing shear, and photometry (through its impact on supernova light curves). The high-level requirement that LSST be a stand-alone Stage IV dark energy experiment is expected to remain fixed, while the detailed requirements may change as our understanding of analysis methods improves.

- We have defined a set of goals, which are quantifiable (like requirements) but are not prerequisites for collaboration success.
- This exercise has highlighted the need for collaboration software for forecasting dark energy analyses self-consistently across all probes. Aspects of the single-probe analyses and systematics models described in this document, whether they were implemented or not in this first DESC SRD version, serve as guides for defining the capabilities of that collaboration software framework.

Future versions of this document will incorporate the following improvements: (a) evolution in our software capabilities and analysis plans; (b) decisions by Rubin Observatory about survey strategy; (c) requirements on sufficiency of models for self-calibrated systematic uncertainties; (d) requirements on calibratable systematic uncertainties beyond those in this version of the DESC SRD (particularly ones for which we currently lack a description of their impact on the observables); and (e) self-consistent treatment of common systematic uncertainties across probes. Currently all objectives, requirements, and goals relate to dark energy constraints; future DESC SRD versions may consider secondary science objectives such as constraints on neutrino mass.

## How to Use This Document

When showing plots, forecasts, or requirements from this document, it should be cited as “the LSST DESC Science Requirements Document v1 (LSST DESC 2018)” in the text, and “LSST DESC SRD v1” in figure legends. (The “DESC” avoids ambiguity with the LSST SRD developed by Rubin Observatory, and “v1” avoids confusion with later versions.) On the LSST DESC community Zenodo page<sup>1</sup> we provide a tarball with the following items: figures, all individual and joint probe Fisher matrices from [Figure G2](#) along with the python script that produced the plot, data vectors and covariances from the weak lensing, large-scale structure, and galaxy clusters forecasts, MCMC chains, simulated strong lens and supernova catalogs, and the software for producing the supernova requirements and forecasts. When using these data products, please cite the Zenodo DOI (for which a BibTeX reference can be downloaded from the Zenodo page) in addition to the arXiv entry for this document. Care should be taken when combining the Fisher matrices with those from other surveys, particularly to ensure common choices of cosmological parameters and consistent choices of priors and that the Fisher matrices being added

---

<sup>1</sup><https://zenodo.org/communities/lstt-desc>



are truly independent (which may not be case if the probed volume overlaps). Finally, internal to the DESC, this document will be used to inform analysis pipeline development, including the development of performance metrics.

## 1 Introduction

Understanding the nature of dark energy is one of the key objectives of the cosmological community today. The objective of the LSST Dark Energy Science Collaboration (DESC) is to prepare for and carry out dark energy analysis with LSST (Ivezic et al. 2008; LSST Science Collaboration 2009). Following acquisition of the LSST images and the processing with Rubin’s LSST Science Pipelines, both carried out by Rubin Observatory, the DESC will use its own “user-generated” software to analyze the LSST data and produce cosmological parameter constraints. In this document, the DESC Science Requirements Document (DESC SRD), we outline the DESC’s scientific objectives, along with the performance requirements that the DESC’s software (including simulations and theoretical modeling capabilities) must meet to ensure that the DESC meets those scientific objectives. Unlike requirements in a Science Requirements Document for a hardware project, the detailed requirements on software pipelines in the DESC SRD may evolve with time, since they are sensitive to assumptions about the entire analysis pathway to cosmological parameters, about which our understanding will continually improve.

Rubin Observatory has its own science requirements document for LSST (the LSST SRD), which can be found on their webpage<sup>2</sup>. The LSST SRD outlines requirements on the hardware, observatory, and the LSST Science Pipelines, all of which fall under the purview of Rubin Observatory. In defining the performance requirements for DESC software, we assume that Rubin Observatory is going to deliver survey data in accordance with the “design specifications” in the LSST SRD (not the more pessimistic “minimum specifications”, or the more optimistic “stretch goals”). We note that the LSST observing strategy will continue to evolve as LSST approaches first light, with the possibility of significant updates in cadence and how depth is build up over time, while still satisfying the LSST SRD requirements. In the subsections below, we highlight relevant LSST Project requirements; more generally, our reliance on Rubin Observatory tools and requirements is summarized in [Appendix A](#).

Following the convention for DOE projects, we quantify the constraining power of dark energy measurements using the figure of merit (FoM) from the Dark Energy Task Force report (DETF; Albrecht et al. 2006). The definition of this quantity, and other relevant terminology for the DESC SRD, is in [Section 2](#). While the main text summarizes the calculations for the sake of brevity, detailed technical appendices describe exactly what was calculated for each probe, with assumptions and systematics models described in a manner designed to ensure reproducibility of the results in this document.

In this document we make the reasonable assumption that already-funded surveys will be carried out and that spectroscopic follow-up and other ancillary telescope resources will continue to be available at similar rates as they are today. We do not assume the acquisition of substantial new ancillary datasets in order to mitigate systematics. See [Appendix C4](#) for a summary of assumptions about follow-up and ancillary telescope resources for each DESC probe.

The outline of this document is as follows. [Section 2](#) includes definitions for terminology used throughout the DESC SRD. In [Section 3](#), we outline the key objectives of the LSST dark energy analysis, while

---

<sup>2</sup><https://docushare.lsstcorp.org/docushare/dsweb/Services/LPM-17>

in [Section 4](#) and [Section 5](#) we derive a set of requirements on the DESC’s analysis software, based on a flow-down from high-level (i.e., targeted constraining power on dark energy) to low-level details of the tolerances for residual systematic uncertainties.

Any changes to the DESC SRD after the first official version (v1) is tagged will be proposed by the Analysis Coordinator following consultation with the Working Groups, Rubin Observatory Liaisons and Management team, and approved by the Spokesperson. In practice this will be achieved by a Pull Request to the master branch of the DESC Requirements repository, which is protected. The Spokesperson will maintain a change log in the document, and tag the repository as changes are merged.

## 2 Definitions

Below we define the terminology used throughout the document.

- *Objectives* ([Section 3](#)): The DESC’s high-level objectives provide the scientific motivation for the LSST dark energy analysis<sup>3</sup>. They provide the context for development of the science requirements and goals, but may not be directly testable themselves.
- *Science requirements* ([Section 4](#) and [Section 5](#)): Requirements are the testable criteria that must be satisfied in order for the collaboration to meet its objectives.
- *Goals*: These are testable criteria that go beyond the science requirements. For example, these could be criteria that must be met in order to achieve secondary science objectives, such as constraining modified gravity theories or neutrino mass. They also could be criteria related to achieving an earlier, or more optimal, use of the data than is needed to meet our requirements. They are “goals” rather than “science requirements” because achieving them is not considered a prerequisite for collaboration success.
- *Dark energy probes*: The DESC currently has five primary dark energy probes: galaxy clusters (CL), large-scale structure (LSS), strong lensing (SL), supernovae (SN), and weak lensing (WL). All details of the associated analyses are given in [Appendix D](#). The general philosophy behind our calculations is that we aim for a state-of-the-art analysis with reasonable (neither overly aggressive nor overly conservative) assumptions about what data we will be able to successfully model to constrain dark energy. In some cases, the analysis choices were constrained by the capabilities of existing software, and hence will need to be updated to be more consistent with this philosophy in future DESC SRD versions when improved software is available. In brief, the baseline analysis for each probe is as follows:
  - The baseline LSST CL analysis includes cluster counts and cluster-galaxy lensing. It will be valuable to update the baseline analysis in future DESC SRD versions to include cluster

---

<sup>3</sup>Some readers may notice that we have adopted similar terminology to the internal Dark Energy Survey (DES) science requirements document for objectives, requirements, and goals. The choices made in this document were influenced by that document.

clustering, which can be beneficial in self-calibrating the mass-observable relation (e.g., [Lima & Hu 2004](#)), when software with this capability is available.

- The baseline LSST LSS analysis includes tomographic galaxy clustering to nonlinear scales, not just the baryon acoustic oscillation (BAO) feature studied in the DETF report. Future DESC SRD versions may define the baseline analysis in terms of a multi-tracer treatment (e.g., [Seljak 2009](#); [Abramo & Leonard 2013](#)), which is beneficial in the cosmic variance-limited regime.
- The baseline SL analysis includes time-delay quasars and compound lenses. Future DESC SRD versions should also include strongly lensed supernovae in the baseline analysis.
- The baseline SN analysis includes WFD (Wide-Fast-Deep, the main LSST survey) and DDF (Deep Drilling Field) supernovae, with the assumption that a commissioning mini-survey will be used to build templates so that the photometric SN analysis can begin in year one of the survey.
- Unlike in the DETF report, the baseline LSST WL analysis is a full tomographic “ $3\times 2$ pt” analysis: shear-shear, galaxy-shear, and galaxy-galaxy correlations. This analysis choice is consistent with the current state of the art in the field, but it means there is some statistical overlap between the LSS and the WL analysis. For completeness we will also report on the constraints from shear-shear alone. When forecasting combined constraints across all probes, we include just the  $3\times 2$ pt analysis to avoid double-counting.

As our understanding of these analyses improves, the baseline analysis may need to be updated, resulting in updates to the forecasts and the requirements.

- *Dark Energy Task Force (DETF) figure of merit (FoM)*: given a dark energy equation of state model with  $w(a) = w_0 + (1 - a)w_a$ , the DETF Report defines a FoM in terms of the Fisher matrix for  $(w_0, w_a)$  marginalized over all other parameters as  $\sqrt{|F|}$ , corresponding to the area of the 68% credible region. See the DETF Report for details.<sup>4</sup>
- *Overall uncertainty*: Following the DETF, we quantify overall uncertainty as the *width*<sup>5</sup> of the posterior probability distribution in the  $(w_0, w_a)$  plane, after marginalizing over nuisance parameters associated with systematic uncertainties.
- *Error budget*: A target overall uncertainty on Dark Energy parameters sets the *error budget* for our LSST analysis. The DESC SRD describes how this error budget can be allocated: each probe will contribute to the overall uncertainty by an amount that will depend on how much information the LSST data contain, how much external information we can provide, and how the probes’

<sup>4</sup>The text of the DETF Report defines the FoM in terms of the area of the 95% contour. However, all numbers tabulated in the report correspond to simply  $\sqrt{|F|}$  without the additional factor needed to get the area of the 95% credible region, and it has become common in the literature to refer to numbers calculated this way as the “DETF FoM”, despite what the text of the report says. The DESC SRD follows this convention as well.

<sup>5</sup>See [Appendix B2](#) for a discussion of how “width” is determined.

likelihood functions interact with each other. Estimating the error budget for each probe, and for each measurement step within those probes, must be done iteratively, making forecasts of overall uncertainty given a set of assumptions, varying those assumptions, and repeating. See the start of [Section 5](#) and [Figure G1](#) for details.

- *Statistical uncertainty*: We use the term “statistical uncertainty” to describe the width of the posterior probability distribution in the  $(w_0, w_a)$  plane when the nuisance parameters associated with systematic uncertainties are fixed at their fiducial values. We expect the statistical uncertainty for each LSST dark energy probe to be small compared to the additional posterior width introduced by marginalizing over systematic effects. This is what we mean by LSST cosmological parameter measurements being “systematics limited.”
- *Systematic biases or systematic errors*: These are known/quantified offsets in our measurements due to some observational or astrophysical issue. We use the noun “systematic” as an abbreviation for “systematic bias” and take “error” and “bias” to be synonymous. Their amplitude is not relevant for the DESC SRD because the known part is presumed to have been removed and does not impact our dark energy constraining power. However, quantifying the uncertainty in these corrections is critical.
- *Systematic uncertainties*: All sources of systematic uncertainty are treated, either explicitly or implicitly, by extending the model to include additional “nuisance parameters” that describe the effect. Marginalization over these nuisance parameters allows us to propagate the uncertainty, which is captured by the prior PDF for their values, through to the cosmological parameters. These systematic uncertainties are hence associated with *residual* (uncorrected or post-correction) offsets, resulting from imperfect knowledge applied in the treatment of systematic biases. Two types of systematic effects are considered in the DESC SRD, defined as follows:
  - *Calibratable systematics*: We refer to systematic biases that can be estimated with some precision, or equivalently, modeled with nuisance parameters that have *informative priors* as “calibratable.” Such biases tend to be associated with some aspect of the measurement process, and their nuisance parameter priors can typically be derived by validating the relevant analysis algorithm against external data or sufficiently realistic simulations. Generally the nuisance parameter values themselves are of no physical importance. Selection bias may also be treated as calibratable, though in that case a meta-analysis may be needed to place priors on its magnitude, since the bias is associated with sample definition rather than per-object measurements. In many cases the marginalization over calibratable systematic nuisance parameters can be done in advance of the cosmological inference, resulting in the apparent application of a “correction” and the corresponding introduction of some additional uncertainty. In the other cases, no well-defined model is available for the nuisance parameters or their priors, and we must estimate the potential impact and propagate this uncertainty. **A key part of any dark energy analysis is demonstrating that systematic uncertainties**

*due to calibratable effects do not dominate, and hence we place requirements on calibratable systematic uncertainties in Section 4 and Section 5 below.* These can be thought of as requirements on the size of the informative priors that we can set on these effects. Informative priors are important in the typical case that we do not have a sufficient model for them. In principle, with a sufficiently descriptive model for a particular source of systematic uncertainty, it could be allocated a larger fraction of our total error budget, moving it into the self-calibrated category defined below.

- *Self-calibrated systematics:* These are sources of systematic uncertainty that cannot be estimated in advance, but that can be “self-calibrated” by marginalizing over the nuisance parameters of a model for them at the same time that the cosmological parameters are constrained. They tend to be astrophysical in nature. Examples include the cluster mass vs. observable relation, galaxy bias, and galaxy intrinsic alignments. The nuisance parameters associated with self-calibrated effects will generally have uninformative or mildly informative priors when considering the analysis of LSST data on their own, and often correspond to astrophysically-meaningful quantities. As mentioned in Section 1, we do not place requirements on factors outside of the DESC’s control, such as the acquisition of substantial ancillary datasets that would provide additional terms in the likelihood to constrain those nuisance parameters more tightly. **When setting requirements on our control of calibratable systematic effects, our convention is to include the additional uncertainty caused by marginalizing over these self-calibrated effects together with the statistical uncertainty, referring to their combination as the *marginalized statistical uncertainty*.** The marginalized statistical uncertainty differs from the *overall uncertainty* in that the latter also includes calibratable systematic uncertainties.

While we do not place requirements on self-calibrated systematic uncertainties in this version of the DESC SRD, one could in principle place requirements on them in the future by requiring *model sufficiency*. Models for self-calibrated systematics must be sufficiently complex, flexible and extensive so as to span the range of realistic possibilities for the physical phenomena in question. If they are not, then our overly-simplified modeling assumptions could result in a bias in cosmological parameter estimates. This bias is often referred to as ‘model bias’, and some meta-analysis may be required to estimate its magnitude. Our current approach, however, is to assume that our models for self-calibrated systematics (which are a topic of active R&D within the DESC analysis working groups) are sufficient. There is a subtlety associated with which systematic uncertainties’ nuisance parameters we marginalize over at different steps of the analysis. When setting requirements on calibratable systematic uncertainties, we marginalize *only over self-calibrated systematic uncertainties* in order to check how the additional uncertainty caused by calibratable systematic uncertainties compares with the marginalized statistical uncertainty. When considering the final dark energy figure of merit, we marginalize over *both self-calibrated and calibratable systematic uncertainties* to determine the *overall uncertainty*, just as we would in the real joint analysis.

- *Cosmological parameters:* Due to practical considerations associated with the software framework used in defining the requirements, we consider a flat  $w$ CDM cosmological model, which results in a seven-dimensional parameter space consisting of  $(\Omega_m, \sigma_8, n_s, w_0, w_a, \Omega_b, h)$ . Future DESC SRD versions may expand this parameter space, e.g., to include massive neutrinos and curvature. Fiducial parameter values and priors are outlined in [Appendix C2](#). For requirements that are placed using forecasts of the constraining power of a single probe, we carry out the likelihood analysis only with the parameters that that probe is able to constrain (e.g., SL and SN do not constrain  $\sigma_8$ ).
- *“Year 1” (Y1) and “Year 10” (Y10) forecasts, requirements, and goals:* Several of our requirements and goals are relevant at all times (not just at the end of the survey), so we provide forecasts for dark energy constraining power with the full survey and with approximately 1/10 of the data. We use “Year 10” (Y10) and “Year 1” (Y1) as shorthand terms for these datasets. See [Appendix C1](#) for details of how we define the Y1 and Y10 survey depths and areas. Note that the time at which we receive a dataset corresponding to this Y1 definition may differ significantly from a single calendar year after the survey starts plus the time for the Project to process and release that data. The LSST SRD has requirements on single-exposure and full-survey performance, but no specifications that collectively guarantee that the Y1 dataset as defined in this document will be delivered by a particular time.

### 3 Objectives

The DESC’s primary scientific objectives are listed and described below.

**Objective O1:** LSST will be a key element of the cosmological community’s Stage-IV dark energy program.

The DETF report ([Albrecht et al. 2006](#)) specifies that the “overall Stage-IV program should achieve, in combination, a factor of 10 improvement over Stage-II.”. In principle, we need not apply this criterion to LSST dark energy analysis on its own, since LSST is being carried out in the context of a broader Stage-IV dark energy program that includes, e.g., DESI. We will nonetheless do so.

**Objective O2:** DESC will produce multiple (at least two) independent dark energy constraints with substantially different dependencies on the growth of structure and the cosmological expansion history.

While one could in principle imagine optimizing dark energy constraints by focusing exclusively on obtaining extremely precise constraints from a single probe or class of probes (e.g., structure growth only, with a focus on WL, CL, LSS), a key part of the Stage-IV dark energy program will be demonstrating consistent results with methods that probe dark energy in different ways and with distinct sets of systematic uncertainties.

**Objective O3:** For the LSST dark energy constraints, calibratable systematic uncertainty should not be the dominant contribution to the overall uncertainty.



In practice, meeting this objective means ensuring that the calibratable systematic uncertainty in the dark energy parameters, which is the most difficult type of uncertainty to model accurately, does not exceed the combination of the statistical uncertainty and the self-calibrated systematic uncertainty (the “marginalized statistical uncertainty”). The latter can be estimated by conditioning on fiducial values of the calibratable biases’ nuisance parameters, and marginalizing over the self-calibrated biases’ nuisance parameters.

#### 4 High-level requirements

In this section, we derive the high-level science requirements from the objectives in [Section 3](#). We start by quantifying requirements on the overall uncertainties, both jointly and from each probe.

**High-level requirement RH1:** DESC dark energy probes will achieve a combined FoM exceeding 500 ( $\sim 10 \times$  Stage-II) with the full LSST Y10 dataset when including both statistical and systematic uncertainties and using Stage III priors.

This requirement is essentially a statement that the DESC dark energy analysis should meet the Stage IV program requirements independent of other Stage IV experiments (which we refer to as being a ‘stand-alone Stage IV experiment’), when combining all probes and using the full ten-year dataset. The Stage II FoM in the DETF report (page 77) includes CL, SN, and WL analysis, corresponding to a FoM of 54. Stage IV surveys should *collectively* exceed this by approximately a factor of 10.

Proper incorporation of Stage III priors for all probes is complicated, especially given the overlap between the LSST and DES footprints. For this reason, we use only SDSS-III BOSS, Planck, and Stage III supernova survey priors, and an  $H_0$  prior (described in more detail in [Appendix C2](#)) rather than all Stage III priors. In future, using SDSS-IV eBOSS will be possible as well.

Note that, when imposing **RH1**, the FoM includes the overall uncertainty: pure statistical uncertainties and marginalization over *both* self-calibrated and calibratable biases (see [Section 2](#) for details of these categories). Indeed, **RH1** is the first step in our systematic error budgeting process: If our forecast FoM exceeds 500 without accounting for calibratable systematic uncertainties, we adjust the amount of the error budget that goes into calibratable systematic uncertainties such that the final FoM after including them is exactly 500. This process is the first step in deriving detailed requirements in [Section 5](#).

Satisfying this requirement will enable DESC to achieve its first objective, **O1**.

**Goal G1:** Each probe or combination of probes that is included as an independent term in the joint likelihood function for the full LSST Y10 dataset will achieve  $\text{FoM} > 2 \times$  the corresponding Stage-III probe when including both statistical and systematic uncertainties. The relevant thresholds for the individual DESC probes<sup>6</sup> are 12, 1.5, 1.3, 19, and 40 for CL, LSS, SL, SN, and WL, respectively.

In addition to the overall FoM requirements in **RH1**, our goal is to substantially improve over the previ-

---

<sup>6</sup>The origin of the Stage-III figures of merit, which are  $0.5 \times$  the thresholds quoted here, is described in [Appendix C3](#). Since the completion of the DETF report, the landscape of measurement has changed significantly and the actual obtained Stage III FoMs are in some cases well below those forecasted in the original report.



ous state of the art in each individual probe analysis. As for **RH1**, the FoM comparison implied by this goal includes the overall uncertainty. Another motivation behind this goal is to ensure that the DESC meets its objective **O2** of deriving dark energy constraints from multiple complementary dark energy probes<sup>7</sup>. To test whether we will meet **G1** for any given dark energy probe, we must define baseline analyses for LSST as well as a corresponding Stage-III FoM. The baseline analyses for LSST are outlined in **Section 2**, and all analysis choices and sources of systematic uncertainty are described in **Appendix D**.

In principle the factor of two in **G1** is arbitrary. However, it is empirically the case that for some of our probes, the LSST Y10 forecasts indicate greater degeneracy breaking between probes such as SN and WL than the Y1 forecasts. By implication, the SN and WL degeneracy-breaking power for Stage IV surveys should be greater than for Stage III surveys assuming that the LSST Y1 and Stage III degeneracy directions may be similar. In that case, the combined probe Stage IV constraining power (a factor of three in overall FoM compared to Stage III; see **RH1**) can be achieved with an increase in FoM for individual probes that is less than a factor of three.

**High-level requirement RH2: Each probe or combination of probes that is included as an independent term in the likelihood function will achieve total calibratable systematic uncertainty that is less than the marginalized statistical uncertainty in the  $(w_0, w_a)$  plane.**

*This requirement, which is the only one of our requirements that can be applied to the Y1 analysis (or any analysis before the completion of LSST), is a way of quantifying whether we have achieved our high-level objective O3.* It is important to note that by comparing against the marginalized statistical uncertainty, we are including self-calibrated systematic uncertainties (e.g., due to astrophysical effects such as scatter in the cluster mass vs. observable relation, galaxy intrinsic alignments, galaxy bias). Hence we are not requiring that systematic uncertainty due to *any* non-statistical error be less than the purely statistical error. We are only requiring that residual uncertainty in *calibratable* systematics be less than the uncertainty after marginalizing over self-calibrated systematics. The reason to frame this requirement in this way is that realistically, some dark energy probes may have astrophysical systematic uncertainties that will always exceed the statistical error for LSST. This basic feature of those probes should not be considered a failure of the DESC’s efforts to utilize those probes. Also note that the line between self-calibrated and calibratable systematics is potentially movable; given a better model for calibratable uncertainties (and possibly a different approach to the analysis of LSST data), they could become self-calibrated. In that case, they would enter **RH2** differently, since they could acceptably become a dominant contributor to the overall uncertainty (leaving **RH1** and **G1** as indirect constraints on how much additional uncertainty they can contribute), modulo any requirements on model sufficiency which would be treated as calibratable uncertainty.

We have not specified precise tolerances (systematic uncertainty equals  $X$  times marginalized statistical uncertainty for some value of  $X$ ) in **RH2** in recognition of the fact that many elements of these forecasts will change as our understanding improves, so  $X$  can be specified only to one significant figure. Chang-

---

<sup>7</sup>Note that **G1** is phrased such that not all probes must meet it, only those probes that enter the final joint likelihood analysis. However, this goal is only part of what is needed to meet **O2**; **RH3** is also relevant to that objective.

ing  $X$  from 1 would coherently shift all of our requirements to be more/less stringent but is unlikely to strongly modify our understanding of which systematics are more/less challenging to control.

While **RH2** applies at all times, its implications for the analysis of each probe depend on time. When the full survey dataset exists, **RH1** constrains how much statistical constraining power we can lose to carry out a more conservative analysis that makes it easier to meet **RH2**. Before then, only **RH2** is relevant. Hence, **Section 5** has Y10 detailed requirements associated with **RH2**, along with Y1 goals. The Y1 goals quantify the needed level of systematics control to enable us to carry out our desired baseline analysis with Y1 data, without sacrificing statistical precision due to difficulties achieving the required control of systematic uncertainties. However, if we cannot meet those goals in Y1 (for example, due to unanticipated systematic uncertainties in the data that require additional time to understand and mitigate), then meeting **RH2** is sufficient.

Finally, note that **RH2** may at times be directly satisfied due to the constraints imposed by **RH1**. As mentioned in the description of **RH1**, we may decrease the allowable calibratable systematic uncertainty if needed to ensure that we meet our high-level requirement of being a stand-alone Stage IV dark energy experiment. In cases where that occurs, as in this version of the DESC SRD, meeting **RH1** automatically ensures that **RH2** will be met.

**High-level requirement RH3: At least one probe of structure growth and one probe of the cosmological expansion history shall satisfy G1 and RH2 for the full LSST Y10 dataset.**

This requirement ensures that we achieve our objective **O2**. **RH3** is motivated by the fact that a Stage IV dark energy experiment should ideally provide not only constraints on the equation of state of dark energy, but also provide a stringent test of gravity. For the purpose of this requirement, we consider CL and WL as probes of structure growth (though they carry a small amount of information about geometry), SN and SL as probes of the expansion history, and LSS in both categories since it includes measurement of the baryon acoustic oscillation feature in addition to smaller-scale clustering. Deviations from General Relativity are best detected with two complementary probes.

**Goal G2: At least one probe of structure growth and one probe of the expansion history should satisfy RH2 for the full LSST Y3 dataset.**

We do not require that **RH3** is met in our early analyses, given the level of technical challenge involved in carrying out an analysis that is not dominated by calibratable systematics with a new dataset. However, we would ideally like to be well on our way to including multiple complementary dark energy measurements after several years – hence the definition of this goal **G2**. Similarly to the definition of Y1 (**Section 2**), the definition of Y3 in **G2** corresponds to the science analyses after a time when roughly 3/10 of the WFD images over the full area have been observed, processed, and released, rather than strictly the end of the third year of the survey.

**High-level requirement RH4: DESC will use blind analysis techniques for all dark energy analyses to avoid confirmation bias.**

Confirmation bias has been highlighted by the field as an important issue for cosmological measure-

ments (Croft & Dailey 2011). Carrying out blind analyses is becoming increasingly common for probes of large-scale structure (DES Collaboration 2017; Hildebrandt et al. 2017) and will be even more important in the era of LSST. Development of methods for blinding that will work for LSST is a non-trivial task, and this procedural requirement is tantamount to saying that this work is high-priority. It will help us to work in a way that is consistent with our objective O3; carrying out blinded analyses avoids confirmation bias. Currently, our inclusion of Stage III priors that originate from non-blinded cosmological analyses in the derivation of our detailed requirements may appear to be in tension with RH4. However, RH4 refers to the actual analyses carried out, and in practice we would strive to use more up-to-date analyses from surveys that are not currently available (DESI, Simons Observatory, CMB-S4, etc.), which will be both more powerful than our current Stage III priors and will hopefully utilize blinded analysis methods given the evolution of the cosmological community in this direction.

## 5 Detailed requirements

This section contains detailed requirements on systematic uncertainties, broken down by DESC dark energy probe. These requirements are derived through a process of *error budgeting*. Our total error budget for calibratable systematic uncertainties that would enable the DESC to meet its high-level requirements is allocated among calibratable systematic effects in order to derive detailed requirements on the treatment of each one. We must make choices about how much of the error budget to allocate to effects that are under our control; these allocations may change in future as we learn more about various sources of systematic uncertainty. Since the error budgeting process will be affected by improvements in our understanding and analysis methods and by the inclusion of requirements on model sufficiency, the detailed requirements (unlike the high-level ones) will evolve in future versions of the DESC SRD.

As a reminder of our overall methodology and a guide to the contents of this section, we note that (as detailed in Section 1 and Section 2), we consider two categories of systematic uncertainties for each probe: self-calibrated systematics (for which we typically have uninformative priors on nuisance parameters) and calibratable ones (for which DESC simulations, theory, other software, or precursor datasets produce informative priors). While both types of systematic uncertainties could be mitigated using new ancillary datasets, we only consider what can be gained from LSST data, precursor and planned ancillary datasets, and follow-up at rates consistent with what can be obtained now.

Consequently, we assume conservative priors for self-calibrated systematics, and *only place requirements on calibratable systematic uncertainties*. If new external data unexpectedly become available, it will be folded into the joint likelihood, and will improve our ability to marginalize over the nuisance parameters of both types of systematic uncertainties, reducing our overall error budget. Given a better model for a given source of calibratable systematic uncertainty, it might be moved into the self-calibrated category, which would change the way it is treated with respect to detailed requirements below. In particular, it would no longer have an associated detailed requirement, and instead would increase the marginalized statistical uncertainty, which would have the additional impact of increasing the tolerances for the remaining sources of calibratable systematic uncertainty and hence loosening other requirements. This tradeoff is acceptable as long as RH1 can still be met. We also note the need for

model sufficiency to reduce systematic biases, but do not place requirements on model sufficiency in this DESC SRD version.

In the subsections below, we place requirements on multiple sources of calibratable systematic uncertainty. In general, our approach (as defined by the need to jointly satisfy **RH1** and **RH2**) is to compute the marginalized systematic uncertainty by conditioning on fiducial values of the calibratable systematic effects’ nuisance parameters, and then allocating some fraction of this marginalized statistical uncertainty across all sources of calibratable systematic uncertainty. The fraction  $f_{\text{sys}}$  that is allocated, i.e., the ratio of calibratable systematic uncertainty to marginalized statistical uncertainty, is determined by **RH1** and **RH2** as follows. Schematically, if we want our overall FoM to be 500, and our FoM with marginalized statistical uncertainty is  $\text{FoM}_{\text{stat}}$ , then **RH1** implies that  $f_{\text{sys}}$  is determined as

$$\frac{\text{FoM}_{\text{stat}}}{500} = 1 + f_{\text{sys}}^2 \quad (1)$$

because the FoM scales like an inverse variance. Clearly if  $\text{FoM}_{\text{stat}}$  exceeds 1000, then  $f_{\text{sys}} > 1$ , which would cause a violation of **RH2**, and hence we cap  $f_{\text{sys}}$  at precisely 1 to jointly meet **RH1** and **RH2**. If  $\text{FoM}_{\text{stat}}$  is only slightly above 500, we would have little room for systematic uncertainty, and the requirements would be extremely tight. In practice, the  $f_{\text{sys}}$  determination is a bit more subtle than **Equation 1** implies, for two reasons. First, the requirement that the overall FoM be 500 includes Stage III priors, which do not get degraded by the LSST systematic uncertainty. Accounting for this involves degrading the Fisher matrices for the DESC probes by the above factor and combining with our Stage III priors, optimizing  $f_{\text{sys}}$  until **Equation 1** is met<sup>8</sup>. Second, the above discussion presumes that all probes will have the same value of  $f_{\text{sys}}$ . While this may be a reasonable default, preliminary calculations with this assumption resulted in unachievably stringent photometric calibration requirements for the supernova science case. As a result, we gave a slightly larger fraction of the systematic error budget to supernovae, and lower fractions for all other probes:  $f_{\text{sys}}^{(\text{SN})} = 0.7$ , and  $f_{\text{sys}}^{(\text{non-SN})} = 0.62$ , again optimizing using the appropriate generalization of **Equation 1**.

Once we determined the overall systematic uncertainty fraction for each probe, we then considered all sources of calibratable systematic uncertainty, and divided them up based on quadrature summation to the probe-specific  $f_{\text{sys}}$  value. This process results in a set of Y10 requirements, as described in **Section 4** below **RH2**. The Y10 error budgeting process described here is illustrated in **Figure G1**. For Y1 goals, the process is slightly different, since **RH1** does not apply, only **RH2**. Hence we use  $f_{\text{sys}}^{(\text{Y1})} = 1$  to set the overall size of the total calibratable systematic error budget for all probes in Y1, while keeping the same breakdown between different sources of systematic uncertainty for a given probe as for Y10.

The mathematical implications of the adopted  $f_{\text{sys}}$  values are described in **Appendix B2**. We define  $N_{\text{class}}$  classes of calibratable systematic uncertainty for each probe, with our current understanding of the tall poles in each analysis being used to define major/minor classes that should get a larger/smaller

<sup>8</sup>There is yet another subtlety, which is that degrading the individual Fisher matrices is not quite the right thing to do; the systematic uncertainties may have a different direction in the 7-dimensional cosmological parameter space. We defer consideration of this effect to future versions of the DESC SRD.

fraction of that error budget. For example, if  $N_{\text{class}} = 2$  then the more major one might get  $0.8f_{\text{sys}}$  and the more minor one  $0.6f_{\text{sys}}$  (note that 0.8 and 0.6 add in quadrature to 1). Each class is thus given a fraction  $f_{\text{class}}f_{\text{sys}}$ . Within each class, there might be  $N_{\text{sub}}$  sources of uncertainty that contribute; these each get  $f_{\text{class}}f_{\text{sys}}/\sqrt{N_{\text{sub}}}$  of the error budget. A crucial assumption here is that there is no covariance between systematic offsets. For example, it is imaginable that the error in mean photometric redshifts could correlate with the error in the redshift scatter determination. Given that the sign of cross-probe correlations can be either positive or negative (i.e. making results better or worse compared to quadrature addition), we proceed with this assumption and will, if necessary, modify our parametrization in the future so that individual contributions will be roughly uncorrelated, or properly account for correlations as needed. In general, we include in the tally of  $N_{\text{class}}$  and  $N_{\text{sub}}$  all sources of calibratable systematic uncertainty outlined in [Appendix D](#) for a given probe, even those for which we do not yet have the infrastructure to set requirements now. This means that in future DESC SRD versions we will not have to revise the fraction of the error budget given to sources of calibratable systematic uncertainty for which requirements already exist when we add requirements on new sources of systematic uncertainty. This statement is only true to the extent that the different contributors to each class of systematic uncertainty are independent of all others (within that class or otherwise).

We emphasize here that there are several layers of subjective choices in the error budgeting beyond what is deterministically specified by our high-level requirements. These include whether to give each probe the same calibratable systematic error budget (specified as a fixed fraction of its statistical error budget), and how to divide up the error budget amongst the different sources of calibratable systematic uncertainty. This feature of our error budgeting provides flexibility, should some of our detailed requirements prove difficult to meet even given a reasonable amount of additional resources (which would be the first avenue to meeting challenging requirements). In short, the paths to dealing with tight requirements on individual sources of systematic uncertainty are (a) devote additional resources to the problem, (b) re-budget within different sources of uncertainty for a given probe to give more room for this source of systematic uncertainty, (c) re-budget the calibratable systematic error budget across probes, and finally (d) re-think where our constraining power is coming from across all probes, potentially changing analysis methods in ways that enable requirements to be loosened.

Several of our technical appendices summarize information and methodology that went into the detailed requirements enumerated below. The full list of self-calibrated and calibratable systematic uncertainties that should be considered for each probe is given in [Appendix D](#), including both the subset that we can currently model and/or place requirements on, the current parametrization, and future improvements. A synthesis of the calibratable effects on which we place requirements across probes is in [Section E1](#). As DESC software pipelines evolve, future DESC SRD versions will naturally be able to describe requirements on additional effects. Finally, the details of how requirements were defined are described in [Appendix B2](#). Several plots that illustrate key aspects of the results in this section are in [Appendix G](#).

## 5.1 Large-scale structure

Here we derive requirements for the galaxy clustering measurements (Appendix D1), which carry information about structure growth and the expansion history of the Universe.

The baseline galaxy clustering analysis used here involves tomographic clustering (auto-power spectra only) across a wide range of spatial scales. This baseline analysis does not include explicit measurement of the baryon acoustic oscillations (BAO) peak, but BAO information is implicitly included (albeit suboptimally) by extending the power spectrum measurements to  $\ell_{\min} = 20$ . In addition to the statistical uncertainties, our cosmological parameter constraints incorporate additional uncertainty due to marginalization over a model for galaxy bias with one nuisance parameter per tomographic bin. Following G1, our target FoM for this analysis after Y10 is 1.5; the forecast FoM with statistical and self-calibrated systematic uncertainties after Y1 and Y10, with informative priors on the non- $(w_0, w_a)$  subset of the space (see Appendix B2), is 13 and 14, respectively. The similarity of these two numbers results from the current design of the baseline analysis for LSS being suboptimal in a way that prevents it from benefiting from the increase in constraining power of the survey as time proceeds; this should be improved in future versions of the DESC SRD. If we achieve RH2, then inclusion of calibratable systematic uncertainties should multiply these numbers by a factor of 0.72 in Y10, which comes from the  $1/(1 + (f_{\text{sys}}^{\text{non-SN}})^2) = 1/(1 + 0.62^2)$  factor motivated in the introduction to Section 5. In practice the FoM reduction is not as severe as that, since it does not apply to the Stage III priors.

We define two classes of calibratable systematic uncertainty for LSS measurements, as described in Appendix D1: redshift and number density uncertainties. The total calibratable systematic uncertainty for LSS split into 0.8 and 0.6 for the two categories, respectively. These numbers are chosen such that the quadrature sum is 1, but the redshift uncertainties (which are expected to be more challenging to quantify and remove) are given a greater share of the error budget. In this version of the DESC SRD, we do not place any detailed requirements on number density uncertainties, and only place requirements on two out of six contributors (see Figure D2) to the redshift uncertainties: the uncertainty associated with the mean redshift  $\langle z \rangle$  in each tomographic bin, and the uncertainty in the width of the redshift distribution in the tomographic bin (presumed to be identical for each bin, modulo a standard  $1 + z$  factor). Hence there are two LSS requirements below, and both effects are allowed to contribute a fraction equal to  $0.8/\sqrt{6} \sim 0.3$  of the total calibratable systematic uncertainty. Here the  $\sqrt{6}$  indicates that eventually we will place requirements on a total of six sources of redshift uncertainty, allocating the total redshift uncertainty budget to each one equally. Finally, as noted previously, the total calibratable systematic uncertainty is allowed to be a factor of  $f_{\text{sys}}^{\text{non-SN}} = 0.62$  times the marginalized statistical uncertainty in Y10.

**Detailed requirement LSS1 (Y10):** Systematic uncertainty in the mean redshift of each tomographic bin shall not exceed  $0.003(1 + z)$  in the Y10 DESC LSS analysis.

**Goal LSS1 (Y1):** Systematic uncertainty in the mean redshift of each tomographic bin should not exceed  $0.005(1 + z)$  in the Y1 DESC LSS analysis.

The above requirement was determined by coherently shifting the mean redshift of all tomographic bins



by the same amount, resulting in tighter requirements than when considering shifts in individual bins, but looser requirements than if we had included a pattern specifically chosen to mimic the impact of dark energy on the tomographic galaxy power spectra. While tighter than what is routinely achieved by existing surveys (e.g., [Davis et al. 2017](#)), which are currently limited by systematic uncertainties that will require additional work to overcome, these requirements are well above the  $0.0004(1+z)$  accuracy that should be achievable through cross-correlation analyses with a DESI-like survey covering the full LSST footprint ([Newman et al. 2015](#)). With the expected 4000 square degrees of overlap between LSST and DESI, combined with the more-dilute 4MOST galaxy and quasar samples covering the remainder of the imaging area, the expected accuracy will be worse than this by a factor of  $\sqrt{2}$  or less for Y10, still well within the requirements.

**Detailed requirement LSS2 (Y10): Systematic uncertainty in the photometric redshift scatter  $\sigma_z$  shall not exceed  $0.03(1+z)$  in the Y10 DESC LSS analysis.**

**Goal LSS2 (Y1): Systematic uncertainty in the photometric redshift scatter  $\sigma_z$  should not exceed  $0.1(1+z)$  in the Y1 DESC LSS analysis.**

The above requirement was determined by computing a data vector in which we coherently broadened the photometric redshift scatter while computing model predictions with the original baseline photometric redshift scatter.

## 5.2 Weak lensing ( $3 \times 2$ -point)

Here we derive requirements for the weak lensing (+LSS, i.e.,  $3 \times 2$ -point) measurements ([Appendix D2](#)), which carry information primarily about structure growth, with a small contribution from the expansion history.

The baseline weak lensing analysis in this version of the DESC SRD involves tomographic shear-shear, galaxy-shear, and galaxy-galaxy power spectra across a wide range of spatial scales. Cross-bin correlations are included for shear-shear and shear-galaxy power spectra, while only auto-power spectra are included for galaxy-galaxy. In addition to pure statistical errors, our cosmological parameter constraints incorporate additional uncertainty due to marginalization over a model for galaxy bias with one nuisance parameter per tomographic bin, and due to intrinsic alignments with four nuisance parameters overall. Following [G1](#), our target FoM for this analysis after Y10 is 40; the forecast FoM with statistical and self-calibrated systematic uncertainties after Y1 and Y10 is 37 and 87, respectively. If we achieve [RH2](#), then inclusion of calibratable systematic uncertainties will multiply these numbers by a factor of  $\sim 0.72$  (see [Section 5.1](#) for details) for Y10, which still enables us to meet [G1](#). Note that if we consider just the shear-shear contribution to the dark energy constraining power, the forecast FoM with statistical and self-calibrated systematic uncertainties after Y1 and Y10 is 19 and 52, respectively. The reason to consider the shear-shear aspect of the analysis separately is that in practice we begin by separately analyzing shear-shear versus galaxy-galaxy correlations to ensure consistent results.

There are four classes of calibratable systematic uncertainty for this analysis, as described in [Appendix D2](#): redshift, number density, multiplicative shear, and additive shear uncertainties. We allocate

0.7, 0.2, 0.7, and 0.2 of the total calibratable systematic error budget to these categories, respectively. These numbers are chosen such that the quadrature sum is 1; the two categories that are given less room in the error budget are more easily diagnosable directly through null tests on the data. Finally, as in [Section 5.1](#), the total calibratable systematic uncertainty is allowed to be a factor of  $f_{\text{sys}}^{(\text{non-SN})} = 0.62$  times the marginalized statistical uncertainty in Y10.

We place requirements on two out of seven sources of systematic uncertainty associated with redshifts (see [Figure D3](#)): the uncertainty associated with the mean source redshifts  $\langle z \rangle$  in each bin and the uncertainty in the photometric redshift scatter (presumed to be identical in each bin, modulo a standard  $1 + z$  factor). These are each allowed to contribute a fraction equal to  $0.7/\sqrt{7} \sim 0.25$  times the total calibratable systematic uncertainty. We also place requirements on our overall knowledge of multiplicative shear calibration (0.7 of the total uncertainty), as well as derived requirements on (a) our knowledge of PSF model size errors, and (b) stellar contamination in the source galaxy sample. Hence there are five WL requirements below. Requirements on control of additive shear systematic biases are deferred to future DESC SRD versions. In general, the sensitivity to additive shear biases depends on their scale dependence and how well it mimics changes in scale dependence due to changes in cosmological parameters; hence more meaningful requirements will be placed after we have templates for the scale dependence of the relevant systematics effects.

**Detailed requirement WL1 (Y10): Systematic uncertainty in the mean redshift of each source tomographic bin shall not exceed  $0.001(1 + z)$  in the Y10 DESC WL analysis.**

**Goal WL1 (Y1): Systematic uncertainty in the mean redshift of each source tomographic bin should not exceed  $0.002(1 + z)$  in the Y1 DESC WL analysis.**

The above requirement was determined by coherently shifting the mean redshift of all source tomographic bins by the same fraction for the shear-shear analysis. Currently the analysis setup for  $3 \times 2$ -point does not allow separate consideration of biases in the lens and source populations, so we rely on [LSS1](#) for lens sample requirements on knowledge of ensemble mean redshifts and [WL1](#) for source sample requirements on knowledge of ensemble mean redshifts (considered entirely separately).

Because of the relatively larger constraining power in this measurement, this requirement is stricter than [LSS1](#). The magnitude of this requirement on the systematic uncertainty in the mean redshifts is comparable to those forecast by [Ma et al. \(2006\)](#), who use different default analysis assumptions but noted that the requirements on knowledge of redshift distribution parameters are especially tight when forecasting requirements with  $w_a \neq 0$ , i.e., in the  $(w_0, w_a)$  space rather than assuming a constant dark energy equation of state. Nonetheless, per discussion following [LSS1](#), the magnitude of the Y10 requirement in [WL1](#) should be within reach for cross-correlation-based calibration methods alone.

**Detailed requirement WL2 (Y10): Systematic uncertainty in the source photometric redshift scatter  $\sigma_z$  shall not exceed  $0.003(1 + z)$  in the Y10 DESC WL analysis.**

**Goal WL2 (Y1): Systematic uncertainty in the source photometric redshift scatter  $\sigma_z$  should not exceed  $0.006(1 + z)$  in the Y1 DESC WL analysis.**



The above requirement was determined by computing a data vector in which we coherently broadened the photometric redshift scatter while computing model predictions with the original baseline photometric redshift scatter. This was done specifically for shear-shear, since the analysis setup does not currently enable us to separately vary the lens and source photo- $z$  scatter values for the  $3 \times 2$ -point analysis. This requirement is substantially more stringent than the requirements for a clustering-only analysis [LSS2](#), reflecting the greater statistical power in the weak lensing analysis.

**Detailed requirement WL3 (Y10): Systematic uncertainty in the redshift-dependent shear calibration shall not exceed 0.003 in the Y10 DESC WL analysis.**

**Goal WL3 (Y1): Systematic uncertainty in the redshift-dependent shear calibration should not exceed 0.013 in the Y1 DESC WL analysis.**

The assumption behind this requirement is that the DESC will carry out its cosmological weak lensing analysis using shear catalogs provided by Rubin Observatory, but will use its own software to quantify and remove any redshift-dependent calibration biases in the ensemble shear signals, and to place bounds on the residuals. This requirement is therefore on our knowledge of the shear calibration: how well can we constrain *the sum of all effects that cause uncertainty in the redshift-dependent shear calibration*, i.e., the residual calibration bias after subtracting off known effects? (For a listing of all effects implicitly included, see [Appendix D2.3](#).) This requirement was placed based on the  $3 \times 2$ -point analysis, though shear-shear requirements are only slightly larger.

The canonical requirement on residual shear calibration that is often quoted in the literature for Stage-IV surveys,  $\Delta m \lesssim 0.002$ , comes from [Massey et al. \(2013\)](#). The Euclid forecasts in that work naturally differ from these forecasts in basic survey parameters (Euclid vs. LSST) and use of shear-shear only, but also in basic methodology: they use Gaussian rather than non-Gaussian covariances; they do not marginalize over intrinsic alignments; and they define shear calibration requirements with  $r \approx 0.15$  ([Equation 2](#) on page 40) rather than  $0.4 = 0.7 f_{\text{sys}}^{\text{(non-SN)}}$  as we have done here. Use of shear-shear alone may make their requirements marginally less stringent than ours, while all the other differences should make them more stringent. In short, it may be surprising that the requirements for Euclid and for LSST Y10 agree so well. In the context of the field, the best state-of-the-art methods can already achieve uncertainty on  $\Delta m = 5 \times 10^{-3}$  in the simplest scenario, *without* accounting for all sources of systematic uncertainty that we are including in this requirement (e.g., blending effects tend to lead to larger shear calibration uncertainties than this). Hence meeting this requirement requires some improvement on the current state of the art to tackle specific contributors to uncertainties on shear calibration that are less well understood such as blending – but does not require an order of magnitude improvement and hence is likely to eventually be achievable with variants of the existing state of the art.

**Detailed requirement WL4 (Y10): Systematic uncertainty in the PSF model size defined using the trace of the second moment matrix shall not exceed 0.1% in the Y10 DESC WL analysis.**

**Goal WL4 (Y1): Systematic uncertainty in the PSF model size defined using the trace of the second moment matrix should not exceed 0.4% in the Y1 DESC WL analysis.**

It is well known (e.g., [Hirata et al. 2004](#)) that biases in the PSF model size can cause a coherent mul-

tiplicative bias in the weak lensing shear signals. While the LSST SRD places explicit requirements on how well the PSF model *shapes* are known, it places no requirement on PSF model size (except the indirect and non-quantitative constraint that most algorithms that can accurately infer the PSF model shape also estimate the PSF model size fairly accurately). Fortunately, there are well-established null tests that can uncover the presence of PSF model size residuals in the real data (e.g., [Jarvis et al. 2016](#); [Mandelbaum et al. 2018](#)). DESC pipelines will use those null tests along with our analysis of image simulations to constrain the magnitude of PSF model size residuals; the above requirement is on our knowledge of those residuals. Many physical effects can cause PSF model size errors; this version of the DESC SRD does not drill down to place separate requirements on each of those effects. While the exact magnitude of the shear calibration bias induced by a PSF model size error depends on the size of the galaxy population compared to the PSF, to within a factor of  $\sim 2$  it is typically the case that the shear calibration bias is set by the size of the typical fractional PSF model size error (i.e.,  $\delta T_{\text{PSF}}/T_{\text{PSF}}$ , where  $T_{\text{PSF}}$  is the trace of the moment matrix of the PSF and hence is related to the area covered by the PSF).

This requirement was derived without additional forecasts; rather, it comes from [WL3](#), along with the aforementioned formalism for estimating how PSF model size residuals propagate directly into shear calibration biases. Since there are many effects that can contribute to shear calibration bias (of order ten) we allocate  $1/\sqrt{10}$  of the shear calibration bias error budget to PSF model size uncertainty.

**Detailed requirement WL5 (Y10): Systematic uncertainty in the stellar contamination of the source sample shall not exceed 0.1% in the Y10 DESC WL analysis.**

**Goal WL5 (Y1): Systematic uncertainty in the stellar contamination of the source sample should not exceed 0.4% in the Y1 DESC WL analysis.**

Inclusion of stars in the WL source sample can, if unrecognized, cause a dilution of the estimated shear signal that is directly related to the fraction of the sample that is stars<sup>9</sup>, because the stars contribute zero shear signal. Hence our overall requirement on shear calibration [WL3](#) can be translated directly into a requirement on how well we have quantified the redshift-dependent contamination of the source sample by stars. Similarly to [WL4](#), we allocate  $1/\sqrt{10}$  of the shear calibration bias uncertainty to stellar contamination.

### 5.3 Galaxy clusters

Here we derive requirements for the galaxy clusters analysis ([Appendix D3](#)), which carries information about structure growth.

The baseline galaxy clusters analysis in this version of the DESC SRD involves tomographic cluster counts and stacked cluster WL profiles in the 1-halo regime. In addition to pure statistical errors, our cosmological parameter constraints incorporate marginalization over a relatively flexible parametrization of the cluster mass-observable relation (MOR). Following [G1](#), our target FoM for this analysis after

---

<sup>9</sup>Or rather, the total *weighted* stellar contamination fraction for whatever weighting scheme is used to infer the ensemble weak lensing shear.

Y10 is 12; the forecast FoM with statistical and self-calibrated systematic uncertainties after Y1 and Y10 is 11 and 22, respectively. If we achieve **RH2**, then as described in **Section 5.1**, inclusion of calibratable systematic uncertainties will multiply these numbers by a factor of  $\sim 0.72$  (see **Section 5.1** for details) in Y10, which enables us to meet **G1**.

There are four classes of calibratable systematic uncertainty for this analysis, as described in **Appendix D3**: redshift, number density, multiplicative shear, and additive shear uncertainties. We allocate 0.7, 0.2, 0.7, and 0.2 of the total calibratable systematic uncertainty to these categories, respectively. These numbers are chosen such that the quadrature sum is 1; the two categories that are given less room in the error budget are more easily diagnosable directly through null tests on the data. We place requirements on two out of seven sources of systematic uncertainty associated with redshifts (see **Figure D4**): the uncertainty associated with the mean source redshifts  $\langle z \rangle$  in each bin, and the uncertainty in the source redshift bin width (presumed to be identical in each bin, modulo a standard  $1 + z$  factor). These are each allowed to contribute a fraction equal to  $0.7/\sqrt{7} \sim 0.25$  times the total calibratable systematic uncertainty. We also place requirements on our overall knowledge of shear calibration (0.7 of the total calibratable systematic uncertainty). Hence there are three CL requirements below. Note that as in **Section 5.1**, the total calibratable systematic uncertainty, for which we have just described its detailed allocation between effects, is allowed to be a factor of  $f_{\text{sys}}^{(\text{non-SN})} = 0.62$  times the marginalized statistical uncertainty in Y10.

**Detailed requirement CL1 (Y10):** Systematic uncertainty in the mean redshift of each source tomographic bin shall not exceed  $0.001(1 + z)$  in the Y10 DESC CL analysis.

**Goal CL1 (Y1):** Systematic uncertainty in the mean redshift of each source tomographic bin should not exceed  $0.008(1 + z)$  in the Y1 DESC CL analysis.

Like **WL1**, the above requirement was determined by coherently shifting the mean redshift of all source tomographic bins by the same amount. This requirement is comparable to the corresponding requirement for WL for Y10, **WL1**, despite differences in cosmological constraining power.

**Detailed requirement CL2 (Y10):** Systematic uncertainty in the source photometric redshift scatter shall not exceed  $0.005(1 + z)$  in the Y10 DESC CL analysis.

**Goal CL2 (Y1):** Systematic uncertainty in the source photometric redshift scatter should not exceed  $0.02(1 + z)$  in the Y1 DESC CL analysis.

Like **WL2**, the above requirement was determined by computing a data vector in which we coherently broadened the photometric redshift scatter for all source tomographic bins while computing model predictions with the original baseline photometric redshift scatter.

**Detailed requirement CL3 (Y10):** Systematic uncertainty in the redshift-dependent shear calibration shall not exceed 0.008 in the Y10 DESC CL analysis.

**Goal CL3 (Y1):** Systematic uncertainty in the redshift-dependent shear calibration should not exceed 0.06 in the Y1 DESC CL analysis.

As for WL, the assumption behind this requirement is that the DESC will carry out its cosmological

weak lensing analysis using shear catalogs provided by Rubin Observatory, but will use its own software to remove any redshift-dependent calibration biases in the ensemble shear signals and to place bounds on any residual calibration biases. This requirement is therefore on our knowledge of the redshift-dependent shear calibration.

**CL3** is weaker than the corresponding shear calibration requirement for WL, **WL3**. Thus any associated requirements defined in [Section 5.2](#) will also be more stringent than similarly derived requirements for CL, so we do not proceed to define requirements related to knowledge of PSF model size and stellar contamination in the source sample for CL analysis.

## 5.4 Supernovae

Here we derive requirements for the supernova analysis ([Appendix D4](#)), which carries information about the expansion rate of the Universe. The detailed requirements presented in this subsection are directly connected to several requirements in the LSST Project SRD, as will be explicitly noted below. Rubin Observatory is responsible for many aspects of photometric calibration, combining information from the in-dome hardware, other system diagnostics, auxiliary telescope data, and the raw science images. As in the rest of this document, we assume that the basic photometric dataset provided by the LSST Facility will meet the requirements of the LSST Project SRD. Where the detailed DESC requirements derived in this subsection are more stringent than those in the LSST Project SRD, the implication is that DESC will need to provide additional resources and expertise, and deploy them in close collaboration with LSST Facility staff, in order to achieve a more precise photometric calibration. Depending on the factors that limit the photometric calibration, this may not be achievable in practice; the LSST SRD requirements were used to set hardware requirements and inform hardware design, resulting in fundamental limitations in some aspects of the system. In that case, what is needed in practice is for the DESC analysis methods to improve (e.g., by updating modeling methods such that any of the DESC probes becomes more constraining, leaving more room in the error budget for the systematic uncertainty associated with photometric calibration). After presenting all the detailed requirements in this section, we will briefly summarize which of them relate to aspects of photometric calibration that are carried out by the Project, and outline the strategy for meeting them.

The baseline supernova analysis in this version of the DESC SRD includes supernova samples derived from both the WFD and the DDF, with conservative estimates of supernova numbers based on simulations that incorporate the `minion_1016`<sup>10</sup> cadence strategy and with plausibly achievable numbers of host spectroscopic redshifts. Currently we neglect the cosmological constraining power of those supernovae for which host spectroscopic redshifts cannot be obtained, relying on them purely for building templates and constraining models for astrophysical systematic uncertainties. The forecasts include marginalization over several self-calibrated systematic uncertainties associated with standardization of the color-luminosity law (including redshift dependence), intrinsic scatter, and host mass-SN luminosity correlations. Following [G1](#), our target FoM for supernova analysis after Y10 is 19; the forecast FoM

---

<sup>10</sup><https://www.lsst.org/scientists/simulations/opsim/opsim-v335-benchmark-surveys>

with statistical and self-calibrated systematic uncertainties after Y1 and Y10 is 44 and 211, respectively. As in the previous subsections, these include informative Stage III priors on the non- $(w_0, w_a)$  subset of the parameter space, which is particularly important due to the  $\Omega_m$  vs.  $w_a$  degeneracy for the supernova constraints and hence substantially increase the FoM. If we achieve **RH1** and **RH2**, then inclusion of calibratable systematic uncertainties will multiply these numbers by a factor of  $\sim 1/(1 + (f_{\text{sys}}^{\text{SN}})^2) \approx 0.67$  (see [Section 5.1](#) for details) in Y10. This which would still enable us to meet **G1**.

There are two classes of calibratable systematic uncertainty for SN as described in [Appendix D4](#) and shown in [Figure D6](#): flux measurement calibration and identification uncertainties. While in general one would include redshift error, we ignore this as we assume that each supernova has an identified host with spectroscopically determined redshift. We allocate 0.95 and 0.3 of the calibratable systematic error budget to these classes (with the constraint that their quadrature sum is 1 and that calibration takes up the largest fraction of the budget because many factors contribute to it).

We then distribute the systematic uncertainty associated with photometric calibration such that the largest fraction of the error budget is given to the source of systematic uncertainty that will most affect cosmology: the zero point uncertainty in each band. We allocate 0.69 of the total systematic uncertainty to zero point uncertainties, and a further 0.39 to the filter mean wavelength uncertainties. In order to account for the fact that the systematic zero point or mean wavelength uncertainties may differ in each band, we draw zero point offsets or mean wavelength offsets from a 4-dimensional normal distribution with a standard deviation set by the magnitude of the systematic uncertainty in either wavelength or zero point. There are only 4 bands because all cosmological constraining power comes from *griz* only<sup>11</sup>. The fact that we can use *griz*-only is beneficial because *u*- and *y*-band come with additional calibration challenges. The bias in the observable quantity  $\mu$ ,  $\Delta\mu$ , is computed from the vector sum of these per-band biases. We then Monte Carlo over this space to determine the covariance in  $(w_0, w_a)$  space due to the systematic uncertainties in zero point and mean wavelength. Given the quadratic relationship between the magnitude of the zero point/wavelength offset and the systematic covariance, one can use the ‘allowed’ systematic error fraction to set requirements on the zero point or mean wavelength uncertainty. In our case, we found that naively allowing equal contributions to the systematic uncertainty from all calibration uncertainties using this process resulted in unachievably tight requirements on the zero point and mean wavelength uncertainty, so we set minimum ‘floor’ values (see Y10 requirements below), and that is what determined the numbers 0.69 and 0.39 given earlier in this paragraph.

This leaves a remaining allowed systematic uncertainty of  $\sqrt{1 - 0.3^2 - 0.69^2 - 0.39^2}/\sqrt{5} = 0.24$  for each of the other five sources of calibration uncertainty. While two of these are currently unmodelled (nonlinearity and wavelength-dependent flux calibration), the constraint on the allowed uncertainty above can be translated to three of the remaining source of photometric calibration error as they affect the light curve quality: wavelength-dependent flux calibration; SN light curve modeling; and Milky Way extinction corrections. Finally, we emphasize that in addition to the error budgeting within the super-

---

<sup>11</sup>The initial forecasts were carried out with *ugrizy*, but comparison of results with *griz*-only calculations indicated that *u* and *y* provide negligible cosmological information and hence are neglected for the rest of this work.

nova systematic uncertainties, there is the factor of  $f_{\text{sys}}^{(\text{SN})} = 0.7$  described above in order to satisfy our high-level requirements. Hence we impose an additional scaling of 0.7 to all requirements in Y10. See [Appendix G](#) for a plot illustrating how these requirements were set, where the relevant numbers come from, and where the systematics trend lines cross the  $r = 0.34$  line for Y1 and  $r = 0.24 = 0.34 \times 0.7$  line for Y10 (with  $r$  defined as in [Equation 2](#)).

The first two requirements below, **SN1** and **SN2**, depend on observations of standard stars by LSST.

**Detailed requirement SN1 (Y10):** Systematic uncertainty in the *griz*-filter zero points shall not exceed 1 mmag in the Y10 DESC SN analysis. As the *griz* requirements represent an ambitious improvement versus the LSST SRD (5 mmag in *griz*), an alternative way to meet this requirement is to improve our analysis methods for all probes until the LSST SRD requirement is sufficient.

**Goal SN1 (Y1):** Systematic uncertainty in the *griz*-filter zero points should not exceed 5 mmag in the Y1 DESC SN analysis.

By “zero point uncertainty”, we mean the difference between the synthetic brightness prediction obtained by integrating the spectra of calibrated standard stars (e.g., HST ‘Calspec’ standards) through the LSST passbands, and the observed LSST magnitudes. Relative zero-point and astrometric corrections are computed for every visit. Sufficient data are kept to reconstruct the normalized system response function (see Eq. 5, LSST SRD) at every position in the focal plane at the time of each visit as required by Section 3.3.4 of the LSST SRD. **SN1** puts strong constraints on (1) the accuracy of the primary flux reference, and (2) the metrology chain, i.e., the chain of flux measurements that links the objects on one image to observations of the primary flux reference.

Table 16 of the LSST SRD gives design specifications of 5 mmag for filter zero points except for *u*-band. Improvement beyond that level in *griz* in later years is primarily a question of resources rather than intrinsic hardware limitations (unlike for *y*-band, which we have not used for SN). Doing so will require the DESC to further constrain the residuals through some other method, such as linking the calibration of the sources to GAIA observations. We expect that using the GAIA Bp/Rp catalog as an external anchor, the uniformity of the LSST measurements may be controlled at the per-mil level. Crucially, the zero point calibration should be valid over a broad color range (e.g.,  $0.5 < g - i < 3$ ). Note that the *griz* design specifications are comparable to our Y1 *griz* goal.

Given the repeat observations required to build up a light curve over time, and the need to have a calibrated dataset across the sky, the LSST SRD requirements in Table 14 (specifications for photometric repeatability) and Table 15 (specifications for spatial uniformity of filter zero points) have impact on the DESC SN science case. These are given as 5, 15 mmag for PA1 and PA2 for the repeatability, and 5, 10 mmag for PA3 and PA4 respectively for spatial uniformity. Our ability to calibrate the LSST photometric system for the supernovae depends on the number of standard stars used for calibration, as any systematic uncertainty related to spatial uniformity reduces as  $\sqrt{N_{\text{standards}}}$ . Observing multiple standard stars over the field of view is therefore central to achieving our calibration goals while staying within LSST SRD requirements.



Regarding photometric repeatability, we expect that our strategies to deal with zero point fluctuations will be beneficial in improving repeatability. Our simulations did not include spatial variation in zero point fluctuations and hence we cannot comment on the quantitative benefit of the LSST SRD requirements on spatial uniformity in this version of the DESC SRD.

**Detailed requirement SN2 (Y10): Systematic uncertainty in the *griz*-filter mean wavelength shall not exceed 1 Å in the Y10 DESC SN analysis.**

**Goal SN2 (Y1): Systematic uncertainty in the *griz*-filter mean wavelength should not exceed 6 Å in the Y1 DESC SN analysis.**

The very large size of the LSST SNIa sample sets very strong requirements on the calibration systematics, including these filter mean wavelength uncertainties. The wavelength uncertainty of 1 Å for Y10 is a strict requirement, but this currently assumes that the errors are not mitigated through light curve modelling. Characterizing filter mean wavelengths at the level of 1–2 Å is well within reach of current metrology techniques. In future simulation-based investigations, it will be valuable to explore the joint marginalization over this systematic uncertainty along with others, rather than considering it completely independently as we have done now.

Unlike SN1, SN2 has no direct analog in the LSST SRD.

**Detailed requirement SN3 (Y10): Systematic uncertainty in the wavelength-dependent flux calibration shall not exceed a slope of 4.4 mmag per 5500 Å in wavelength in the Y10 DESC SN analysis.**

**Goal SN3 (Y1): Systematic uncertainty in the wavelength-dependent flux calibration should not exceed a slope of 5 mmag per 5500 Å in wavelength in the Y1 DESC SN analysis.**

This source of systematic uncertainty relates to our knowledge of the wavelength-dependent flux calibration of the external photometric system to which we tie LSST’s calibration (e.g., the HST photometric system). This calibration extends over the entire wavelength range considered. In this analysis we restrict ourselves to considering only the *griz* bands, hence we require this slope on the external calibration over  $\simeq 5500$  Å.

The LSST SRD has an overall 10 mmag calibration requirement. The supernova dark energy science case is not sensitive to an overall calibration offset, as this is degenerate with the intrinsic magnitude of the supernova population (or alternatively the Hubble constant). However, the calibration of the LSST photometric system to the standards (e.g., the HST standards Bohlin 2014) cannot vary in a wavelength-dependent way by more than 2.2 mmag per 7000 Å for the Y10 survey. This requirement is linked to SN1 in that the zero point calibration allows the LSST SNe to map onto the low- $z$  sample, while SN3 relates to our ability to relate the LSST supernovae (and the low- $z$  sample itself) to the standard stars (see e.g. Scolnic et al. 2015). However, unlike SN1, SN3 has no direct analog in the LSST SRD.

Our ability to meet this requirement depends on how well the standard stars are modeled. The extent to which the wavelength-dependent flux calibration is required also depends on how low-redshift samples are included in any analysis. In this simulation, an independent low- $z$  sample was included, and the

SALT model uncertainty and HST calibration uncertainty were varied for this low- $z$  sample. Care will have to be taken to ensure calibration between high-quality low- $z$  surveys and the LSST sample. This is an active area of research, and future studies will investigate the optimal combinations of current and future low-redshift data to anchor the LSST Hubble diagram.

**Detailed requirement SN4 (Y10): Systematic uncertainty in the light curve modeling shall not exceed 3% of current SALT2 model errors in the Y10 DESC SN analysis.**

**Goal SN4 (Y1): Systematic uncertainty in the light curve modeling should not exceed 22% of current SALT2 model errors in the Y1 DESC SN analysis.**

This requirement is on our uncertainty in the SALT2 light curve model due to calibration uncertainties in and statistical limitations of the training sample. Improving the error on the SALT2 model will be critical especially for the Y10 LSST SN analysis; there is a clear path to dealing with this systematic uncertainty by using some of the LSST sample to retrain the SALT2 models. The training sample we will obtain from LSST observations is expected to be 10 to 50 times larger than the current SALT2 training sample. This will permit us to significantly decrease the statistical uncertainty affecting the light curve model. Furthermore, this will allow us to capture more of the SN variability than currently captured by SALT2. Finally, the calibration requirements in **SN1–SN3** will be important in enabling an improved calibration of the SALT2 model.

**Detailed requirement SN5 (Y10): Systematic uncertainty in Milky Way extinction corrections shall not exceed 30% of current systematic Galactic extinction uncertainties in the Y10 DESC SN analysis.**

**Goal SN5 (Y1): Systematic uncertainty in Milky Way extinction corrections should not exceed 100% of current systematic Galactic extinction uncertainties in the Y1 DESC SN analysis.**

The reason why this source of systematic uncertainty is so important is that the WFD and DDF locations have different extinction and their supernovae have different redshift distributions. For context, the Milky Way extinction model is generally determined using data and methods external to LSST, and the current uncertainty in the normalization of the global Milky Way extinction is  $\pm 5\%$  (Schlafly et al. 2014). The Y1 sample does not require any improvement on the current Milky Way extinction model. However, the Y10 sample will require the model of systematic uncertainty related to Galactic extinction to be 30% of its current value, Schlafly et al. (2014) from Table D8.

Work that will enable the above requirements to be met occurs in several different contexts. The first two requirements in this subsection, **SN1** (zero points) and **SN2** (filter mean wavelengths), relate to aspects of photometric calibration that are driven by Rubin Observatory. These detailed requirements are more stringent than their counterparts in the LSST SRD; as indicated at the start of this subsection, by providing additional DESC resources and expertise, and working closely with the LSST Facility, we aspire to achieve, together, a more precise photometric calibration than the Facility is *required* to produce on its own. Moreover, the DESC is actively pursuing research methods that might result in eventual loosening of the detailed requirements on photometric calibration. Some of these are methods that directly relate to photometric calibration; e.g., methods of marginalizing over astrophysical



systematics that may be able to reliably absorb certain photometric calibration uncertainties. This is particularly the case for requirements [SN3](#), [SN4](#), and [SN5](#); [SN3](#) partly depends on the photometric calibration provided by Rubin Observatory and partly on what external datasets that DESC chooses to include in its analysis, while [SN4](#) and [SN5](#) are most likely to be met (or loosened) by further development of modeling methods on the DESC side. However, even [SN2](#), which is ostensibly dependent on photometric calibration provided by Rubin Observatory, has the potential to be loosened in the future given that filter mean wavelength uncertainties may be absorbed in the light curve model retraining that will be performed for the LSST supernova sample, and may additionally be absorbed by our techniques for marginalizing over astrophysical systematic uncertainties. Progress on this high-priority work will be reflected in future versions of the DESC SRD. However, we reiterate that the high-level requirement of being a Stage IV dark energy survey ties together all of the probes, such that even methodological improvements in e.g. weak lensing that result in increased constraining power could enable a relaxation of the photometric calibration requirements for SN.

Finally, as a consistency check, we note that an independently conducted study carried out within the DESC Photometric Corrections working group<sup>12</sup> with somewhat different methodology, including the retraining of the SALT2 models, came to similar conclusions as [SN1](#) and [SN2](#).

## 5.5 Strong lensing

This section describes the strong lensing analysis, which yields information about the expansion rate of the Universe.

As described in [Appendix D5](#) in more detail, the baseline strong lensing analysis in this version of the DESC SRD includes time delay and compound lens systems, with sample sizes defined based on conservative assumptions about follow-up resources. The forecasts include marginalization over several self-calibrated systematic uncertainties; this marginalization is implicitly done, via increased uncertainties in the per-lens distance measurements, rather than explicitly via marginalization over models for those uncertainties. Following [G1](#), our target FoM for strong lensing after Y10 is 1.3; the forecast FoM with statistical and self-calibrated systematic uncertainties after Y1 and Y10 is 2.0 and 9.4, respectively. As in the previous subsections, these include informative Stage III priors on the non- $(w_0, w_a)$  subset of the parameter space. If we achieve [RH2](#), then inclusion of calibratable systematic uncertainties will multiply these numbers by a factor of  $\sim 0.72$  (see [Section 5.1](#) for details) in Y10, which still enables us to meet [G1](#).

In this version of the DESC SRD, we do not place requirements on calibratable systematic uncertainties for strong lensing, because developing models for how those systematic uncertainties affect the observable quantities is work that will begin during DC2.

---

<sup>12</sup>F. Hazenberg, M. Betoule, S. Bongard, L. Le Guillou, N. Regnault, P. Gris, *et al.*, 2018, “Impact of the calibration on the performances of the LSST SN survey”, DESC internal note

## 5.6 Combined probes and other requirements

Now that we have described the detailed requirements and the baseline forecasts for individual probes, we revisit our requirement on the joint probe constraining power of LSST. First, we describe how the joint forecast was carried out. In principle, we would like to undertake a full joint forecast with software that is capable of describing the likelihood analyses for all five probes, and combine all probes at the level of likelihoods. However, at present three different software tools are used to produce the forecasts (see [Appendix B](#)). Currently our method for combining them is through Fisher matrix approximations of their posterior probability distributions for cosmological parameters (ignoring any non-Gaussian distributions). Future DESC SRD versions should work at the likelihood level as additional DESC software products become available. Following [RH1](#), our target FoM for all probes including Stage III priors and factoring in all sources of systematic uncertainty is 500. The forecast joint FoMs with statistical and self-calibrated systematic uncertainties after Y1 and Y10 are 156 and 711, respectively, after including Stage III priors. See [Appendix G](#) for a plot illustrating the joint constraining power in the  $(w_0, w_a)$  plane. The error budgeting process described in the preamble of [Section 5](#), aimed at jointly satisfying [RH1](#) and [RH2](#), ensures that calibratable systematic uncertainties will lower the Y10 number to something very close to 500 (actually 505 in practice).

In addition, here we include requirements that are not probe-specific. These relate to our high-level blinding requirement [RH4](#).

**Detailed joint probes requirement J1 (Y1): Blinding methods will involve failsafes to avoid accidental unblinding (e.g., redundancy of blinding both summary statistics and cosmological parameter plots, use of public key encryption).**

**Detailed joint probes requirement J2 (Y3): DESC dark energy analyses will employ blind analysis techniques that self-consistently work for individual and joint probe analyses.**

Requirements [J1](#) and [J2](#) apply not only to the analyses listed explicitly (Y1 and Y3, respectively) but to all later analyses.

## 6 Conclusion and outlook

The baseline analysis for all five probes defined in this document represents the first DESC-wide forecasting exercise, including adoption of common analysis methodology and key sources of systematic uncertainty across all probes. In this section we briefly summarize the key findings from this exercise.

First, the estimated DETF FoM values for each of our baseline analyses and for all probes together, based on current forecasts, are summarized in [Table 6.1](#).

Second, as noted in [Section 1](#), the overarching purpose of the exercise carried out here is to place requirements on the DESC’s analysis pipelines to enable an analysis of LSST data corresponding to a stand-alone Stage IV dark energy experiment. Here we briefly discuss the connection between the requirements placed in this version of the DESC SRD and the relevant analysis pipelines:

Analysis	Priors	Y1 FoM (ceiling)	Y10 FoM (ceiling)	Target
LSS	Stage III (not $w_0, w_a$ )	10 (13)	10 (14)	1.5
LSS	None	6.7 (8.4)	6.6 (9.1)	1.5
WL+LSS	Stage III (not $w_0, w_a$ )	31 (37)	66 (87)	40
WL+LSS	None	22 (27)	49 (68)	40
CL	Stage III (not $w_0, w_a$ )	9 (11)	17 (22)	12
CL	None	6.5 (8.2)	12 (17)	12
SN	Stage III (not $w_0, w_a$ )	36 (44)	157 (211)	19
SN	None	10 (12)	32 (48)	19
SL	Stage III (not $w_0, w_a$ )	1.6 (2.0)	6.9 (9.4)	1.3
SL	None	1.3 (1.7)	4.4 (6.1)	1.3
All	Stage III	142 (156)	505 (711)	500
All	None	108 (135)	461 (666)	-

Table 6.1: Summary of forecast DETF FoMs after Y1 and Y10 for each probe and their combination, synthesizing target and forecast numbers from across Section 5. The FoM values correspond to our calculated baselines from current forecasts including all sources of uncertainty, while “ceiling” values in parenthesis indicate those without any contribution from calibratable systematic uncertainties, which in practice should not be reachable with current analysis methodology. The “Target” column corresponds to the Y10 targets defined by RH1 and G1, to be compared with the first number in the previous column. For individual probes, our goal (G1) is that the Y10 forecast FoM should meet or exceed the target value, while for combined probes, it is a requirement (RH1). Note that since our methodology is to make a forecast with reasonable assumptions of what is achievable in all probes (including statistical and astrophysical systematic uncertainties), and then degrade that forecast by tuning the size of the calibratable systematic error budget to meet RH1, in general the Y10 forecast and target will match precisely as described in Section 5.6 and the introduction to Section 5. This is a feature of our flowdown from our high-level science requirements rather than a feature of the baseline analysis for each probe that goes into the forecasts. Note that only the individual-probe FoM values without priors should be compared with the individual probe contours in Figure G2. Finally, the individual probe results include Stage III priors on non-dark energy parameters (to stabilize the Fisher matrix calculations), while the “All” results include full Stage III priors because they are included in the definition of overall constraining power in RH1. The Stage III priors on their own give a FoM of 23.

- We placed requirements on our knowledge of mean redshifts and redshift bin widths for tomographic LSS, WL, and CL analyses. These essentially amount to requirements on the performance of the `PZCalibrate` pipeline that is being developed by the PZ working group during the DC2 era. The purpose of that pipeline is to use cross-correlation analysis and spectroscopic training data to provide calibrated  $N(z)$  (not just mean and width, but full  $N(z)$  including the impact of photometric redshift outliers) for tomographic samples defined using photometric redshifts. The requirements for WL and CL analyses, such as **WL1**, represent a substantial improvement beyond the current state of the art. Current analyses are limited by the availability of spectroscopic surveys within the footprint of the imaging survey, so the 4000 deg<sup>2</sup> overlap with DESI and the more dilute samples expected from 4MOST in the rest of the area will provide some of the improvement in control of redshift uncertainties for LSST. The rest of the improvement will rely on algorithmic improvements, and rigorous development and testing of `PZCalibrate`. Additional spectroscopic redshifts for training and calibration, particularly at the faint end (near and beyond the limit of the C3R2 survey; [Masters et al. 2017](#)) would provide additional margin on this source of systematic uncertainty. However, this approach has several serious challenges: (a) the necessary amount of telescope time on 8m-class telescopes ([Newman et al. 2015](#)) is very large, (b) spectroscopic incompleteness is still an issue and difficult to assess at the necessary tolerances, and (c) direct calibration is very sensitive to small numbers of incorrect redshifts.
- We placed requirements on our knowledge of the redshift-dependent ensemble shear calibration (**WL3**). This corresponds to a requirement on `shearMeasurementPipe`, the pipeline being developed by the WL working group in order to quantify the calibration of the LSST Science Pipelines shear estimator for the selected tomographic shear samples at the required level of accuracy. As mentioned in the text associated with **WL3**, state-of-the-art shear estimation methods can already achieve uncertainty on shear calibration that is comparable to this requirement, but *without* accounting for all effects that are included in this requirement (e.g., blending). The implications for weak lensing pipeline development are that it is important to integrate at least one of these state-of-the-art shear estimation methods into the pipeline in the near term to enable work that must be done on less well-understood effects such as blending.
- We also placed requirements on our knowledge of specific contributors to shear calibration bias, such as PSF model size errors and stellar contamination. These will be quantified with the WL null testing pipeline, `WLNullTest`.
- The requirements on photometric calibration for the SN science case correspond to requirements on (a) the software provided by the Photometric Corrections working group to quantify aspects of photometric calibration that go beyond what is provided by Rubin Observatory (for **SN1** and **SN2**), (b) the SN working group light curve modeling software (**SN4**), and (c) the SN working group likelihood analysis software, since our stringent requirements suggest it will be important to investigate avenues for jointly (and efficiently) marginalizing over observational and astrophysical systematic uncertainties, converting some of our calibratable systematic uncertainties to

self-calibrated ones through development of appropriate models (for [SN3](#) and [SN5](#)). In some cases, meeting the detailed requirements on photometric calibration may require investment of DESC resources on work with the Facility to achieve more accurate photometric calibration than the design specifications in the LSST SRD.

Finally, the baseline analyses defined in this version of the DESC SRD do not necessarily correspond to each working groups' aspirations; limitations were imposed both by the capabilities in existing software and the fact that further R&D is needed into several key questions about the analysis process. Here we briefly summarize anticipated updates in future DESC SRD versions (with further details available in [Appendix B](#), [C](#), and [D](#)). Such updates will inevitably lead to improved forecasts and hence revised values in [Table 6.1](#):

- The LSS analysis may be defined with different samples (e.g., including multitracer analysis), a longer redshift baseline, inclusion of cross-power spectra between redshift bins, modified  $\ell$  binning to better resolve the BAO feature, and other updates to make it more optimal. In addition, marginalization over nonlinear (rather than just linear) bias must be included, which will also enable the  $k_{\text{max}}$  value to be shifted to smaller scales, potentially providing more cosmological information.
- The WL+LSS analysis may be defined with a different sample than the LSS-alone analysis for lenses, and may benefit from the LSS improvements described above. The powerfully constraining  $3\times 2$ -point analysis is particularly sensitive to what scales can be used; improvements in theoretical modeling of nonlinear bias has the potential to produce substantial gains.
- The galaxy clusters baseline analysis will be updated to include further realistically-achievable priors on the MOR, and to include large-scale cluster clustering and cluster lensing, which can improve the self-calibration of the MOR.
- For all probes of structure growth, more optimal choices of tomographic binning schemes will be explored. Aside from possible gains in statistical constraining power, different choices may enable more optimal self-calibration of redshift-dependent effects, and/or changes in the requirements in control of redshift-related systematic biases.
- The SN analysis will include the impact of photometric redshift uncertainties for the photometric SN sample, probabilistic SN inference, and SN type misclassification.
- The SL analysis should include lensed supernovae.
- We will place requirements on model sufficiency for self-calibrated systematic uncertainties.
- The cosmological parameter space should be widened to include massive neutrinos.

- In this DESC SRD version we only placed requirements on a subset of calibratable systematic uncertainties, occasionally due to limitations in existing software but in other cases due to insufficient knowledge in the field as to how to parametrize the effects of interest in terms of how they affect our observable quantities. The DESC’s DC2 and other non-simulation-based work happening during the DC2 era should deepen our understanding of how to describe these sources of systematic uncertainty, resulting in both requirements and more capable analysis software. Notable areas in which substantial development of systematics models is needed include the impact of photometric redshift errors on photometric SN analysis; more flexible photometric redshift uncertainties for structure growth probes; the impact of residual blending systematics on number densities, redshifts, and shear; the impact of survey inhomogeneity on the galaxy density field; a description of how many types of observational systematics impact the strong lensing observables.
- The interaction between models for different types of systematic uncertainties, and their potential for very different behavior in the 7-dimensional cosmological parameter space, will be more thoroughly considered. In addition, we will take care to adopt common models of specific sources of systematic uncertainty across probes wherever possible.
- Future versions of this document will use DESC software for describing cosmological observables and their covariances, so as to enable collaboration-wide development of forecasts and requirements within a common software framework that meets DESC coding guidelines. It will also incorporate lessons learned about the dependence of the forecasts on observing strategy produced by the DESC’s Observing Strategy Task Force during the second half of 2018, along with any subsequent updates in the LSST baseline survey definition (see baseline used for the DESC SRD in [Appendix C1](#)).
- More concrete statements should be made about blinding as our understanding of blinding techniques develops.
- Requirements should be placed on the accuracy of modeling of cosmological quantities such as power spectra, mass functions, etc.

Some of the above improvements will be the subject of R&D in the coming years, the results of which will be incorporated into our baseline analyses as our understanding evolves. Further details of planned updates are given in the aforementioned appendices. All changes will be subject to the change control process outlined at the end of [Section 1](#).

## Acknowledgments

The DESC acknowledges ongoing support from the Institut National de Physique Nucléaire et de Physique des Particules in France; the Science & Technology Facilities Council in the United Kingdom; and the Department of Energy, the National Science Foundation, and the LSST Corporation in the United States. DESC uses resources of the IN2P3 Computing Center (CC-IN2P3–Lyon/Villeurbanne - France) funded by the Centre National de la Recherche Scientifique; the National Energy Research Scientific Computing Center, a DOE Office of Science User Facility supported by the Office of Science of the U.S. Department of Energy under Contract No. DE-AC02-05CH11231; STFC DiRAC HPC Facilities, funded by UK BIS National E-infrastructure capital grants; and the UK particle physics grid, supported by the GridPP Collaboration. This work was performed in part under DOE Contract DE-AC02-76SF00515.

We are grateful for the support of the University of Chicago Research Computing Center for assistance with the calculations carried out in this work, and also acknowledge the use of the Glamdring cluster in the Department of Physics at the University of Oxford. Part of the research was carried out at the Jet Propulsion Laboratory, California Institute of Technology, under a contract with the National Aeronautics and Space Administration and is supported by NASA ROSES ATP 16-ATP16-0084 grant. We thank Chris Hirata for providing input on various approaches to placing requirements.

**References**

- Abramo, L. R. & Leonard, K. E. 2013, MNRAS, 432, 318
- Aihara, H., Armstrong, R., Bickerton, S., et al. 2018, PASJ, 70, S8
- Albrecht, A., Bernstein, G., Cahn, R., et al. 2006, astro-ph:0609591
- Betoule, M., Kessler, R., Guy, J., et al. 2014, A&A, 568, A22
- Bhattacharya, S., Habib, S., Heitmann, K., & Vikhlinin, A. 2013, ApJ, 766, 32
- Biswas, R., Cinabro, D., & Kessler, R. 2017, simlib\_minion
- Blazek, J., Vlah, Z., & Seljak, U. 2015, JCAP, 8, 015
- Bohlin, R. C. 2014, ArXiv e-prints
- Campbell, H., D’Andrea, C. B., Nichol, R. C., et al. 2013, ApJ, 763, 88
- Chang, C., Jarvis, M., Jain, B., et al. 2013, MNRAS, 434, 2121
- Chotard, N., Gangler, E., Aldering, G., et al. 2011, A&A, 529, L4
- Collett, T. E. 2015, ApJ, 811, 20
- Croft, R. A. C. & Dailey, M. 2011, arXiv:1112.3108
- Davis, C., Gatti, M., Vielzeuf, P., et al. 2017, arXiv:1710.02517
- DES Collaboration. 2017, arXiv:1708.01530
- Eisenstein, D. J. & Hu, W. 1999, ApJ, 511, 5
- Foley, R. J., Scolnic, D., Rest, A., et al. 2018, MNRAS, 475, 193
- Font-Ribera, A., McDonald, P., Mostek, N., et al. 2014, JCAP, 5, 023
- Goliath, M., Amanullah, R., Astier, P., Goobar, A., & Pain, R. 2001, A&A, 380, 6
- Guy, J., Astier, P., Baumont, S., et al. 2007, A&A, 466, 11
- Guy, J., Sullivan, M., Conley, A., et al. 2010, A&A, 523, A7
- Harnois-Déraps, J., van Waerbeke, L., Viola, M., & Heymans, C. 2015, MNRAS, 450, 1212
- He, S., Wang, L., & Huang, J. Z. 2018, arXiv:1802.06125
- Hildebrandt, H., Viola, M., Heymans, C., et al. 2017, MNRAS, 465, 1454



- Hinton, S. R. 2016, *The Journal of Open Source Software*, 1, 00045
- Hirata, C. M., Mandelbaum, R., Seljak, U., et al. 2004, *MNRAS*, 353, 529
- Hlozek, R., Kunz, M., Bassett, B., et al. 2012, *ApJ*, 752, 79
- Hounsell, R., Scolnic, D., Foley, R. J., et al. 2017, [arXiv:1702.01747](https://arxiv.org/abs/1702.01747)
- Howlett, C., Lewis, A., Hall, A., & Challinor, A. 2012, *Journal of Cosmology and Astro-Particle Physics*, 2012, 027
- Huterer, D. & Peiris, H. V. 2007, *Phys. Rev. D*, 75, 083503
- Ivezic, Z., Tyson, J. A., Abel, B., et al. 2008, [arXiv:0805.2366](https://arxiv.org/abs/0805.2366)
- Jarvis, M., Sheldon, E., Zuntz, J., et al. 2016, *MNRAS*, 460, 2245
- Joachimi, B. & Bridle, S. L. 2010, *A&A*, 523, A1
- Jones, D. O., Scolnic, D. M., Riess, A. G., et al. 2017, *ApJ*, 843, 6
- Kessler, R., Bernstein, J. P., Cinabro, D., et al. 2009, *PASP*, 121, 1028
- Kim, A. G., Aldering, G., Antilogus, P., et al. 2014, *ApJ*, 784, 51
- Kim, A. G., Thomas, R. C., Aldering, G., et al. 2013, *ApJ*, 766, 84
- Krause, E. & Eifler, T. 2017, *MNRAS*, 470, 2100
- Krause, E., Eifler, T., & Blazek, J. 2016, *MNRAS*, 456, 207
- Laigle, C., Pichon, C., Arnouts, S., et al. 2018, *MNRAS*, 474, 5437
- Lewis, A., Challinor, A., & Lasenby, A. 2000, *ApJ*, 538, 473
- Lima, M. & Hu, W. 2004, *Phys. Rev. D*, 70, 043504
- LSST Science Collaboration. 2009, [arXiv:0912.0201](https://arxiv.org/abs/0912.0201)
- Ma, Z., Hu, W., & Huterer, D. 2006, *ApJ*, 636, 21
- Macaulay, E., Davis, T. M., Scovacricchi, D., et al. 2017, *MNRAS*, 467, 259
- Mandelbaum, R., Miyatake, H., Hamana, T., et al. 2018, *PASJ*, 70, S25
- Marriner, J., Bernstein, J. P., Kessler, R., et al. 2011, *ApJ*, 740, 72
- Massey, R., Hoekstra, H., Kitching, T., et al. 2013, *MNRAS*, 429, 661
- Masters, D. C., Stern, D. K., Cohen, J. G., et al. 2017, *ApJ*, 841, 111

- Murata, R., Nishimichi, T., Takada, M., et al. 2018, ApJ, 854, 120
- Najita, J., Willman, B., Finkbeiner, D. P., et al. 2016, ArXiv e-prints
- Newman, J. A., Abate, A., Abdalla, F. B., et al. 2015, Astroparticle Physics, 63, 81
- Oguri, M. & Marshall, P. J. 2010, MNRAS, 405, 2579
- Planck Collaboration, Ade, P. A. R., Aghanim, N., et al. 2016, A&A, 594, A13
- Roberts, E., Lochner, M., Fonseca, J., et al. 2017, JCAP, 10, 036
- Sako, M., Bassett, B., Connolly, B., et al. 2011, ApJ, 738, 162
- Schlafly, E. F., Green, G., Finkbeiner, D. P., et al. 2014, ApJ, 789, 15
- Scolnic, D., Casertano, S., Riess, A., et al. 2015, ApJ, 815, 117
- Scolnic, D., Rest, A., Riess, A., et al. 2014, ApJ, 795, 45
- Scolnic, D. M., Jones, D. O., Rest, A., et al. 2018, ApJ, 859, 101
- Seljak, U. 2009, Physical Review Letters, 102, 021302
- Takahashi, R., Sato, M., Nishimichi, T., Taruya, A., & Oguri, M. 2012, ApJ, 761, 152
- Tinker, J. L., Robertson, B. E., Kravtsov, A. V., et al. 2010, ApJ, 724, 878
- Treu, T. & Marshall, P. J. 2016, AAPR, 24, 11
- Wolz, L., Kilbinger, M., Weller, J., & Giannantonio, T. 2012, JCAP, 9, 009
- Zhang, P. 2015, ApJ, 806, 45
- Zuntz, J., Paterno, M., Jennings, E., et al. 2015, Astronomy and Computing, 12, 45
- Zuntz, J., Sheldon, E., Samuroff, S., et al. 2017, arXiv:1708.01533

## Appendices

### A Connections to Rubin Observatory tools and documents

In this Appendix, we briefly summarize how this document depends on Rubin Observatory tools and requirements.

First, our assumptions about the cadence (affecting the time-domain science cases), the coadded depth as a function of time in each band, and the area reaching some criteria for homogeneous coverage as outlined in [Appendix C1](#) are entirely based on Rubin Observatory tools, specifically the operations simulator (OpSim<sup>13</sup>) `minion_1016` run. The LSST observing strategy has not been finalized, and hence these assumptions may need to be revisited. The DESC is working to quantify the impact of LSST observing strategy on the dark energy science cases so as to communicate with Rubin Observatory on this important topic through the mechanism of contributing to the community white paper on the LSST Observing Strategy<sup>14</sup>.

We also rely on the LSST catalog simulator (CatSim<sup>15</sup>) to estimate the weak lensing source number density and redshift distribution ([Appendix F](#)) using simulated LSST images that have parameters based on Rubin Observatory Project inputs such as filter throughputs, and anticipated survey image characteristics such as typical PSF FWHM, sky brightness, and so on from Table 2 of [Ivezic et al. \(2008\)](#).

Finally, there are many relevant requirements in Rubin Observatory’s LSST SRD<sup>16</sup>. Below we briefly comment on the LSST SRD requirements and their relevance to enabling our science cases. All appendices, tables, and equations listed below without links are in the LSST SRD, while those with direct links are in this document.

- Basic aspects of the instrument in Appendix A, Table 1 (filter complement), Table 11 (pixel size specification), Table 22 (area coverage), Table 23 (median number of visits per filter), Table 24 (coadded depth), Table 25 (distribution of visits over time) were implicitly encoded in our forecasts through our reliance on OpSim to define depths and cadence.
- Tables 5 (single image depth) and 6 (variation of single image depth with bandpass) are primarily relevant in enabling transient science. Our assumptions about the number of supernovae with a given light curve quality described in [Appendix D4](#) depend heavily on this specification; the excellent single-image depth is an important enabler of our dark energy constraints from supernovae, including both the statistical and systematic uncertainties (e.g., associated with light curve modeling).
- There are several requirements associated with image quality, along with assumptions that are not framed as requirements. First, regarding assumptions, Appendix D of the LSST SRD shows the

---

<sup>13</sup><https://github.com/lsttsims/operations>

<sup>14</sup><https://github.com/LSSTScienceCollaborations/ObservingStrategy>

<sup>15</sup><https://www.lsst.org/scientists/simulations/catsim>

<sup>16</sup><https://docushare.lsstcorp.org/docushare/dsweb/Services/LPM-17>

distribution of atmospheric seeing at the site. The LSST SRD then places requirements on image quality through Table 9, which is effectively a requirement that the total PSF size for a given atmospheric seeing should have no more than 15% contribution due to the LSST system. Our weak lensing cosmology constraints are enabled by the excellent image quality that is implied by the expected atmospheric seeing and the requirement on the overall PSF size in Table 9, given that the constraining power of weak lensing improves when the image quality is better. Image quality has a more difficult-to-quantify impact on all probes through its impact on blending systematics. At fixed depth, blending effects become worse as the PSF size increases, with impacts on galaxy photometry and shear estimation that are not yet well-quantified.

- At a lower level, we also are sensitive to Tables 12 and 13 in the LSST SRD, which cover the spatial profile of the PSF (not too much power in the wings) and the PSF ellipticity distribution, respectively. If the latter is imperfectly removed in software when estimating shear, it can generate additive systematics in the shear-shear correlation functions. However, state-of-the-art shear estimation methods are quite effective at removing the PSF anisotropy from weak lensing shear estimates, and there are null tests to effectively diagnose this issue, so these are lower level effects than the image quality assumptions in the bullet point above.
- Tables 14-17 in the LSST SRD cover various aspects of photometric calibration. The connection between these requirements and the DESC supernova science case is explored in detail in [Section 5.4](#). In this version of the DESC SRD, we have not quantified to what extent the Rubin Observatory requirements on photometric calibration are important for meeting our goals with respect to control of photometric redshift uncertainties.
- Section 3.3.5 covers requirements on the astrometry, which enters our dark energy observables in ways that we have not explicitly quantified in this version of the DESC SRD.
- Table 27 provides requirements on the PSF model ellipticity residuals (i.e., difference between PSF model ellipticity and the true PSF ellipticity). Significant PSF model ellipticity residuals would mean we are effectively removing the wrong PSF anisotropy from galaxy shear estimates, which generates additive biases in the weak lensing shear-shear correlation functions that must be quantified and removed through null tests. Hence, the requirements in Table 27 in the LSST SRD reduce the burden on the DESC in diagnosing such effects.

## B Software

### B1 Software packages

Here we briefly describe the software used for forecasting and setting requirements in this version of the DESC SRD.

For weak lensing, galaxy clustering, and galaxy cluster analysis, we use CosmoLike<sup>17</sup> ([Krause & Eifler](#)

<sup>17</sup><https://github.com/CosmoLike>, <http://www.cosmolike.info/>

2017). Use of the same software is important, as these three probes of large-scale structure are correlated with each other and hence must be treated self-consistently especially in joint probe forecasts. CosmoLike can model all cross-correlations among probes, with analytical non-Gaussian covariances, and a variety of self-calibrated and calibratable systematic uncertainties. Indeed, the choice of which systematic uncertainties to include (and in what form) in this version of the DESC SRD was largely driven by the existing capabilities of CosmoLike, though in a few highlighted cases in [Appendix D](#) our approach represents a departure from [Krause & Eifler \(2017\)](#). All CosmoLike forecasts in the DESC SRD are carried out through a Fisher forecasting approach. The limitations of this approach include the fact that it assumes a multivariate Gaussian likelihood and the fact that the results are numerically somewhat sensitive to the step size of the derivatives (resulting in potentially 5–10% variations in figures of merit). The assumption of a multivariate Gaussian likelihood is generally more problematic for geometric probes than it is for probes of structure growth ([Wolz et al. 2012](#)). Having many poorly-constrained directions in parameter space, even in dimensions that are being marginalized over, can be particularly problematic for convergence of the FoM calculated from the Fisher matrices. Our default priors on cosmological parameter space ([Appendix C2](#)) are relatively broad. To achieve more stable results, the individual probe calculations from CosmoLike used Stage III priors on the five cosmological parameters that are marginalized over, i.e., everything but  $w_0$  and  $w_a$ , as described in [Appendix C2](#).

As a comparison point with CosmoLike, we used GoFish<sup>18</sup>, a completely independent code base that can carry out Fisher forecasting. Our comparison between CosmoLike and GoFish<sup>19</sup> involved forecasting constraints in the  $(w_0, w_a)$  plane for the  $3 \times 2$ pt analysis without any systematic uncertainties, but very similar baseline data vectors. CosmoLike used non-Gaussian covariance matrices, took a conservative approach in not including LSS cross-bin correlations, and both codes used slightly different redshift bins and bandpowers. This comparison showed that the parameter constraints from CosmoLike were indeed weaker than those found with GoFish by roughly 30–40% for  $w_0$  and 10–20% for  $w_a$ . This can be expected given the differences in both baseline analysis and approaches to covariances. As a more quantitative validation of CosmoLike, both codes generated forecasts for exactly the same baseline data vector (the shear-shear power spectrum for the Y1 survey parameters) in the absence of systematics. To isolate the impact of the non-Gaussian covariance, GoFish was modified to take in the covariance estimated by CosmoLike as input. In this case, the values for the DETF FoM found by both codes were the same within 1%, well within the expected numerical fluctuations due to the instability associated to the numerical derivatives. This test case was also used to quantify the impact of the non-Gaussian terms in the covariance matrix. For this GoFish was re-run using the same data vector as well as its internally-computed Gaussian covariance. The effect of the non-Gaussian terms was found to be minimal ( $\sim 2$ –5% of the FoM, in agreement with expectations given the large sky fraction assumed for LSST).

For the shear-shear forecasts, an MCMC vs. Fisher matrix comparison was carried out using CosmoLike, including marginalization over self-calibrated systematic uncertainties. The results between the two methods were found to agree to within our aforementioned  $\sim 10\%$  tolerance.

<sup>18</sup><https://github.com/damonge/GoFish>

<sup>19</sup>See the end of <https://github.com/LSSTDESC/Requirements/issues/6> for details.

The software frameworks used for supernova and strong lensing forecasts are dedicated probe-specific frameworks that are described in Appendices D4 and D5, respectively.

The joint forecasts were carried out in CosmoLike, by combining Fisher matrices from the three different code bases described above. As noted in Section 5.6, this implies that we are treating the SL, SN, and the combination of WL+LSS+CL as carrying completely independent information, allowing us to combine Gaussian approximations to their posterior probability distributions rather than doing a full joint likelihood analysis. This should be an excellent assumption for the foreseeable future.

Future versions of the DESC SRD will use DESC software for describing cosmological observables and their covariances, TJPCosmo and TJPCov, so as to enable the forecasts to use the same models for systematic uncertainties and how they impact dark energy observables as DESC working groups are defining for their likelihood analysis of real LSST data. This will allow us to carry out cross-checks on the software more easily than can be done now, while also ensuring that all calculations use software that has undergone collaboration-wide review.

## B2 How requirements are set

In practice, the detailed requirements in Section 5 were placed by (a) generating contaminated data vectors with some systematic bias, (b) carrying out cosmological parameter constraints via Fisher forecasts while ignoring the fact that the initial data vectors had a systematic bias in some calibratable effect (while marginalizing over self-calibrated systematic uncertainties). This process was carried out until the best-fitting parameters in the  $(w_0, w_a)$  plane reached the edge of the  $1\sigma$  ellipse defined by the marginalized statistical uncertainties. The question of whether a particular systematic reached the edge is determined as follows: given a choice of baseline systematic parameter  $s_0$  (such as a bias in shear calibration); a 2D vector of biases in  $w_0$  and  $w_a$  determined by comparing the best-fitting and fiducial cosmological parameters, called  $\mathbf{b}$ ; and a covariance matrix for  $w_0$  and  $w_a$  after marginalization over nuisance parameters and the other cosmological parameters<sup>20</sup>,  $\mathbf{C}$ , the linear distance between the best-fitting point and the edge of the ellipse is

$$r = \sqrt{\mathbf{b} \cdot \mathbf{C}^{-1} \cdot \mathbf{b}}. \quad (2)$$

The  $1\sigma$  (systematic and statistical uncertainty are equivalent) requirement value is  $s_0/r$ . In other words, if our calculation results in  $r = 1$ , it means that our baseline systematic parameter  $s_0$  has gotten us precisely to the boundary of the error ellipse defined by the covariance matrix. If this is the only systematic bias under consideration, and if  $f_{\text{sys}}$  defined by Equation 1 is 1, then our requirement would be that the residual systematic bias must be less than or equal to  $s_0$ . Since individual sources of systematic uncertainty are not allowed to take up the entire error budget, this number is then further rescaled by whatever fraction of the error budget is to be allocated to this effect. In doing so, we use the quadrature

---

<sup>20</sup>To be more specific, given a covariance  $\mathbf{C}$  with rows for all cosmological parameters and nuisance parameters, we take the submatrix corresponding to the  $(w_0, w_a)$  dimensions. This is implicitly marginalized over all other dimensions. In contrast, taking the subset of the Fisher matrix ( $\mathbf{C}^{-1}$ ) would correspond to all other dimensions being fixed, resulting in overly small uncertainties and too-conservative requirements.

summation, i.e., if there are two sources of uncertainty that are to be given equal fractions of the error budget, we set the requirement such that  $r = 1/\sqrt{2}$  for each of them; this assumes independence of the systematic errors under consideration, such that variances of the systematic error distribution add<sup>21</sup>.

We implicitly assume a linear scaling of  $\mathbf{b}$  with the value of  $s_0$ , which was confirmed to be a good approximation for the sources of systematic uncertainty considered in the supernova analysis (Appendix G) for small values of systematic contamination, but is unlikely to be true when considering very large variations in  $s_0$ . For this reason, convergence tests were carried out for a few limited cases where  $r$  differed by orders of magnitude from 1, by modifying the value of  $s_0$  and re-estimating the  $\mathbf{b}$  and the requirement.

In the case that  $w_0$  and  $w_a$  confidence ellipses are aligned with the axes in that 2D space, Equation 2 reduces to

$$r = \sqrt{\left(\frac{b(w_0)}{\sigma(w_0)}\right)^2 + \left(\frac{b(w_a)}{\sigma(w_a)}\right)^2} \quad (3)$$

which intuitively makes sense: the biases for  $w_0$  and  $w_a$  are rescaled by their uncertainties, and we measure the hypotenuse of a right triangle in that rescaled space.

The choice to aim for  $r = 1$  in RH2 was motivated, as previously mentioned, by the intent to not allow offsets in the  $(w_0, w_a)$  plane in any direction to be outside the  $1\sigma$  error ellipse. One could interpret the quantity  $\mathbf{b} \cdot \mathbf{C}^{-1} \cdot \mathbf{b}$  as a  $\Delta\chi^2$  for the biased measurement; in our 2D parameter space, it may seem natural to set requirements at  $r^2 = 2.3$ , the  $\Delta\chi^2$  for  $1\sigma$  offsets in the case of a Gaussian likelihood. What would effectively happen in this case is that there could be some specific subsets of directions in our 2D space for which the systematic bias would go outside the  $1\sigma$  ellipse. Since we are likely to care about such offsets in the era of LSST, when there are other Stage-IV experiments that will further reduce the interesting area in this parameter space, we use the stricter cut at  $r = 1$ . Situations in which one might cut based on the  $\Delta\chi^2$  for a multivariate Gaussian with the dimensionality of the space in which  $\mathbf{b} \cdot \mathbf{C}^{-1} \cdot \mathbf{b}$  is calculated are generally those in which the tests for biases are being done in a high-dimensional space that has many dimensions that are not physically interesting, unlike here.

When estimating biases in cosmological parameter space due to use of a contaminated data vector as described above, with marginalization over models for self-calibrated systematic uncertainties, it is possible that the biases can be absorbed into the self-calibrated systematic model, if it is sufficiently flexible (as are some of our adopted models). This has the potential to result in very loose requirements on calibratable systematic uncertainties. In a realistic measurement, we would have done much more careful tests for interactions between models for various systematic uncertainties, and would be explicitly controlling for such effects rather than allowing for very large calibratable systematic uncertainties while counting on self-calibrated systematics models to absorb residual biases. Understanding the interactions between various types of systematic uncertainties, their parametrizations, and priors on nuisance parameters is an active area of research within DESC, and future DESC SRD versions will consider this

<sup>21</sup>It does not assume Gaussianity of these distributions, just that they can be considered independent, such that their error distributions are convolved. In that case, the variances add even if the distributions are non-Gaussian.

issue more carefully.

Finally, we note that [Equation 2](#) is agnostic of the space in which the analysis is carried out. That is, one could in principle carry it out using the observables ( $C_\ell$ , etc.) and their covariance, or in cosmological parameter space. As described above, we have opted to do this in cosmological parameter space. There are advantages and disadvantages to this choice. The main advantage is that if you have a systematic error that causes a large shift in the observables  $\hat{X}$  that looks very different from  $\partial\hat{X}/\partial w_0$  or  $\partial\hat{X}/\partial w_a$  (the response of the observables to a change in the dark energy equation of state), working in  $(w_0, w_a)$  space produces appropriately weaker requirements on that source of systematic uncertainty compared to those that actually do mimic the change in observables due to dark energy. This may in principle be the right thing to do, relying on the fact that systematic biases that look nothing like changes in dark energy models would be flagged and corrected due to what they do elsewhere in cosmological parameter space (e.g., produce results for other parameters that are inconsistent with Stage III priors, or yield a terrible overall  $\chi^2$ ). However, it does mean that our requirements are somewhat more sensitive than they might otherwise be to our parametrization and whether it results in changes in observables  $\Delta\hat{X}$  that mimic those induced by dark energy; see for example the relevant discussion on shear calibration bias in [Appendix D2.3](#).

Several of these issues with systematics parametrizations and priors have also been raised previously in e.g. [Massey et al. \(2013\)](#) and [Krause & Eifler \(2017\)](#).

### B3 Ensuring reproducibility

To ensure reproducibility of the calculations in this version of the DESC SRD, we take the following steps.

First, for calculations in [Appendix F](#), all analysis scripts are in the DESC’s Requirements repository<sup>22</sup>. The relevant version of each script is associated with the tag of the repository for that document version.

For CosmoLike calculations, there are two private repositories that are relevant. The first is the ‘cosmo-like\_core’ repository, which has the bulk of the CosmoLike infrastructure. The second (DESC\_SRD<sup>23</sup>) is a dedicated repository containing scripts, configuration files, and other analysis routines specific to this document. Both repositories have a v1 tag containing scripts used to produce v1 of this document; moreover, plotting routines and associated data products are made available in the tarball released with v1 of this document on Zenodo.

For strong lensing forecasts, the associated scripts are stored in the ‘forecasting/SL’ directory in the Requirements repository and in the tarball released with v1 of the document. Instructions on how to rerun the forecasts are given in the file README.md in that directory. Similarly, the software for supernova forecasts and requirements can be found in the ‘forecasting/SN’ directory of the repository and tarball.

<sup>22</sup><https://github.com/LSSTDESC/Requirements>

<sup>23</sup>[https://github.com/CosmoLike/DESC\\_SRD](https://github.com/CosmoLike/DESC_SRD)



## C Assumptions

### C1 The LSST observing strategy

We use the OpSim<sup>24</sup> v3 minion\_1016 run<sup>25</sup> to define the Y1 and Y10 survey depths and area, and to simulate the sample of supernovae and estimate the number with well-sampled light curves. Our Y1 definition involves taking the first 10% of the WFD observations<sup>26</sup>, which gives median (across the survey)  $5\sigma$  point-source detection depths of 24.07, 25.60, 25.81, 25.13, 24.13, 23.39 in *ugrizy* after 1 year, and 25.30, 26.84, 27.04, 26.35, 25.22, 24.47 after 10 years. These median depths were determined after discarding areas that have a depth shallower than  $i < 24.5$  and 26 for Y1 and Y10, respectively. (These were chosen to be 0.4 and 0.7 magnitudes deeper than the LSS galaxy samples for Y1 and Y10.) The resulting areas after this homogenization process are 12.3k deg<sup>2</sup> (Y1) and 14.3k deg<sup>2</sup> (Y10). Note that the depth cut removes areas of high extinction near the Galactic plane, because the depths used for the above cuts are after accounting for dust extinction. We have explicitly confirmed that regions near a Galactic latitude of zero and those with  $E(B - V) \gtrsim 0.2$  are eliminated by our depth cut (more specifically, 3.8% and 0.7% of the area exceeds  $E(B - V) = 0.2$  in Y1 and Y10, or 0.7% and 0% for  $E(B - V) = 0.3$ ).

### C2 The cosmological parameter space

For forecasting, we assume a  $w_0w_a$ CDM cosmology.

Our forecasts for the static probes use the Fisher matrix formalism, with weak priors necessary to regularize the Fisher matrix when individual probes exhibit significantly non-Gaussian likelihoods. Following Krause & Eifler (2017) Table 1, we fit for the following seven parameters, with fiducial parameter values and  $\sigma$  of the Gaussian prior listed in parenthesis:  $\Omega_m$  (0.3156; 0.2);  $\sigma_8$  (0.831; 0.14);  $n_s$  (0.9645; 0.08);  $w_0$  (-1.0; 0.8);  $w_a$  (0.0; 2.0);  $\Omega_b$  (0.0492; 0.006);  $h$  (0.6727; 0.063).

The supernova forecasts begin with MCMC, and involve only the four of the aforementioned cosmological parameters to which supernova measurements are sensitive:  $\Omega_m$ ,  $w_0$ ,  $w_a$ , and  $h$ . We also vary the supernova intrinsic magnitude  $\mathcal{M}$  (which is completely degenerate with the Hubble constant) using a flat prior over the prior range  $-20 < \mathcal{M} < -18$ . Beyond the weak priors mentioned above, the supernova forecasts have one additional prior imposed within CosmoSIS:  $w(a) < 0$  for all  $a$ . We note that the direction of the degeneracy ellipse in the  $w_0 - w_a$  plane depends sensitively on the width of the assumed priors on these or other parameters. In particular, we find that for wide priors on  $\Omega_m$ , the degeneracy lies along the  $w_a \approx -(w_0 + 1)$  line, but rotates towards a line of  $w_a \approx +(w_0 + 1)$  as the  $\Omega_m$  priors are tightened (assuming uninformative priors on intrinsic magnitude parameter), as it changes the pivot point in redshift space where the dark energy constraints are tightest. This effect is

<sup>24</sup>[https://github.com/lstts/sims\\_operations](https://github.com/lstts/sims_operations)

<sup>25</sup><https://www.lsst.org/scientists/simulations/opsim/opsim-v335-benchmark-surveys>

<sup>26</sup>For details of why this is not simply the first 10% of nights, see extensive discussion in <https://github.com/LSSTDESC/Requirements/issues/9>. In short, the OpSim run has a spurious preference for the Deep Drilling Fields in the first year that leads to the wide survey area being under-observed. Since this is not expected to be part of the actual survey strategy, we used an ad-hoc correction for this.

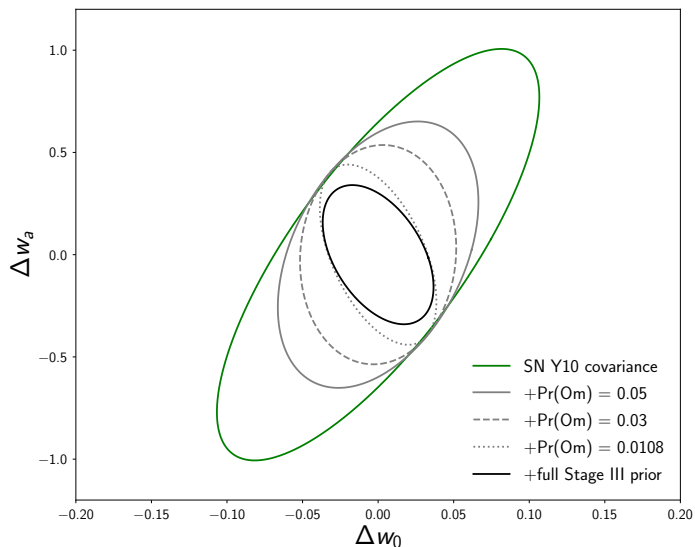


Figure C1: 95% confidence ellipses for the supernova science case as a function of prior on  $\Omega_m$ . For low-matter universes, the dark energy equation of state lies along the positive  $w_0 - w_a$  degeneracy direction, however a tight prior around the fiducial matter density focuses and rotates the dark energy equation of state parameters along the degeneracy direction for acceleration.

seen for generic dark energy models and is not specific to the dark energy parameterization considered here (Huterer & Peiris 2007). This effect has been studied previously for upcoming surveys (see e.g. Goliath et al. 2001). The exact slope of the line is also dependent on the redshift distribution of the sample, the particular systematics included and the prior on the intrinsic magnitude; a more exhaustive study is forthcoming in a separate paper. We show the behavior for changing the  $\Omega_m$  prior in Figure C1. The supernova parameters ( $\mathcal{M}, H_0, \Omega_m, w_0, w_a$ ) are sampled via MCMC and the resultant chains are processed to produce a covariance matrix. That covariance matrix is then sampled with the other three cosmological parameters not relevant to the SN likelihood to produce the full 7-parameter chains.

We show parameter constraints in the  $(X, Y)$  plane for any pairs of parameters as  $(\Delta X, \Delta Y)$  after subtracting off the fiducial values, to de-emphasize our choice of fiducial values (which do have some impact on the forecasts). Note that we are fixing the neutrino mass  $m_\nu = 0$  for the forecasts in the baseline analysis even though neutrinos have mass. This is for the sake of expediency: fixing the neutrino mass to a nonzero value should have little impact on the  $(w_0, w_a)$  constraints while inflating the run-time by a factor of  $\sim 2$ . For future DESC SRD versions, it may be worth revisiting this choice. Also, this forecast does not allow for curvature, unlike the forecasts in the DETF report. In principle, this means that our comparison of FoMs against ones from that report is overly optimistic. However,

this is only important for supernovae, not the other probes and not the joint forecast<sup>27</sup>. Since our primary concern is the joint forecast, we do not attempt to account for this over-optimism in the comparison of the supernova forecasts against those from Stage III.

When including Stage III priors, the ones that we use correspond to the scenario described in section 6.3 and shown with dark blue contours in figure 28 of [Planck Collaboration et al. \(2016\)](#), the “TT+TE+EE+lowP+lensing+ext” chain with  $w_0$  and  $w_a$  free. This prior includes Planck polarization and lensing (neglecting all cross-terms with LSST probes) and the following external data (“ext”): BOSS, JLA, and  $H_0$ , with the exact analysis used for these three probes described in subsections 5.2–5.4 of [Planck Collaboration et al. \(2016\)](#). Without a prior on the matter density, the supernova posterior is considerably non-Gaussian and so the contours produced by computing the covariance of the supernova chains are broader than the Fisher matrix contours from the SN likelihood. The addition of the Stage III prior significantly Gaussianizes the contours.

### C3 Stage III dark energy surveys

We must assume some Stage-III DETF FOM for each probe in order to quantify whether we meet [G1](#). The derivation of the Stage-III numbers is described below.

- **WL:** Both scenarios presented in the DETF report for Stage-III WL are too optimistic in certain key respects, using an area comparable to the full DES<sup>28</sup> survey area but a much higher effective source number density ( $15/\text{arcmin}^2$ ) and redshift ( $\langle z \rangle \sim 1$ ). These can be compared with the DES Y1 shear catalog paper ([Zuntz et al. 2017](#)), which reports number densities from two catalogs, the larger of which has  $6.5/\text{arcmin}^2$  and a mean redshift  $\langle z \rangle \sim 0.6$ , constructed using state-of-the-art methodology that is unlikely to evolve in ways that bring DES substantially closer to the DETF configuration. The increased depth in later years, with roughly doubled exposure time, should yield tens of percent higher number densities, but not a factor of 2.5. In addition the DETF assumes 20% lower shape noise (lower  $\sigma_\gamma^2$ ) than is found in DES in practice. For all of these reasons, the signal is lower and the noise is higher in DES than in the DETF forecast, meaning that the real Stage III numbers will be substantially more shape noise-dominated than even the DETF pessimistic scenario. In the absence of a more realistic Stage III forecast, we use the DETF pessimistic FoM (20) as our benchmark for LSST WL. The fact that we will compare it with an LSST forecast 3x2-point analysis partially accounts for the fact that even the pessimistic forecast may be too optimistic in terms of statistical precision.
- **LSS:** The DETF report only considers BAO, not a full LSS analysis to smaller scales. We nonetheless use a geometric mean of their Stage-III pessimistic and optimistic photometric BAO FoMs,

<sup>27</sup>To quote from the DETF report: “Setting the spatial curvature of the Universe to zero greatly strengthens the dark energy constraints from supernovae, but has a modest impact on the other techniques once a dark-energy parameterization is selected. When techniques are combined, setting the spatial curvature of the Universe to zero makes little difference to constraints on parameterized dark energy, because the curvature is one of the parameters well determined by a multi-technique approach.”

<sup>28</sup><https://www.darkenergysurvey.org/>

which yields a value of 0.76.

- CL: The DETF considers number counts and cluster lensing. Their optimistic cluster lensing forecasts assume too much prior knowledge of the mass-observable relation compared to our assumptions here, so we use the DETF pessimistic FoM of 6.
- SL: The DETF does not include strong lensing time delays among the probes they consider, so we must estimate the Stage III FoM some other way. Based on reasonable assumptions about what Stage III strong lensing dark energy analysis will include<sup>29</sup>, we assume 3 compound lenses each with 1.7% distance measurements, and 15 time delay lenses each with 7% distance measurements. Given this Stage III survey definition and our adopted priors, the Stage-III FoM is 0.65.
- SN: The geometric mean of the optimistic and pessimistic scenarios in the DETF report gives a FoM of 9.4.

#### C4 Follow-up observations and ancillary data

As described in [Section 1](#), some of our science cases assume that already-funded surveys will be carried out and that spectroscopic follow-up and other ancillary telescope resources will continue to be available at similar rates as they are today. Below the assumptions for specific science cases are summarized, with references to where further discussion can be found.

- WL: The WL baseline analysis outlined in [Appendix D2](#) does not rely directly on ancillary telescope resources. It is expected that spectroscopic samples will be needed to meet the requirements on knowledge of photometric redshift bias and scatter presented in [Section 5.2](#). However, as described in [Section 5.1](#), the overlaps of the LSST footprint with DESI and 4MOST should enable us to meet those requirements.
- LSS: The LSS baseline analysis outlined in [Appendix D1](#) does not rely directly on ancillary telescope resources, though the same considerations about spectroscopic data to meet the requirements on knowledge of photometric redshift errors mentioned for WL apply to LSS.
- CL: The CL baseline analysis outlined in [Appendix D3](#) makes conservative assumptions about available multiwavelength (X-ray and SZ) data to help place priors on the mass-observable relationship, as described in [Appendix D3.3](#).
- SL: The SL baseline analysis outlined in [Appendix D5](#) assumes readily achievable amounts of follow-up both to constrain the lens model parameters over which we must marginalize and to provide lens and source spectroscopic redshifts. The modest sample size is set in part by the need for follow-up, with the follow-up needs described in detail there.

---

<sup>29</sup>See discussion in <https://github.com/LSSTDESC/Requirements/issues/17>, which resulted in a Stage-III configuration slightly more conservative than that described in [Treu & Marshall \(2016\)](#) for time delay lenses, but with the inclusion of the compound lenses not discussed there.

- SN: The SN baseline analysis outlined in [Appendix D4](#) assumes (a) the presence of a low-redshift external supernova sample (based on an ongoing survey), and (b) host spectroscopic redshifts, with the usable sample size strictly limited by reasonable assumptions about host spectroscopy using 4MOST for the WFD supernova sample and PFS or DESI for the DDF sample. See that appendix for more details.

## D Baseline analyses

Each subsection within this appendix outlines the baseline analysis for a single probe or probe combination.

### D1 Large-scale structure

The default LSS (galaxy clustering only) analysis is a tomographic one with galaxy two-point correlations. BAO information is implicitly included in the tomographic analysis of the 2-point correlations. For this DESC SRD version, the baseline LSS analysis is simply the galaxy-galaxy part of the WL+LSS analysis described in the next subsection. That is, the WL+LSS analysis has a “lens” sample and a “source” sample for which auto- and cross-correlations are measured. The sample described in this section is the lens sample for WL+LSS (while the source sample is described in [Appendix D2](#)).

#### D1.1 Analysis choices

Here we describe the essential points of the LSS analysis setup in this version of the DESC SRD:

- We assume 10 tomographic bins spaced by 0.1 in photo- $z$  between  $0.2 \leq z \leq 1.2$  for Y10, and 5 bins spaced by 0.2 in photo- $z$  in that same redshift range for Y1.
- The data vector consists of the angular power spectra,  $C_\ell$ . For clustering, unlike for shear, we only use the auto-power spectra (which carry the vast majority of the cosmological information), not cross-spectra between different redshift bins.
- Since the astrophysical issues determining what scales to use are tied to physical scale, we use  $k_{\max} \sim 0.3 h/\text{Mpc}$ . This cut is based on work in progress indicating that this is the scale where nonlinear bias results in  $\sim 10\%$  deviations from the linear bias for  $z \sim 0.5$  galaxies. Following [Font-Ribera et al. \(2014\)](#), this should be taken as an effective maximum wavenumber. Statistical precision of LSST will be considerably better than 10%, but it is assumed that these differences will be accounted for by fitting for beyond-linear bias parameters using scales slightly larger than  $k_{\max}$ .
- In order to enable combined probe analysis, we define a common set of  $\ell$  bins for all large-scale structure analyses (LSS, WL, CL). There are 20 logarithmically-spaced  $\ell$  bins, covering  $20 \leq \ell \leq 15000$  (where this value is adopted to accommodate the galaxy cluster lensing profiles

in the 1-halo regime). These limits are the bin edges, not centers. For the LSS analysis, an  $\ell_{\max}$  is chosen for each redshift bin based on its  $k_{\max}$  and redshift distribution as follows:

$$\ell_{\max} = k_{\max} \chi(\langle z \rangle) - 0.5. \quad (4)$$

All  $\ell$  bins above that  $\ell_{\max}$  value in our standardized  $\ell$  binning are discarded.

- The nonlinear matter power spectrum and covariances are calculated following [Krause & Eifler \(2017\)](#), using the [Takahashi et al. \(2012\)](#) prescription for the nonlinear power spectrum and the transfer function from [Eisenstein & Hu \(1999\)](#).
- For the Y10 lens sample, we use the gold sample<sup>30</sup> which has a limiting magnitude of  $i_{\text{lim}} = 25.3$ . The overall normalization of the number density is estimated based on the HSC Deep survey (see [Appendix F1](#) for details),  $48 \text{ arcmin}^{-2}$ , and the intention was to use other parameters from the LSST Science book<sup>31</sup>:  $b(z) = 0.95/G(z)$ , where  $G(z)$  is the normalized growth factor with  $G(z=0) = 1$ ; and  $\sigma_z = 0.03(1+z)$ . In practice, after tagging v1 we found that a different set of bias values was used<sup>32</sup> for the data vectors and covariances, but for a cosmic variance-dominated sample and when marginalizing over a separate galaxy bias in each bin, this should not affect the forecasts. We use a parametric redshift distribution,

$$\frac{dN}{dz} \propto z^2 \exp[-(z/z_0)^\alpha] \quad (5)$$

with (0.28, 0.90) for Y10. See [Appendix F3](#) an explanation of the origin of the best-fitting values given here and a comparison with real and simulated data.

- For the Y1 lens sample, we use the equivalent of the gold sample, cut off 1 magnitude brighter than the (shallower) median survey depth, giving  $i_{\text{lim}} = 24.1$  (see [Appendix C1](#) for an explanation of how the limiting magnitudes were determined). Again we define the number density following empirical results from the HSC survey ([Appendix F1](#)), finding a value of  $18 \text{ arcmin}^{-2}$ . Similarly the parametric form for the redshift distribution is above, with  $(z_0, \alpha) = (0.26, 0.94)$  for Y1 (see [Appendix F3](#)). Based on the typical luminosity-bias relation, we use<sup>33</sup>  $b(z) = 1.05/G(z)$  and use the same photo- $z$  scatter,  $\sigma_z = 0.03(1+z)$ .

<sup>30</sup>See chapter 3 of the LSST science book, [LSST Science Collaboration \(2009\)](#), [http://www.lsst.org/sites/default/files/docs/sciencebook/SB\\_3.pdf](http://www.lsst.org/sites/default/files/docs/sciencebook/SB_3.pdf) (Equation 3.8).

<sup>31</sup>This  $\sigma_z$  value is optimistic; it is close to the LSST design specifications without inclusion of effects such as template uncertainty or the impact of incomplete spectroscopic training samples. However, we defer a more realistic model (including a more realistic distribution, not just the width, and including stronger redshift evolution) to future DESC SRD versions; in any case, the statistical power of the LSS analysis is largely limited by the need to marginalize over galaxy bias rather than by the photo- $z$  scatter.

<sup>32</sup>For Y1, the per-bin bias values that were actually used were [1.562362, 1.732963, 1.913252, 2.100644, 2.293210]. For Y10, they were [1.376695, 1.451179, 1.528404, 1.607983, 1.689579, 1.772899, 1.857700, 1.943754, 2.030887, 2.118943].

<sup>33</sup>The text states the intended bias-redshift relation, but see previous footnote for numbers that can be used when comparing data vectors and covariances with those from the DESC SRD v1.

## D1.2 Anticipated improvements

Ideally the LSS analysis would make use of a red sample with better photo- $z$  in a multitracer analysis using both the gold sample and the red sample. Future DESC SRD versions should use multitracer analyses if possible, and also enable use of the “lens” galaxies beyond  $z = 1.2$  in the clustering analysis. While most information about cosmology is included in the auto-spectra, there is some additional information in the cross-spectra between bins that it would be useful to include in the future (especially once our analysis has a more complicated treatment of photo- $z$  errors, which tend to increase the cross-bin correlations). Modified  $\ell$  binning will be important to more optimally include the BAO feature; the current broad  $\ell$  binning scheme is likely quite suboptimal. **Figure D1** may be used to guide future efforts to derive a better binning scheme. Finally, incorporating the impact of survey inhomogeneity in Y1 would be valuable, if a simple parametrization for its effect on the observables can be derived.

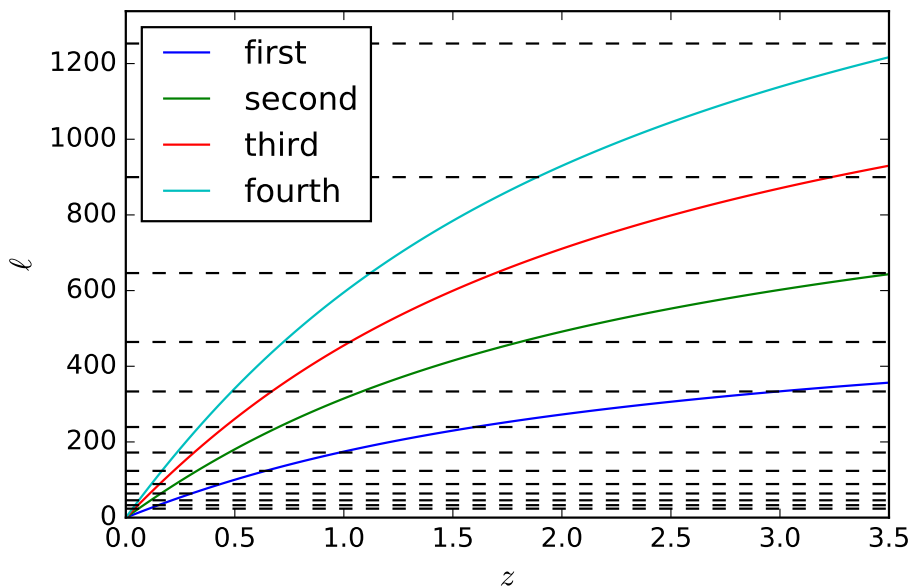


Figure D1: The positions of the first four BAO peaks as a function of redshift are shown in color, while the horizontal lines show the centers of our  $\ell$  bins in this DESC SRD version. In order to Nyquist sample, we need two  $\ell$  bins (i.e., horizontal lines) between each colored line. A finer binning, and possibly linear rather than logarithmic  $\ell$  binning, would yield a more optimal measurement of the BAO feature from the galaxy angular power spectrum.

## D1.3 Systematic uncertainties

For LSS, we consider the following classes of systematic uncertainties in our two categories:

- Self-calibrated systematics: galaxy bias, magnification, baryonic effects on the matter power spectrum.
- Calibratable systematics on which we place requirements: any photo-z issue, sky contaminants.

The models for the self-calibrated systematic uncertainties are summarized in [Table D1](#). For each source of systematic uncertainty, we describe how it is included in this DESC SRD version, as well as aspirations for more complex models to be included in future. Currently, our data vectors are produced assuming linear galaxy biasing due to lack of an adopted and validated  $b(k)$  model, and marginalization will use  $b$  defined in redshift bins without assuming a parametrized  $b(z)$  model – hence  $N$  bins leads to  $N$  nuisance parameters. For a given  $z$  bin, the fact that we do not have to marginalize over nonlinear bias implies more statistical power left for cosmology constraints than would be present in reality (since we will have to marginalize over nonlinear bias); but the fact that we need a per-bin bias (rather than having a parametrized model) does result in many bias parameters. Incorporating a realistically complex nonlinear bias model with an appropriate number of nuisance parameters is the highest-priority update to make for the LSS analysis in the next DESC SRD version.

Self-calibrated systematic uncertainty	Current model	Future plans
Galaxy bias	Linear galaxy bias, one value per tomographic bin (Gaussian prior, mean= 1.9 and $\sigma = 0.9$ )	Nonlinear galaxy bias with a redshift-dependent parametrization of the linear bias vs. redshift, and at least one nonlinear bias parameter
Magnification	None	Self-consistent convergence field and luminosity function as what goes into the shear and intrinsic alignments in 3x2pt analysis, following e.g. <a href="#">Joachimi &amp; Bridle (2010)</a> ; marginalize over uncertainty in slope of number counts
Baryonic effects	None	Sufficiently complex nonlinear galaxy bias model that it can absorb modifications to the matter power spectrum due to baryonic effects

Table D1: Self-calibrated systematic uncertainties for LSS.

The residual calibratable systematic uncertainties on which we will place requirements can be divided into two categories: those that cause uncertainties in the galaxy number density as a function of position on the sky (and hence in the galaxy power spectrum), and those that cause redshift uncertainties. Both classes of uncertainty are coupled by systematics such as dust extinction or photometric calibration. A



diagram of these calibratable systematics is shown in [Figure D2](#), while the current models and future plans for how to represent them can be found in [Table D2](#). The DESC’s DC2 analysis effort will provide useful guidance on how to incorporate our need for knowledge of systematic uncertainty due to observational effects like airmass and PSF effects and how to connect them to cosmological parameter estimates, so some models for inclusion of these effects and how to place requirements on our knowledge of them (or associated scale cuts) are still to be defined in future DESC SRD versions. Additional updates to our modeling might result from DC2- or DC3-era decisions about whether the analysis will proceed in bins (which requires the calibration of photo- $z$ ’s in each bin) or will rely on photo- $z$  PDFs (in which case misspecification of PDFs may also be an issue, similar but not identical to catastrophic photo- $z$  outliers in impact). In either case, a more sophisticated model for the redshift-dependent photo- $z$  bias, scatter, and outlier rate is needed.

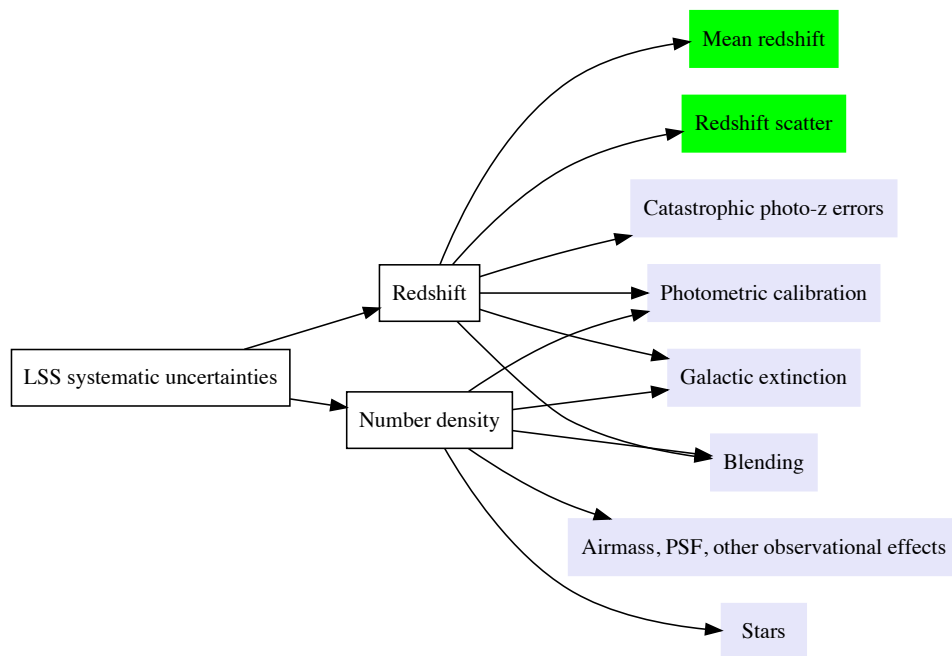


Figure D2: Diagram indicating sources of systematic uncertainty for the LSS analysis on which we would like to place requirements in the DESC SRD. The direction of the arrows indicates the flow from overall systematic uncertainty to broad systematics categories to the specific physical effects on which we place requirements. As shown, there are several issues that contribute to both redshift and number density uncertainty. The green / lavender boxes indicate sources of uncertainty on which we do / do not place requirements in this DESC SRD version, respectively.

Calibratable systematic uncertainty	Current model	Future plans
Redshift uncertainties		
Mean redshift	Uncertainty in $\langle z \rangle$ for each tomographic bin	Investigate bins separately
Redshift width	A redshift bin width that is the same for each bin modulo $1 + z$ factors	Account for inflation of $\sigma_z$ at higher redshift compared to the $1 + z$ model; use DC2 guidance on $\sigma_z$
Catastrophic photo- $z$ errors	None	To be decided based on DC2
Galactic extinction	None	To be decided
Photometric calibration	None	To be decided
Blending	None	To be decided
Number density uncertainties		
Galactic extinction	None	To be decided
Photometric calibration	None	To be decided
Stars	None	Templates for incomplete detection near bright stars, impact of bright stars on background estimates, stellar contamination of galaxy sample, ...
Airmass, PSF, other observational effects	None	To be decided based on DC2
Blending	None	To be decided based on DC2

Table D2: Calibratable systematic uncertainties for LSS.

## D2 Weak lensing (3×2-point)

The default weak lensing analysis is a tomographic analysis of shear-shear, galaxy-shear, and galaxy-galaxy correlations (or “3×2-point” analysis), which has become the standard in the field of weak lensing due to the way it enables marginalization of both astrophysical and observational systematic uncertainties in the shear signal. Currently, this analysis is implemented such that the LSS analysis described in the previous subsection is a strict subset of the  $3 \times 2$ -point analysis, but that might not always be the case in future DESC SRD versions. In other words, the lens sample for the 3×2-point analysis was described in [Appendix D1](#), while the source sample is described here.

### D2.1 Analysis choices

Here we describe the essential points of the WL analysis setup in this version of the DESC SRD:

- For the “lens” sample, we assume 10 tomographic bins spaced by 0.1 in photo- $z$  between  $0.2 \leq z \leq 1.2$  for Y10, and 5 bins spaced by 0.2 in photo- $z$  in that same redshift range for Y1. This is the same as for the LSS analysis in the previous subsection.
- For the “source” sample, we assume 5 redshift bins defined with equal numbers of source galaxies per bin for both Y1 and Y10. This is done using the true redshift distribution, and then the bins are convolved with the photo- $z$  error distribution to make the photo- $z$  distributions. While this technically does not mimic what is done in reality, it is quite a close approximation and easier to implement. Unlike for the lens sample described in [Appendix D1](#), there is no upper redshift cutoff at  $z = 1.2$  for the source sample. While this use of only 5 redshift bins is pessimistic compared to previous LSST and other Stage-IV survey forecasts, there are a few reasons to do this here: First, there were relatively larger numerical convergence issues seen with CosmoLike forecasts with 10 bins, and stronger discrepancies between CosmoLike and GoFish than for the 5-bin case (where agreement was excellent as described in [Appendix B](#)). Second, the requirements on calibration of the mean redshift of each tomographic bin were extremely tight in the 10-bin case, possibly unachievable even with acquisition of substantial additional data; hence opting for fewer tomographic bins and less constraining power constitutes a more realistic analysis choice. Third, there were concerns that the overly simplistic photometric redshift error model may be particularly limiting in the 10-bin case, where each bin is relatively narrower and the impact of outliers (not yet modeled) is more important.
- The data vector consists of the angular power spectra,  $C_\ell$ . Both auto- and cross-power spectra are included in the analysis for shear-shear and galaxy-shear correlations, but as in the previous subsection, only auto-power spectra are included for galaxy-galaxy correlations.
- We use the same set of globally defined  $\ell$  bins as described for the LSS analysis. The actual choice of bins to include in the forecasting is made as follows:

- For galaxy-shear and galaxy-galaxy correlations, the  $k_{\max}$  value is chosen in the same way as for the LSS analysis (based on our ability to model galaxy bias), and  $\ell$  bins are eliminated for each tomographic redshift bin based on the relationship between  $k_{\max}$  and  $\ell_{\max}$  as described in the previous subsection.
  - For shear-shear correlations, since the  $C_\ell$  are determined based on an integral that goes from redshift  $z = 0$ , it does not make sense to define a physical  $k_{\max}$ . Instead, we adopt  $\ell_{\max, \text{shear}} = 3000$  in all tomographic bins. This is based on assuming some improvements in our ability to model the impact of baryons on the matter power spectrum compared to the current state-of-the-art, though we have not factored in the fact that baryonic physics mitigation schemes will prevent our use of the full constraining power of the data on those scales.
  - For galaxy-shear tomographic cross-correlations, for bins  $i$  and  $j$  where  $i \neq j$ , we use the value of the  $\ell_{\max}$  for the lens sample (since the restriction is based on our ability to model nonlinear bias in the lens sample), and in all cases require  $\ell_{\max} \leq \ell_{\max, \text{shear}}$ .
- We use the same prescription for the nonlinear matter power spectrum as described in the previous subsection.
  - The covariance matrix estimation follows the same numerical prescription as in Krause & Eifler (2017), with the only changes being those required by our new baseline analysis definition, tomographic binning, etc.
  - The number density and redshift distribution for the Y1 and Y10 lens samples are as described in the previous subsection.
  - We use a process similar to that of Chang et al. (2013) to estimate  $n_{\text{eff}}$  for lensing source galaxies. Following the calculations in Appendix F2 of this document, we use 10 and 27 arcmin<sup>-2</sup> as the lensing  $n_{\text{eff}}$  in Y1 and Y10 as given in Figure F4. We also use  $\sigma_e = 0.26$  per component, and  $\sigma_z = 0.05(1 + z)$ . This  $\sigma_z$  value is somewhat optimistic for  $z \gtrsim 1.2$ ; future DESC SRD versions should incorporate a stronger redshift-dependence of the scatter for greater realism.
  - For  $n_{\text{eff}}(z)$ , we use the same parametric form as Equation 5, with  $(z_0, \alpha) = (0.13, 0.78)$  for Y1 and  $(0.11, 0.68)$  for Y10 (see legends of Figure F4 and discussion in Appendix F4 for details). These give mean effective source redshifts of  $\sim 0.85$  and  $\sim 1.05$ , respectively.

## D2.2 Anticipated improvements

In future DESC SRD versions, we may consider versions of the baseline WL analysis that allow a different choice of “lens” galaxies from what goes into the LSS analysis, in order to optimize the two science cases. If multitracer analysis is deemed useful for WL, it may be pursued in future. Other potential improvements include: use of “lens” galaxies beyond  $z = 1.2$  in the clustering analysis; use of galaxy-galaxy cross-power spectra; more optimal tomographic binning; and incorporating the impact of survey inhomogeneity in Y1, if a simple parametrization for its effect on the observables can be derived.

### D2.3 Systematic uncertainties

For the WL analysis, we consider the following classes of systematic uncertainties in our two categories:

- Self-calibrated systematics: intrinsic alignments, baryonic effects, galaxy bias, magnification
- Calibratable systematics on which we place requirements: any shear, photo- $z$ , detector, or image processing issue

The models for the self-calibrated systematic uncertainties are summarized in [Table D3](#). For each source of systematic uncertainty, we describe how it is included in this DESC SRD version, as well as aspirations for more complex models to be included in future. Currently, our data vectors are produced assuming linear galaxy biasing, and marginalization will use  $b$  defined in redshift bins without assuming a parametrized  $b(z)$  model – hence  $N$  bins leads to  $N$  nuisance parameters. For a given  $z$  bin, the fact that we do not have to marginalize over nonlinear bias implies more statistical power left for cosmology constraints than would be present in reality (since we will have to marginalize over nonlinear bias); but the fact that we need a per-bin bias (rather than having a parametrized model) does result in many bias parameters. In one sense we are overestimating the number of needed bias parameters, and in another we are underestimating compared to reality.

For intrinsic alignments (IA), we currently use the nonlinear alignment model as in section 4.4 of [Krause & Eifler \(2017\)](#) for red galaxies, assuming that blue galaxies have no IA. The red galaxy fraction is computed from equation 25 and subsequent text in [Krause et al. \(2016\)](#); the red galaxy luminosity function is from GAMA. The definition of IA amplitude and luminosity dependence is in the text around equations 7-8 and section 4.1 of that paper. For the DESC SRD, the luminosity function parameters were fixed and the four IA parameters allowed to vary within the ranges defined by the following Gaussian priors:

- Overall intrinsic alignment amplitude  $A_{\text{IA}}$ : mean= 5,  $\sigma = 3.9$
- Power-law luminosity scaling  $\propto L^{\beta_{\text{IA}}}$ :  $\beta_{\text{IA}}$  with mean= 1,  $\sigma = 1.6$
- Redshift scaling  $\propto (1+z)^{\eta_{\text{IA}}}$ :  $\eta_{\text{IA}}$  with mean= 0,  $\sigma = 2.3$
- Additional high-redshift scaling parameter  $\eta_{\text{high-}z}$ : mean= 0,  $\sigma = 0.8$

The residual calibratable systematic uncertainties on which we will place requirements can be divided into four categories: redshift, number density, multiplicative shear, and additive shear uncertainties. A diagram of these calibratable systematics is shown in [Figure D3](#), while the current models and future plans for how to represent them is in [Table D4](#). We note that the residual multiplicative shear calibration bias  $\Delta m$  is in principle a function of redshift, and indeed it is redshift evolution of  $\Delta m$  that can mimic changes in dark energy models (because it implies a change in structure growth). As a result, our model for  $\Delta m(z)$  is not simply a constant  $m_0$ ; we confirmed that this gives extremely weak requirements on

Self-calibrated systematic uncertainty	Current model	Future plans
Galaxy bias	Linear galaxy bias, one value per tomographic bin (Gaussian prior, mean= 1.9 and $\sigma = 0.9$ )	Nonlinear galaxy bias with a redshift-dependent parametrization of the linear bias vs. redshift, and at least one nonlinear bias parameter
Magnification	None	Self-consistent convergence field and luminosity function as what goes into the shear and intrinsic alignments in WL analysis, following e.g. <a href="#">Joachimi &amp; Bridle (2010)</a> ; marginalize over uncertainty in slope of number counts
Intrinsic alignments	Nonlinear alignment model as in section 4.4 of <a href="#">Krause &amp; Eifler (2017)</a> , but with different priors as described in <a href="#">Appendix D2.3</a>	More complex model such as <a href="#">Blazek et al. (2015)</a> , with IA and luminosity function parameters marginalized
Baryonic effects	None	Hydrodynamic simulation-motivated emulator for baryonic effects in WL (e.g., <a href="#">Harnois-Déraps et al. 2015</a> )

Table D3: Self-calibrated systematic uncertainties for WL.

$m_0$  because, as noted previously by [Massey et al. \(2013\)](#),  $\partial C_\ell/\partial m_0$  differs significantly from  $\partial C_\ell/\partial w_0$  (or  $w_\alpha$ ) when considering the full data vector of  $C_\ell$  across all redshift bins. In order to identify sensitivity of cosmological parameter constraints to multiplicative shear calibration uncertainties, it is important to use a redshift-dependent model; we adopted

$$\Delta m(z) = m_0 \left( \frac{2z - z_{\max}}{z_{\max}} \right) \quad (6)$$

with  $z_{\max}$  set to the middle of the highest tomographic redshift bin. Given this parametrization, the total variation in shear calibration across the redshift range used for the weak lensing analysis is  $2m_0$ , and requirements on shear calibration should be interpreted as a requirement on our knowledge of redshift-dependent shear calibration trends across the sample. In principle, there is some higher-order dependence on the redshift-dependent function adopted, but do not explore this further in this version of the DESC SRD.

The DESC’s DC2 analysis effort will provide useful guidance on how to incorporate our need for knowledge of systematic uncertainty due to observational effects like airmass and PSF effects and how to connect them to cosmological parameter estimates, so some models for inclusion of these effects and how to place requirements on our knowledge of them (or associated scale cuts) are still to be defined in future DESC SRD versions. Additional updates to our modeling might result from DC2- or DC3-era decisions about whether the analysis will proceed in bins (which requires the calibration of photo- $z$ ’s in each bin) or will rely on photo- $z$  PDFs (in which case misspecification of PDFs may also be an issue, similar but not identical to catastrophic photo- $z$  outliers in impact). In either case, a more sophisticated model for the redshift-dependent photo- $z$  bias, scatter, and outlier rate is needed.

It is worth noting that several of the effects listed in the right-most column of [Figure D3](#) contribute to systematic uncertainties for WL in several ways (number density, redshift, and shear-related uncertainties); it will be important to develop a self-consistent approach for how systematic uncertainties due to blending, photometric calibration, galactic extinction, stars, galaxy characterization, selection bias, detector effects, and PSF modeling errors propagate into all of the observables.

Calibratable systematic uncertainty	Current model	Future plans
Redshift uncertainties		
Mean redshift	Uncertainty in $\langle z \rangle$ for each tomographic bin	Investigate bins separately
Redshift width	A redshift bin width that is the same for each bin modulo $1+z$ factors	Account for inflation of $\sigma_z$ at higher redshift compared to the $1+z$ model; use DC2 guidance on $\sigma_z$
Catastrophic photo- $z$ errors	None	To be decided based on DC2
Galactic extinction	None	To be decided
Photometric calibration	None	To be decided

Blending	None	To be decided
Number density uncertainties		
Galactic extinction	None	To be decided
Photometric calibration	None	To be decided
Stars	None	Templates for incomplete detection near bright stars, impact of bright stars on background estimates, stellar contamination of galaxy sample, ...
Airmass, PSF, other observational effects	None	To be decided based on DC2
Blending	None	To be decided based on DC2
Shear (multiplicative) uncertainties		
Blending	None	To be decided based on DC2
Stars	Fractional contamination of galaxy sample by stars	To be decided based on DC2
Galaxy characterization	None	To be decided
Galaxy selection bias	None	To be decided
Detector effects	None	To be decided based on DC2
PSF modeling errors	PSF model size requirement based on second moments	To be decided based on DC2
Shear (additive) uncertainties		
Blending	None	To be decided based on DC2
Galaxy characterization	None	To be decided
Galaxy selection bias	None	To be decided
Detector effects	None	To be decided based on DC2
PSF modeling errors	$\rho$ statistics	To be decided based on DC2
Member galaxy contamination	None	To be decided

Table D4: Calibratable systematic uncertainties for WL.

Finally, several boxes in the right-most column of [Figure D3](#) implicitly include multiple effects. For completeness, we note the primary contributors to these, which will eventually be important for modeling their impact on the observable quantities:

- Detector effects: brighter-fatter, glowing edges, tree rings, and others.
- PSF modeling errors: differential chromatic refraction, chromatic seeing, other chromatic effects in the optics and sensors, color gradients, relative astrometry between exposures, model bias, PSF interpolation, contamination of the PSF star sample by binaries.



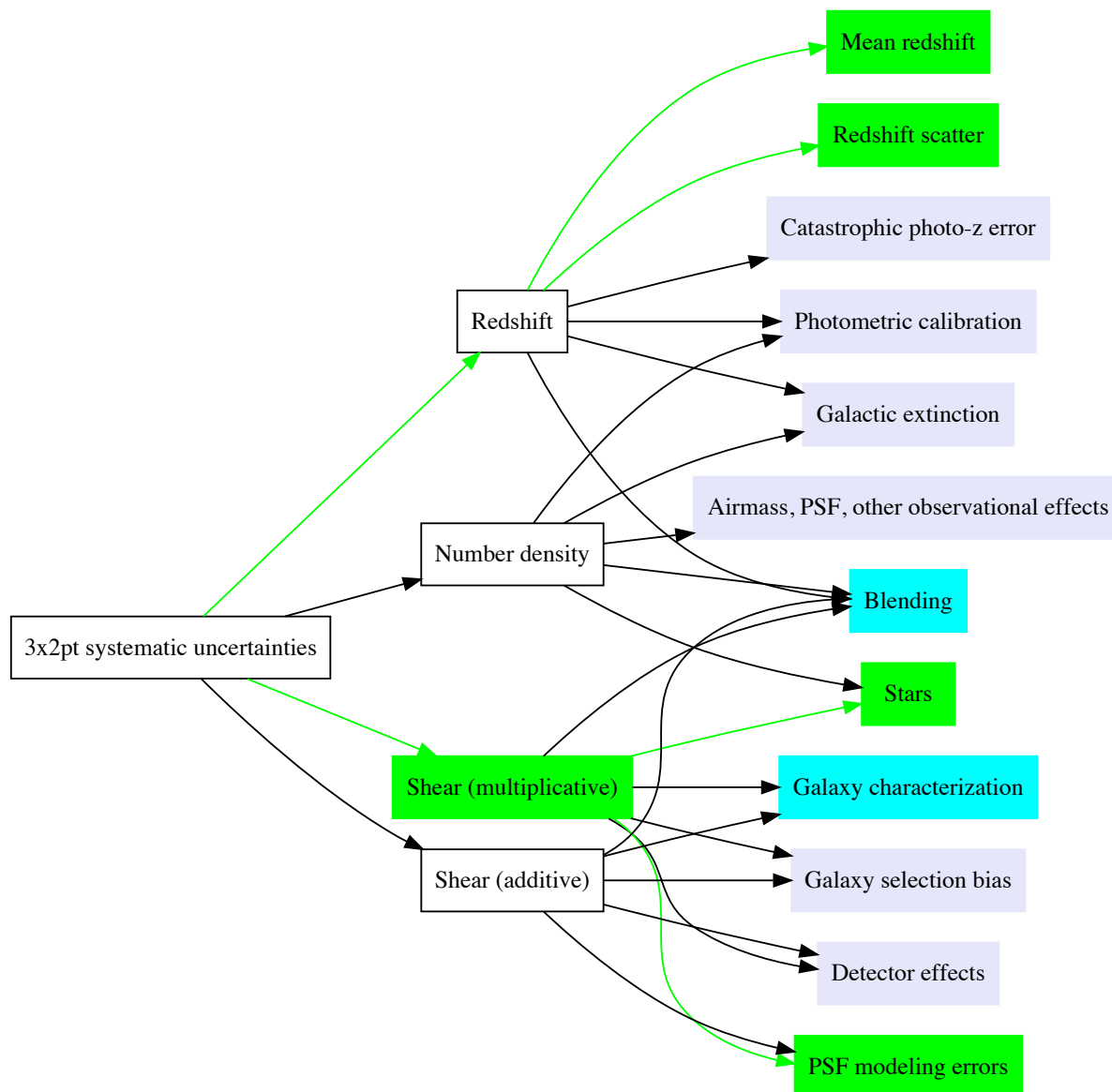


Figure D3: Diagram indicating sources of systematic uncertainty for the WL analysis on which we would like to place requirements in the DESC SRD. The direction of the arrows indicates the flow from overall systematic uncertainty to broad systematics categories to the specific physical effects on which we place requirements. As shown, there are several low-level issues in the right-hand column that contribute to multiple categories of uncertainty in the middle column. The green / lavender boxes indicate sources of uncertainty on which we do / do not place requirements in this DESC SRD version, respectively. The cyan boxes indicate those for which more R&D beyond the DESC's DC2 may be needed in order to place requirements. For some of the green boxes, we currently only have software infrastructure to place requirements through their impact on one class of uncertainty; such connections are shown as green arrows.

- Galaxy characterization: insufficient PSF correction method, pixel-noise bias, model bias
- Blending: effects on detection, astrometry, photometry, and shapes due to undetected blended objects, selection effects, increased model and/or noise bias

These may not be explicitly modeled independently in the end, but understanding the nature of these contributing factors may be important for building up templates for systematics.

### D3 Galaxy clusters

For the purpose of this first version of the DESC SRD, the default galaxy cluster abundance analysis incorporates the cluster counts as a function of richness and redshift, along with stacked cluster weak lensing in the 1-halo regime to constrain parameters of the cluster mass-observable relation (MOR).

#### D3.1 Analysis choices

Here we describe the essential points of the CL analysis setup in this version of the DESC SRD. It largely follows the treatment in [Krause & Eifler \(2017\)](#), with a few variations:

- For the source sample, we use the same sample as defined for WL in Y1 and Y10. See [Appendix D2](#) for number densities, redshift distributions, tomographic bin definitions, and other relevant parameters.
- The cluster-shear data vector consists of the angular power spectra,  $C_\ell$ , defined in redshift and richness bins, along with the cluster counts on those bins  $N(\lambda, z)$ .
- We use the same set of globally defined  $\ell$  bins as described for the LSS analysis. Since the analysis for now uses only the 1-halo regime, we restrict to  $382 \leq \ell \leq 15000$ . The choice of lower  $\ell$  limit is due to technical issues in covariance estimation; lower  $\ell$  values may be used in future DESC SRD versions.
- The cluster-shear data vector is a stack of the Fourier transform of NFW profiles given the redshift and mass distribution of the clusters and a concentration-mass relation from [Bhattacharya et al. \(2013\)](#). At high redshift, the lowest  $\ell$  bins contain a contribution from the 2-halo term. This term is constructed using the nonlinear matter power spectrum along with the halo bias vs. mass relation from [Tinker et al. \(2010\)](#). Currently the bias is fixed and is not fit for as a free parameter.
- Covariances are calculated following [Krause & Eifler \(2017\)](#).
- The cluster sample binning is defined as follows:
  - $\lambda = [20, 30], [30, 45], [45, 70], [70, 120], [120, 220]$
  - $z = [0.2, 0.4], [0.4, 0.6], [0.6, 0.8], [0.8, 1.0]$  for Y10, with the highest redshift bin omitted in Y1 due to the shallower depth of the Y1 imaging data.

- For the first version of the DESC SRD, we assume perfect knowledge of cluster redshift, i.e., there is no photo- $z$  error.

### D3.2 Anticipated improvements

The above baseline analysis does not correspond to either cluster cosmology analysis approach that is under consideration within the DESC. The clusters working group is considering two approaches, at least one of which should be included in a future DESC SRD version. The two approaches are as follows:

- An extension of the approach described above to include cluster-shear correlations in the 2-halo regime, along with cluster-cluster correlations.
- An approach that involves using individual cluster shear profiles, rather than a stacked analysis.

In addition, external X-ray and SZ data will be used to place priors on certain astrophysical nuisance parameters (MOR, optical cluster miscentering). A more direct connection to that data, given some reasonable assumptions about what will be available when the LSST survey starts, would be desirable – i.e., using sample sizes to connect to the size of the priors on the MOR parameters.

Additional extensions for consideration include stacking in real space using physical coordinates for better reconstruction of cluster profiles, going to lower  $\ell$ , and a comparison of stacking shear vs. surface densities.

### D3.3 Systematic uncertainties

For the CL analysis, we consider the following classes of systematic uncertainties in our two categories:

- Self-calibrated systematics: mass-observable relation, intrinsic alignments, other theory uncertainties (e.g., mass function), cluster miscentering, cluster large-scale bias, baryonic effects on cluster halo profiles and mass function, projection effects
- Calibratable systematics on which we place requirements: any shear, photo- $z$ , detector, or image processing issue

The models for the self-calibrated systematic uncertainties are summarized in [Table D5](#). For cluster abundance measurements, the MOR tends to be the dominant self-calibrated systematic uncertainty (and dominates over purely statistical uncertainties). For each source of systematic uncertainty, we describe how it is included in this DESC SRD version, as well as aspirations for more complex models to be included in future.

For the first version of the DESC SRD, we use the MOR from [Murata et al. \(2018\)](#) with an extension of redshift dependence. Specifically, the mean relation is defined as

$$\ln \lambda(M, z|A, B, C) = A + B \ln \left( \frac{M}{M_{\text{pivot}}} \right) + C \ln(1 + z), \quad (7)$$

and the mass-dependent mass-observable scatter is defined as

$$\sigma_{\ln \lambda|M}(M, z|\sigma_0, q_M, q_z) = \sigma_0 + q_M \ln \left( \frac{M}{M_{\text{pivot}}} \right) + q_z \ln(1+z). \quad (8)$$

This is a slight update from Krause & Eifler (2017) where they used a constant mass-observable scatter. We assume fiducial values for  $A$ ,  $B$ , and  $\sigma_0$  used in Murata et al. (2018), fiducial values 0 for  $C$ ,  $q_m$ , and  $q_z$ . The pivot mass is  $M_{\text{pivot}} = 3 \times 10^{14} h^{-1} M_{\odot}$ . We use Gaussian priors for  $A$  and  $B$  with a width corresponding to 80% of the probability within the flat prior ranges for  $A$  and  $B$  used in Murata et al. (2018) and a Gaussian prior with  $\sigma = 1.2$  for  $C$ . For nuisance parameters in the mass-observable scatter, we use priors which are not directly on these parameters but on scatters at three different richnesses and redshifts,  $P(\sigma_{\ln \lambda|M}(M_{\text{fid}}(\lambda_i, z_i), z_i|\sigma_0, q_M, q_z)) = \text{Gauss}[\sigma_{\ln \lambda|M}(M_{\text{fid}}(\lambda_i, z_i), z_i|\sigma_{0,\text{fid}}, q_{M,\text{fid}}, q_{z,\text{fid}}), \sigma_i]$ , where  $\sigma_i = 0.1$  and  $M_{\text{fid}}(\lambda_i, z_i)$  is the inverse of the mean relation with the fiducial nuisance parameters; there are different sets of  $(\lambda_i, z_i)$  and different assumptions about how well the scatter can be constrained for Y1 and Y10. The priors for Y1 and Y10 are based on reasonable assumptions of ancillary datasets that will be available at those times:

- Y1: The constraints are  $\sqrt{N}$  extrapolations from current constraints of  $\sim 10\%$  on the scatter in the mass-observable relation for  $N = 30$  clusters. Based on this assumption, we use  $(\lambda_i, z_i) = (90, 0.2)$ ,  $(30, 0.1)$ , and  $(100, 0.8)$ , assuming the scatter in the MOR is known to 0.06, 0.05, and 0.04 respectively, corresponding to 100, 150, and 200 clusters. The 100 cluster assumption is based on expectations for Chandra+SPT follow-up, the 150 cluster assumption is based on an already-completed observing program with Swift, and the 200 cluster assumption is from combined SPT+ACT.
- Y10: We use  $(\lambda_i, z_i) = (80, 0.2)$ ,  $(30, 0.1)$ , and  $(90, 0.8)$ , assuming the scatter in the MOR is known to 0.03, 0.05, and 0.03 respectively, corresponding to 500, 150, and 500 clusters, respectively. The 500 cluster assumption is based on expectations for eROSITA and CMB-S4, and is conservative for those surveys (but we assume there will be some systematics floor that prevents further constraint on scatter in the MOR even for higher  $N$ ). The 150 cluster assumption for low redshift is based on an already-completed observing program with Swift.

The residual calibratable systematic uncertainties on which we will place requirements can be divided into four categories: redshift, number density, multiplicative shear, and additive shear uncertainties. A diagram of these calibratable systematics is shown in Figure D4, while the current models and future plans for how to represent them is in Table D6. The DESC’s DC2 analysis effort will provide useful guidance on how to incorporate our need for knowledge of systematic uncertainty due to observational effects like airmass and PSF effects and how to connect them to cosmological parameter estimates, so some models for inclusion of these effects and how to place requirements on our knowledge of them (or associated scale cuts) are still to be defined in future DESC SRD versions. It is worth noting that several of the effects listed in the right-most column of Figure D4 contribute to systematic uncertainties for CL in several ways (number density, redshift, and shear-related uncertainties); it will be important

Self-calibrated systematic uncertainty	Current model	Future plans
MOR	See discussion surrounding <a href="#">Equation 7</a> and <a href="#">Equation 8</a>	Further exploration of parametrizations with more complexity and possibly modified priors
Intrinsic alignments	None	Self-consistent model with WL analysis
Mass function uncertainty	None	At least one parameter overall rescaling, but possibly with mass-dependence as well
Baryonic effects	None	Self-consistent inclusion of baryonic effects on mass function, cluster shear profiles
Cluster large-scale bias	None	Once 2-halo regime and/or cluster clustering is included, will need a model that includes nonlinear bias.
Other theoretical uncertainty (e.g., halo definition biases)	None	Further exploration needed to determine approach
Cluster miscentering	None	Approach to be decided after DC2
Projection effects	None	Approach to be decided after DC2

Table D5: Self-calibrated systematic uncertainties for CL.

to develop a self-consistent approach for how systematic uncertainties due to blending, photometric calibration, galactic extinction, stars, galaxy characterization, selection bias, detector effects, and PSF modeling errors propagate into all of the observables.

The parameters related to shear calibration, shear sample tomographic bins, and source photo- $z$  are shared with the WL analysis ([Appendix D2](#)).

Calibratable systematic uncertainty	Current model	Future plans
Redshift uncertainties		
Mean redshift	Uncertainty in $\langle z \rangle$ for each tomographic bin	Investigate bins separately
Redshift width	A redshift bin width that is the same for each bin modulo $1 + z$ factors	Account for inflation of $\sigma_z$ at higher redshift compared to the $1 + z$ model; use DC2 guidance on $\sigma_z$
Catastrophic photo- $z$ errors	None	To be decided based on DC2
Cluster photo- $z$ errors	None	To be decided
Galactic extinction	None	To be decided
Photometric calibration	None	To be decided
Member galaxy contamination	None	To be decided
Number density uncertainties		
Galactic extinction	None	To be decided
Photometric calibration	None	To be decided
Blending	None	To be decided based on DC2
Stars	None	Templates for incomplete detection near bright stars, impact of bright stars on background estimates, stellar contamination of galaxy sample, ...
Airmass, PSF, other observational effects	None	To be decided based on DC2
Member galaxy contamination	None	To be decided
Shear (multiplicative) uncertainties		
Blending	None	To be decided based on DC2
Stars	Fractional contamination of galaxy sample by stars	To be decided based on DC2
Galaxy characterization	None	To be decided
Galaxy selection bias	None	To be decided
Detector effects	None	To be decided based on DC2

PSF modeling errors	PSF model size requirement based on second moments	To be decided based on DC2
Non-weak shear re-sponse and flexion	None	To be decided
Shear (additive) uncertainties		
Blending	None	To be decided based on DC2
Galaxy characterization	None	To be decided
Galaxy selection bias	None	To be decided
Detector effects	None	To be decided based on DC2
PSF modeling errors	$\rho$ statistics	To be decided based on DC2
Member galaxy contamination	None	To be decided

Table D6: Calibratable systematic uncertainties for CL.

Finally, we note that several boxes in the right-most column of [Figure D4](#) implicitly include multiple effects. The primary contributors to these are listed in [Appendix D2.3](#). Where possible, adopting a common approach to these systematics and their impact on LSS, WL, and CL would be desirable.

## D4 Supernovae

### D4.1 Analysis choices

Here we describe the essential points of the SN analysis setup in this version of the DESC SRD:

The surveys are simulated in four separate parts: a one-year DDF survey, a ten-year DDF survey, a ten-year WFD survey and an external low-redshift sample. For all simulations we use simulation libraries from [Biswas et al. \(2017\)](#) to take the OpSim `minion_1016` run and provide inputs to the SuperNova ANALysis (SNANA [Kessler et al. 2009](#)) software to generate supernova light curves. Then we fit those light curves with the SALT2 model ([Guy et al. 2007](#); [Betoule et al. 2014](#)), and compute distance moduli using the [Marriner et al. \(2011\)](#) approach. The analysis follows the prescription of [Scolnic et al. \(2018\)](#), which was most recently used for the Pantheon sample of supernovae.

These statements assume that a commissioning mini-survey will reach ‘template depth’ of 5-10 times the single night coadd depth of the DDF (around 3000s exposures) in the DDF regions to produce deep templates in order to detect SN from difference images in the first year of operation. In the absence of such a mini-survey, the first year survey results should be considered to have significantly fewer SN<sup>34</sup> – or, effectively, the first year forecasts actually describe our capabilities after 2-3 years rather than one year. Similarly, the first few years of observation of the wide field will be used to generate templates, hence we do not assume a WFD year-one survey, and restrict ourselves to those obtained after 10 years.

<sup>34</sup>This is not just because of the time to make the observations that will be used to build the templates, but because of the need for a time lag to avoid the supernovae we want to measure being in the templates.

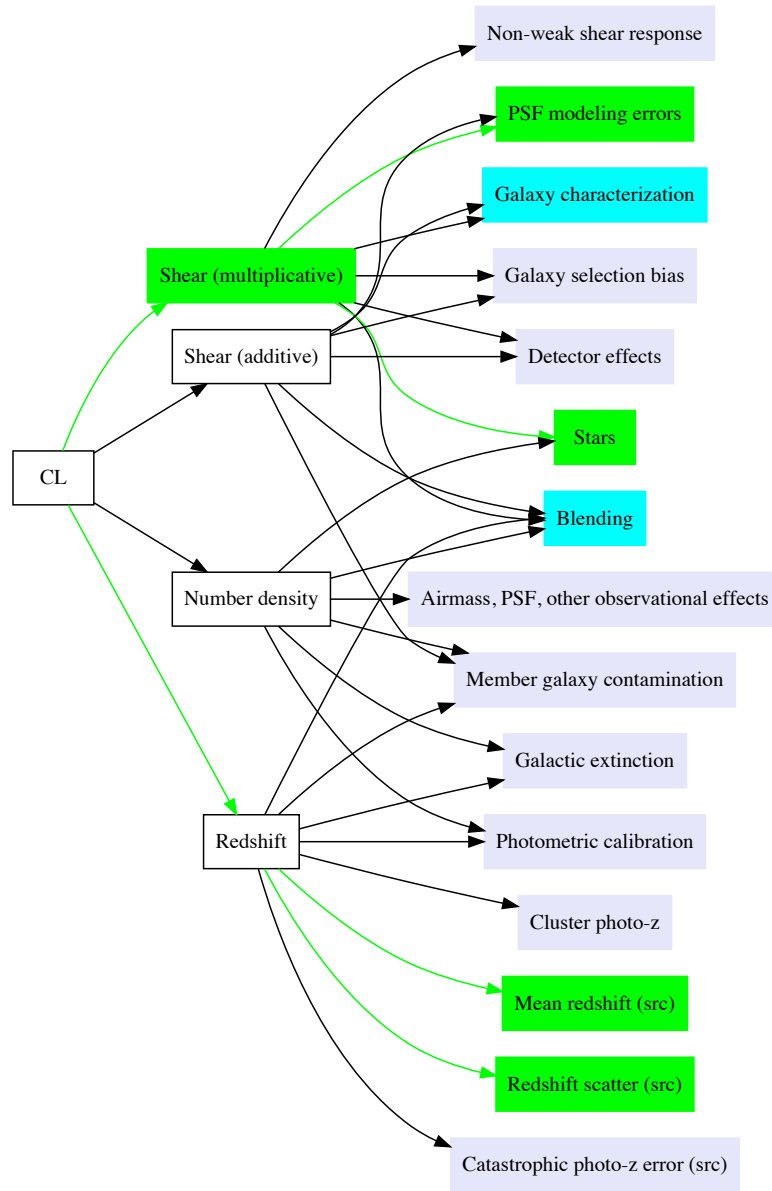


Figure D4: Diagram indicating sources of systematic uncertainty for the CL analysis on which we would like to place requirements in the DESC SRD. The direction of the arrows indicates the flow from overall systematic uncertainty to broad systematics categories to the specific physical effects on which we place requirements. As shown, there are several low-level issues in the right-hand column that contribute to multiple categories of uncertainty in the middle column. The green / lavender boxes indicate sources of uncertainty on which we do / do not place requirements in this DESC SRD version, respectively. The cyan boxes indicate those for which more R&D beyond the DESC’s DC2 may be needed in order to place requirements. For some of the green boxes, we currently only have software infrastructure to place requirements through their impact on one class of uncertainty; such connections are shown as green arrows.



The current software framework for forecasting cosmological constraining power with SNe and the impact of systematics involves a sample of simulated Type Ia supernovae, with selection cuts, that get passed through light curve fitters. The simulated SN analyses currently assume that the supernova redshifts are being determined through spectroscopic follow-up of the host galaxies. Such spectroscopic follow-up of hosts is considerably simpler than spectroscopic followup of active supernovae, as it does not need to be done during the few-week window when a supernova is bright. Also, several supernova hosts within a small patch of sky aggregated over time may be simultaneously followed up using suitable multi-object spectrographs<sup>35</sup>.

250,000 fiber hours have been allocated on 4MOST for the 4MOST-TiDES observations of transients, SN hosts, and AGN reverberation mapping – with LSST being the primary source of transients. The usage of that allocated time is being decided, with a view to target as many viable hosts as possible (including galaxies where the SN candidate is not obvious). 4MOST can reach a depth of  $r \sim 22$  with 1-hour exposures, which corresponds to roughly  $z \sim 0.4 - 0.6$  (in OzDES). This will cover the bulk of the wide-survey candidates. In future, it will be valuable to estimate how many of the WFD supernovae may have redshifts from the DESI survey, but this is likely to be subdominant to the number that will be acquired by 4MOST. For the purpose of this forecast we assume the redshifts in the DDF will come from Subaru (see below).

We reduce the full simulated sample to a subset which would have spectroscopic host information assuming 20 nights of observing time with the Prime Focus Spectrograph on the Subaru telescope in the Deep Drilling Fields, which can reach  $i = 22.86$  hosts, plus 250k fiber-hours with the 4MOST survey spread over the WFD area, which can reach  $i = 22$  with the maximum possible 6 visits per fiber. The fraction of Type Ia supernovae at a given redshift which are expected to have hosts bright enough for spectroscopy based on the stellar mass/SFR/photometric redshift catalogs of [Laigle et al. \(2018\)](#) are shown in [Figure D5](#). We note that a similar (same order of magnitude) amount of observing time on DESI in the DDFs could garner a comparable number of host redshifts, given that DESI has a larger FoV, compensating for its smaller collecting area. Hence there are two potential pathways to obtain host redshifts for the DDF supernovae.

The restriction on fiber hours leads to a total restriction of 100k supernovae which we obtain by scaling the overall efficiency curves until we obtain the 100k objects in the final sample (see the note on fitting light curves below). For both surveys we also assume an 80% secure redshift rate given the S/N for the assumed exposure times, and assuming that some time is spent obtaining redshifts for non-Ias and other objects (converting an initial estimate of 125k supernova candidates to 100k). In this forecast, we assume the supernovae without redshifts will not be used for cosmological constraints. Work is ongoing within the DESC to study both the impact of host photo- $z$  contamination on the overall science FoM, including mis-identification of hosts, and the best practice for mitigating redshift error ([Roberts et al. 2017](#); Malz, Peters, Hlozek et al. in preparation<sup>36</sup>). It is worth noting that the dark energy task force

<sup>35</sup>Such follow-up, which is used in current photometric supernova surveys like DES and Pan-STARRS, might be easiest to combine with needs of other working groups like photometric redshifts.

<sup>36</sup><https://github.com/aimalz/scippr>

(DETF) assumed a much larger sample of 400k photometric supernovae with an ‘optimistic photo- $z$ ’ error. We restrict ourselves to the more conservative case described above.

The Foundation survey (Foley et al. 2018) will observe  $\sim 800$  low redshift SNe by the time it completes the survey in 2020. For the Y10 survey, we triple this number of low-redshift SNe, given the number of low-redshift surveys (e.g. ZTF) that will be online and will yield impressive numbers of supernovae by the end of the LSST Y10 survey. We include this sample by decreasing the error on the distance modulus in our final Y10 sample by  $\sqrt{3}$  for  $z < 0.05-0.1$ . This low- $z$  sample is an essential anchor to the Hubble diagram. For the low- $z$  sample, we do not include here any individual calibration systematics for the different samples and filters. Instead, we include the SALT2 calibration systematic and uncertainty in the HST calibration which affects both low- $z$  and LSST supernovae. Future versions of the DESC SRD should factor in a reasonable level of calibration uncertainties for the external low- $z$  sample, which will mildly change its constraining power.

The supernovae are then fit in two stages: the data are fit with light curve templates based on the SALT2 model (Guy et al. 2007; Betoule et al. 2014). At this stage, detection quality cuts are applied, and the number of supernovae reduces slightly compared to the original simulated light curve points. There is a quality cut to restrict the number of objects that we would put fibers on (for host- $z$  determination): we require objects to have three epochs that have signal-to-noise ratios in the nightly coadds of greater than five. An epoch here is based on a detection where the likelihood of detection follows an SNR-dependence as modelled by the Dark Energy Survey. The quality cut at this stage is to ensure that any fibers used to obtain host galaxy spectra are placed on ‘high quality’ candidates.

The separate subsamples described above are then combined to form the overall Y1 and Y10 samples as follow: DDF Y1 and an 800-SN low- $z$  sample to form the overall Y1 sample; DDF Y10, a 2400-SN low- $z$  sample, and WFD Y10 sample to form the overall Y10 sample.

We apply the following quality cuts for inclusion of the SNe in the final cosmological sample:  $|c| < 0.3$ ,  $|x_1| < 3$ ,  $\sigma(x_1) < 1$ ,  $\sigma(t_0) < 2$ , where  $c$ ,  $x_1$ ,  $t_0$  are the color, stretch and explosion time respectively. Following the cuts on light curve fit quality, we arrive at a sample of  $\sim 2400$  SNe for the Y1 sample, and  $\sim 104000$  SNe for the Y10 sample. The distance moduli are included as a likelihood in CosmoSIS<sup>37</sup> (Zuntz et al. 2015), which makes use of algorithms for efficient sampling of cosmological parameter space (Lewis et al. 2000; Howlett et al. 2012).

The number of SNe obtained and their light curve quality depend strongly on the survey cadence. Initial studies show that the total number of high-quality SNe in the 10-year survey can change by a factor of  $\sim 1.5$  with cadences that are optimized for their detection, which will not only improve the statistical uncertainty, but also allow for new studies of supernova systematics<sup>38</sup>.

For the WFD survey, the corresponding numbers depend even more strongly on the cadence strategy employed. With that caveat, we obtain a final sample combining the WFD and DDF and low- $z$  data of

<sup>37</sup><https://bitbucket.org/joezuntz/cosmosis/wiki/Home>

<sup>38</sup>Exploration of the impact of cadence on cosmology with SNe is a key ongoing DESC activity.

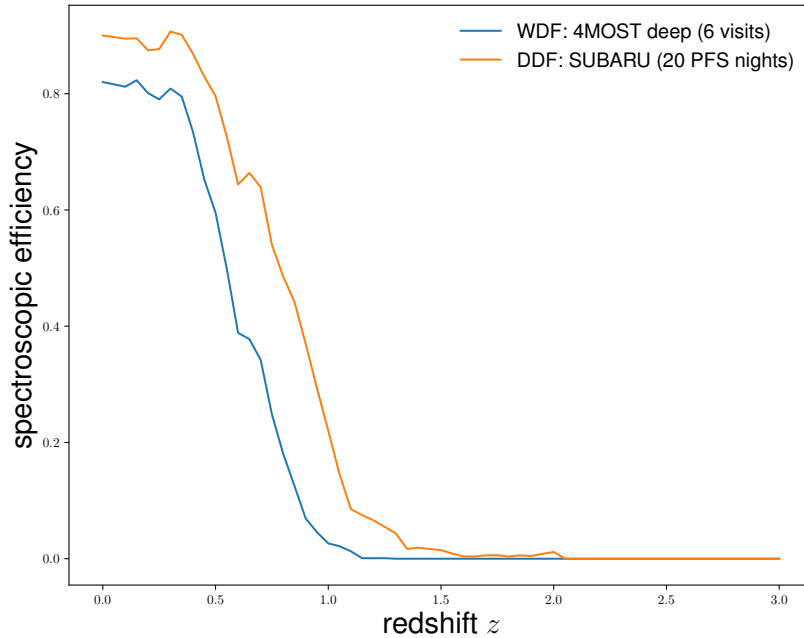


Figure D5: Host spectroscopic redshift efficiencies for the WDF and DDF fields, assuming follow-up using a combination of maximum-depth observations with the 4MOST survey (for WDF) and 20 nights of observing time with the Prime Focus Spectrograph on the Subaru telescope (for DDF). The curves correspond to the fraction of Type Ia supernovae at a given redshift which have hosts bright enough to be targeted for spectroscopy (corresponding to a limit of  $i = 22$  for the maximum possible 6 visits with 4MOST, or  $i = 22.86$  for this Subaru survey). We place additional restrictions on the total number of SNe that can be followed up with 4MOST, given the total allocation of 250k fiber-hours. In addition to the losses from hosts too faint to target that are plotted here, we assume that 20% of targets will fail to yield highly-secure redshifts based on past experience with data of the expected S/N.

$\sim 112\,000$  SNIa with sufficiently well-sampled light curves, host galaxy redshifts, with a distribution peaking around  $z \sim 0.4$ . The WFD and low- $z$  sample significantly improve the SN science case for the following reasons:

- The resulting low-redshift sample is complete up to  $z \sim 0.4$ , which adds significantly to the quality of the Hubble diagram constraints.
- $z < 0.5$  is roughly the redshift range where BAO is limited by cosmic variance. An all-sky  $z \lesssim 0.5$  SN sample over ten years is unique as a distance indicator in this region. Further, we note that there is no other SN survey capable of producing a sample of around 100 thousand supernovae.
- A rolling cadence or other more optimal cadence may substantially increase the number of SNe with well-sampled light curves, allowing us to reach the nominal statistics in a fraction of the duration of the survey (modulo uncertainties in the host redshift), and providing a larger sample with which to study systematic effects. It may also enable the construction of a deeper supernova sample, extending the redshift lever arm for this probe.
- The low-redshift sample will also be useful both in constraining non-standard cosmological models and improving our understanding of the SN population and underlying correlations with environments. Moreover, it allows for the opportunity of probing structure growth with supernovae.

In contrast, the deep drilling fields will generate a superb ‘gold’ sample of supernovae out to  $z \sim 1.2$ , which not only allow for cosmological constraints, but will enable us to study the redshift evolution of supernova systematics (e.g., evolution of SN populations).

#### D4.2 Anticipated improvements

In future DESC SRD versions, we believe we can improve both the precision and accuracy of supernova cosmology with several changes to the baseline analysis presented here. These new approaches are still a subject under development, and the tradeoff in terms of quantitative success versus additional computational cost will determine which approaches are adopted in the end. We present a brief outline of such newer analysis methods below:

1. Standardization of supernova light curves: Historically, supernova cosmology has used a two-step standardization approach of (a) compressing SNIa light curves into a universal function of a few light curve model parameters thereby dimensionally reducing the multi-band time series dataset, and then (b) using a correlation between these light curve model parameters to an intrinsic brightness or distance of the supernova. Currently, surveys use models (Guy et al. 2007) which include a scatter  $\sim 0.1$  mags in the resultant redshift-distance relationship, part of which correlates with the environment of the supernova, potentially leading to biases in cosmological analysis.

Following current standard approaches, the baseline analysis tries to account for this via post-facto correctional terms based on host galaxy stellar mass, and an attempt to distribute the scatter in the different model parameters. A better approach that minimizes the intrinsic dispersion and accounts for such environmental dependence in training the model itself requires the development of newer SN light curve models (Kim et al. 2013, 2014; He et al. 2018), which is a key project in the SRM. These more sophisticated models will also make it possible to incorporate redshift dependencies of the components of the models, which presumably are primarily related to the environmental correlations with redshift (known and unknown).

2. **Supernova selection:** The selection criteria for the supernova sample in the baseline analysis is designed to yield a sample which has a small impurity of moving objects. While this might have a small impact on surveys designed for SN cosmology, it is possible that this choice has a large impact on the supernova sample for a multipurpose survey like LSST. Therefore, we would like to investigate the possibility of less aggressive selection combined with a more computationally-intensive filtration step to a sample purity similar to the current strategy. For certain observing strategies, this could result in an increase in good quality supernovae in the final cosmological sample.
3. **Cosmology Inference:** The current baseline analysis uses a method of estimating the distance modulus (Marriner et al. 2011) and intrinsic dispersion which has been validated on SDSS data, and compares binned theoretical and ‘observed’ values of distance moduli for supernovae binned in redshift. In the future, we would like to better model the relationships between different parameters used in the cosmological inference (e.g. Hinton et al. in preparation<sup>39</sup>), including the systematic parameters, leading to a likelihood of a large number of parameters. An important feature of these methods is that they enable better treatment of systematics, leading to better knowledge of them after the analysis. A problem with these methods is the integration with other probes in the joint likelihood analysis (e.g. with TJP tools due to software and parallelization issues).
4. **Photometric Classification and Cosmological Inference:** The current baseline analysis assumes that (binary) photometric classification (using PSNID; Sako et al. 2011; Campbell et al. 2013) is performed accurately. In practice, any photometric classification algorithm will mis-classify objects, causing biases. This can be accounted for using algorithms like BEAMS (Hlozek et al. 2012; Jones et al. 2017) in the future. Further, we plan to study the extension of cosmological inferences with photometric classification to include supernovae whose host redshifts are not known (Roberts et al. 2017; Malz, Peters, Hlozek et al. in preparation<sup>40</sup>).
5. **Cross-correlations between probes:** Some of the systematic effects that affect the supernova science case can be mitigated by cross correlating supernova with other probes, and indeed can

---

<sup>39</sup><http://dessn.github.io/sn-doc/doc/out/html/index.html>

<sup>40</sup><https://github.com/aimalz/scippr>

mitigate the systematics of other probes. For example, measurements of the LSST SN magnifications could be used to calibrate multiplicative errors in the LSST cosmic shear measurements (Zhang 2015), while measurements of the skewness and kurtosis of the SN magnitude distribution (see Macaulay et al. 2017) will help constrain  $\sigma_8$ . Further study of the impact of systematics on these cross-correlations will be an important area of research and development with DC2 data and beyond.

6. Retraining the SALT2 model: SN4 shows that it is essential to retrain the SALT2 models as part of the analysis. Also, doing this retraining simultaneously with the cosmology inference has the potential to add constraints on filter wavelength calibration.

On a more technical note, non-Gaussian contours in cosmological parameter space may need to be more fully addressed in future DESC SRD versions; they were neglected in this one.

The issue of redshift uncertainty and its impact on the supernova science case is an active area of study within the DESC SNWG. In this analysis we assume the existence of host spectroscopic redshifts for all supernovae that form part of the final sample. In the next iteration of the DESC SRD, we will deviate from this default, by also assuming a simple photo- $z$  model for the majority of objects. This subsample will again be selected with an efficiency that roughly matches expected spectroscopic redshift yield. This source of systematic uncertainty is one of the most important ones to model in the future, as this affects both axes on the Hubble diagram ( $\mu$  fits in addition to  $z$ ).

In this analysis, we have also made a large simplifying assumption that the cosmology sample consists of only Type Ia supernovae that have been selected with perfect efficiency and purity. The potential bias from misclassification (so-named classification uncertainty), will be introduced in the future by including some percentage (a few percent, given reasonable estimates of classification purity, see e.g. Campbell et al. 2013) of non-Ias for which the light curves get fit as if they were Ias, and checking the induced bias. This results in a conservative requirement that ignores improvements that can be gained from probabilistic inference methods (e.g., Roberts et al. 2017), and would represent our ‘worst case’ scenario for classification bias.

### D4.3 Systematic uncertainties

For the SN analysis, we consider the following classes of systematic uncertainties in our two categories:

- Self-calibrated systematics: astrophysical systematics (errors in the modelling of SN and their standardization based on the supernova light curve, the environment, and any other redshift dependencies, including those induced by weak lensing magnification and peculiar velocities)
- Calibratable systematics on which we place requirements: calibration (uncertainty on filter zero points, the transmission function wavelength, wavelength-dependent flux calibration, uncertainties in Galactic extinction corrections); redshift uncertainty; detection, classification

The models for the self-calibrated systematic uncertainties are summarized in [Table D7](#). For each source of systematic uncertainty, we describe how it is included in this DESC SRD version, as well as aspirations for more complex models to be included in the future. Generally speaking, the systematic uncertainties are estimated by simulating the supernova sample with the given systematic effect included and comparing the distance modulus to the case where no systematic is included. This difference in the distance modulus redshift-by-redshift produces a systematics covariance matrix for each systematic, which is added to the intrinsic scatter. In these cases, the systematic uncertainty is naturally estimated as a data covariance ( $\mu$  estimates) and then propagated into cosmological parameter space.

We assume that the error in the intrinsic dispersion modelling will be reduced by two times its current value given the large sample of SNe in the full survey that can be used to study the scatter, in combination with spectra from the ground-based collaboration. Similarly, for the host mass-SN luminosity correlations, a bias in the high-mass sample following the model from [Hounsell et al. \(2017\)](#) is introduced into the simulations and ignored in the fitting, and this is used to estimate the resulting systematic uncertainty.

We introduce a SN-color population drift (again following the prescription in [Hounsell et al. 2017](#)) that gets ignored in the fitting to determine the systematic uncertainty. Finally, we include a systematic due to the potential from evolution of the  $\beta$  SALT2 parameter which describes the colour-luminosity correlation, which we include as half of the measurement uncertainty of  $d\beta/dz$  as determined from our simulated LSST sample, because we can take the average of the observed and expected values.

Self-calibrated systematic uncertainty	Current model baseline	Future plans
Standardization of color-luminosity law and its $z$ -dependence	Marginalization over SALT-II parameter $\beta$ <a href="#">Scolnic et al. (2014)</a> at half the predicted measurement uncertainty	Same as current model
Intrinsic scatter	Modelling differences between <a href="#">Guy et al. (2010)</a> and <a href="#">Chotard et al. (2011)</a> at half model differences	To be decided
Host mass-SN luminosity correlations	High-mass sample bias as in <a href="#">Hounsell et al. (2017)</a>	To be decided
Magnification-induced covariances (especially for DDFs)	Not modeled	To be decided
Individual low- $z$ calibration uncertainty	Not modeled	To be decided

Table D7: Self-calibrated systematic uncertainties for SN.

The residual calibratable systematic uncertainties on which we will place requirements can be divided into 3 categories: calibration, redshift, and identification-related systematic uncertainties. A diagram of these calibratable systematics is shown in [Figure D6](#), while the current models and future plans for how to represent them is in [Table D8](#).

The DESC’s DC2 analysis effort will provide more sophisticated models for the impact of several of these effects than the ones used in these simulations.

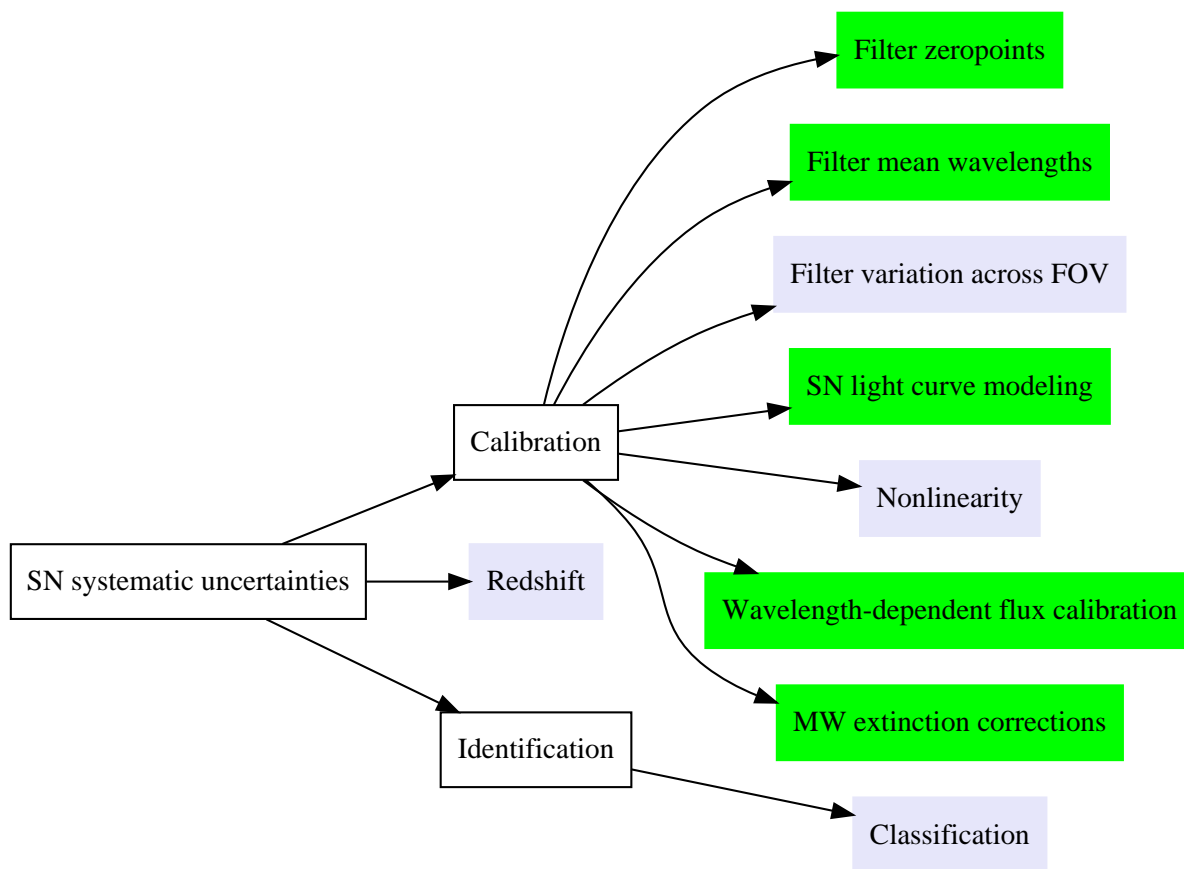


Figure D6: Diagram indicating sources of systematic uncertainty for the SN analysis on which we would like to place requirements in the DESC SRD. The direction of the arrows indicates the flow from overall systematic uncertainty to broad systematics categories to the specific physical effects on which we place requirements. The green boxes indicate sources of uncertainty on which we place requirements in this DESC SRD version, respectively. In some cases, as discussed in [Table D8](#), the systematics models will have to be updated.

One might expect systematic errors to be correlated (for example the filter mean wavelengths and cutoff positions). Here we have assumed that all systematics can be varied individually, and estimated the



Calibratable systematic uncertainty	Current model baseline	Future plans
Calibration		
Filter zero points	$\mathcal{N}(0, 1 \text{ mmag})$ offset per band	Same as current model
Filter mean wavelength	$\mathcal{N}(0, 1)$	Same as current model
Filter variation across FOV	None	10 measurements across FoV with 5 Å mean wavelength uncertainty
SN light curve modeling	One-third scaling of <a href="#">Betoule et al. (2014)</a> SALT2 parameter covariance matrix	Same as current model
Nonlinearity	None	3 mmag over 5 mag
Wavelength-dependent flux calibration	5 mmag slope over 7000 Å	Same as current model
MW extinction corrections	5% scaling of <a href="#">Schlafly et al. (2014)</a> model	Same as current model
Redshift		
Redshift	None	To be included based on DC2
Identification		
Classification	None	To be included based on DC2 or DC3

Table D8: Calibratable systematic uncertainties for SN. The numbers given in the table represent a base value for the level of uncertainty; the requirements given in [Section 5.4](#) were placed using contaminated data vectors with various multiples of this best guess. Note that the ‘base’ value of the systematics was chosen as larger than our intended baseline, in order to fully investigate the systematics requirements.

impact of them separately. For the band-dependent systematics we then include their combined contribution through a Monte Carlo simulation of the individual bias vectors. This allows for the separate uncertainties for different bands.

Finally, we note that the extinction requirement is placed without allowing for uncertainty in the Milky Way dust law, which is yet another layer of complexity with the potential to introduce apparent differences between low- and high-redshift supernova populations. We defer consideration of this effect to future versions of the DESC SRD.

## D5 Strong lensing

### D5.1 Analysis choices

Here we describe the essential points of the SL analysis setup in this version of the DESC SRD:

The Y10 strong lensing sample for our baseline analysis consists of time delay systems and compound lenses. The time delay cosmography sample is defined as 400 lensed quasar systems monitored with LSST through 2032 and followed-up with TMT/GMT/JWST/E-ELT, so as to provide a 7% time delay distance measurement after marginalization over lens model parameters (including lens galaxy mass distribution, environment and line of sight structure). This marginalization is implicit, not explicit. The sample size was estimated using OM10 predictions<sup>41</sup> (Oguri & Marshall 2010) and results of the DESC’s Time Delay Challenge, with requirements on length of the time delay, image separation, and ability to obtain follow-up data.

The Y10 compound lens sample is assumed to include 87 double source plane lenses. This calculation uses LensPop<sup>42</sup> (Collett 2015) modified to include compound lenses using best seeing single epoch imaging alone. Thus all systems are bright enough that follow up is practicable. We assume that each is followed up with TMT/GMT/JWST/E-ELT so as to provide fractional precision on  $\beta$  of  $[(0.01/R_{\text{ein},1})^2 + (0.01/R_{\text{ein},2})^2 + 0.01^2]^{1/2}$  after marginalization over lens model parameters.

For Y1, lensed quasars are challenging due to the need to generate high-quality template imaging that can be used as a reference for identifying time-varying objects in the first  $\sim 2$  years of the survey. As for supernovae, we assume that a commissioning mini-survey may result in templates being available slightly earlier than would otherwise be possible. We assume 20 of the brightest and most variable lenses will get measured time delays early. We can, however, reliably assume there will be of order ten compound lenses in Y1.

In both Y1 and Y10, the likelihood function is taken as gaussian in  $D_{dt}$  for time delay lenses (no requirement on  $D_A$  from lens velocities). For compound lenses the likelihood is taken as Gaussian.

These forecasts assume 1 high resolution image per lens (space or AO), and spectroscopic redshifts for lens and source in each system. In Najita et al. (2016), it was estimated that adaptive optics IFU spectroscopy for characterizing lens galaxy velocity dispersions and image positions for 100 strong lens

<sup>41</sup><https://github.com/drphilmarshall/OM10>

<sup>42</sup><https://github.com/tcollett/LensPop>

systems would require roughly 100 hours on GSMTs in total (or greater amounts of time on 8-10m telescopes). Given the relatively modest requirements when spread out over a number of years, we therefore assume that the needed spectroscopy will be done. As a backup plan, WFIRST or Euclid could provide some of the high-resolution imaging.

## D5.2 Anticipated improvements

This version of the DESC SRD does not include lensed supernovae in the forecasts, because of the additional need for high-resolution cadenced imaging. Further developments with respect to follow-up telescope resources may lead to their inclusion in the future. We anticipate that the Y10 sample could include 50-500 lensed SNe systems (strongly dependent on follow-up resources), each providing a 5% time delay distance measurement after marginalization over lens model parameters.

There are also  $\sim 3500$  lensed quasars that could yield precise time delays with supplementary data points on their light curves. There are up to 2000 fainter compound lenses that are discoverable with LSST coadds. Exploiting these fainter systems will require significantly more high-resolution imaging time, and hence we defer consideration of these additional systems for the future.

## D5.3 Systematic uncertainties

For the SL analysis, we consider the following classes of systematic uncertainties in our two categories:

- Self-calibrated systematics: lens model assumptions (lens galaxy mass distribution), environment effects (including halo vs. stellar mass relation), line-of-sight structure, compound lensing in double source plane
- Calibratable systematics on which we will eventually place requirements: time delay measurement systematics, selection bias, photometry issues including blending, photo- $z$  and  $M_*$  errors in environment analysis

Currently the self-calibrated systematics are all included implicitly in the forecasts through adoption of a larger uncertainty in distance estimates than are obtained from statistical error in the time delay measurements. Future work within the DESC will include a more physical forward-modeling of these effects and their impact on dark energy observables.

Developing models for how the calibratable systematics enter the observable quantities for LSST (specifically through challenges in time delay estimation or sample characterization) will be an important task for the DESC SL working group during DC2 and DC3. In this DESC SRD version, in the absence of such models, no requirements will be placed for the SL analysis.

## E Synthesis of systematic uncertainties across all probes

### E1 Systematic uncertainties in this DESC SRD version

In this section, we synthesize the list of systematic uncertainties on which requirements are placed in this DESC SRD version (see [Table E1](#)). As in the appendices on individual probes, we divide them into categories (e.g., uncertainties in redshifts, number densities, and so on). The top two categories are considered only for probes of structure growth, while the last is considered only for SN.

Systematic uncertainty	Probes	Note
Redshift uncertainties		
Mean redshift	LSS, WL, CL	For CL, only source redshift uncertainties were considered
Redshift scatter	LSS, WL, CL	
Shear (multiplicative) uncertainties		
Overall multiplicative bias	WL, CL	This requirement encompasses all sources of multiplicative bias
Stellar contamination	WL, CL	Subset of “Overall multiplicative bias”
PSF modeling errors	WL, CL	Subset of “Overall multiplicative bias”
Photometric calibration uncertainties		
Filter zeropoints	SN	
Filter mean wavelengths	SN	
Wavelength-dependent flux calibration	SN	
Light curve modeling	SN	
MW extinction corrections	SN	

Table E1: List of all sources of systematic uncertainty for which we place requirements in this version of the DESC SRD.

### E2 Systematic uncertainties deferred for future work

In this DESC SRD version, we have focused on a limited list of systematic uncertainties for which there is a clear prescription for describing how they modify the observable quantities for dark energy analysis. More complete wish-lists for calibratable systematic uncertainties on which requirements could be placed in future may be found for each probe in [Appendix D](#). More generally, as the DESC’s analysis pipelines are constructed and models for systematics characterization and mitigation are built, interconnections between classes of uncertainties should be noted. For example, if a given effect could result in systematic uncertainty in both redshift and number densities, a self-consistent model for those un-

certainties should be built. Similarly, self-consistent models should be built for how a given systematic uncertainty affects the observables in different cosmological probes.

As described in [Section 2](#), the choice not to place requirements on model-sufficiency for either type of systematic uncertainty may also be revisited in future DESC SRD versions.

While not strictly a systematic uncertainty, one issue affecting all probes that is important for fulfilling our high-level objectives ([O3](#)) and requirements ([RH4](#)) is the development of blinding methods that work at the level needed for single and joint probe analysis.

## F Defining number densities

For the WL, LSS, and CL analyses, we need to define Y1 and Y10 source galaxy number densities and redshift distributions. LSS and WL also require number densities and redshift distributions for the photometric lens sample. Older estimates, e.g., in the LSST Science Book ([LSST Science Collaboration 2009](#)), used the best deep ground-based data and spectroscopic redshift samples available at the time. We would like to confirm these estimates for Y10 using more recent datasets, and produce a Y1 estimate.

Below we derive the photometric sample number density ([Appendix F1](#)), the source sample number density ([Appendix F2](#)), the photometric sample redshift distribution ([Appendix F3](#)), and the source sample redshift distribution ([Appendix F4](#)). These numbers are somewhat different than common assumption on LSST densities found in the LSST science book based on updates in our understanding both in observations and simulations, as will be described in detail in each subsection.

### F1 Photometric sample number density

To estimate the overall galaxy number density for a photometric sample with a given flux limit, we use the HSC<sup>43</sup> Deep field *i*-band catalogs from the HSC Survey Public Data Release<sup>44</sup> 1 ([Aihara et al. 2018](#)). This sample is useful because it requires relatively minimal extrapolation to LSST depths, is a large enough field that cosmic variance is not too significant, and the bandpass is similar to the expected LSST *i*-band.

The HSC data were downloaded with an SQL query that was designed to get a complete galaxy sample that goes as deep as possible, with only minimal flag cuts (e.g., star/galaxy classification, only primary detections, and nothing with saturated/interpolated pixels near the center of the galaxy). A bright star mask was imposed. Random points were also downloaded from the HSC deep database while imposing the same flag cuts, in order to properly calculate the area<sup>45</sup>.

Using the random points, we calculated the area as 26.1 deg<sup>2</sup>. Note that this includes a  $\sim 12\%$  reduction factor for masks due to various image defects, bright stars, and so on. The number densities we calculate

<sup>43</sup><http://hsc.mtk.nao.ac.jp/ssp/survey/>

<sup>44</sup><https://hsc-release.mtk.nao.ac.jp/doc/>

<sup>45</sup>The real and random SQL queries can be found in the Requirements repository, ‘number\_density/hsc.sql’ and ‘number\_density/hsc\_rand.sql’. The script that used the resulting HSC catalogs to carry out the calculations described below and make [Figure F1](#) is ‘number\_density/dndmag\_hsc.py’.

do *not* include this reduction at the outset. Since our adopted survey area does not account for masking, we need to include it by reducing our number densities at the end by a factor we will call  $1 - f_{\text{mask}}$ . Assuming that  $f_{\text{mask}} = 0.12$  would amount to an assumption that HSC and LSST will have similar levels of masking.

The differential  $dN/d\text{mag}$  (using the  $i$ -band forced `cmode1` magnitudes) is shown in the top panel of [Figure F1](#), along with a power-law fit that is extrapolated to faint magnitudes. Analysis of deep pencil-beam HST surveys suggests that extrapolating a power-law  $dN/d\text{mag}$  is a reasonable approximation.

We can use this power-law and the area of the survey to get the cumulative counts as a function of limiting  $i$ -band magnitude  $i_{\text{lim}}$ . The result is shown in the bottom panel of [Figure F1](#). Including the factor of  $f_{\text{mask}}$ , our adopted number density as a function of  $i_{\text{lim}}$  is

$$N(< i_{\text{lim}}) = 42.9 (1 - f_{\text{mask}}) 10^{0.359(i_{\text{lim}} - 25)} \text{ arcmin}^{-2} \quad (9)$$

For the calculations in this version of the DESC SRD, we define the Y1 and Y10 gold samples using  $i_{\text{lim}} = 24.1$  and  $25.3$ , respectively. These limiting magnitudes come from defining the gold sample magnitude limit one magnitude brighter than the median survey depth at any given time (see [Appendix C1](#) for assumptions about survey depth). We also adopt  $f_{\text{mask}} = 0.12$ . This results in Y1 and Y10 photometric sample number densities of 18 and 48  $\text{arcmin}^{-2}$ , respectively.

## F2 Source sample number density

For weak lensing forecasts, we need the source effective number density  $n_{\text{eff}}$  (accounting for the necessary downweighting for low signal-to-noise shear estimates; e.g., [Chang et al. 2013](#)) for Y1 and Y10. To estimate this quantity, we use a method similar to that of [Chang et al. \(2013\)](#). Specifically, we use the WeakLensingDeblending (WLD<sup>46</sup>) package to simulate the LSST CatSim galaxy catalog in the  $i$  and  $r$  bands, and use the following values for each simulated galaxy:

- True redshift  $z$ ,
- Estimated measurement error  $\sigma_m$  for each shape component calculated using the parameterization  $\sigma_m(\nu, R)$  of [Chang et al. \(2013\)](#), and
- Estimated purity  $\rho$  (a measure of blendedness in the range 0–1, with 1 for a perfectly isolated source).

The code used for this analysis is in a jupyter notebook<sup>47</sup> in the Requirements repository. We have performed detailed comparisons of WLD results against [Chang et al. \(2013\)](#) and discovered some issues that were later determined to be a problem in that work rather than in this notebook, but the overall agreement is good.

<sup>46</sup><https://github.com/LSSTDESC/WeakLensingDeblending>

<sup>47</sup>`notebooks/RedshiftDistributions.ipynb`

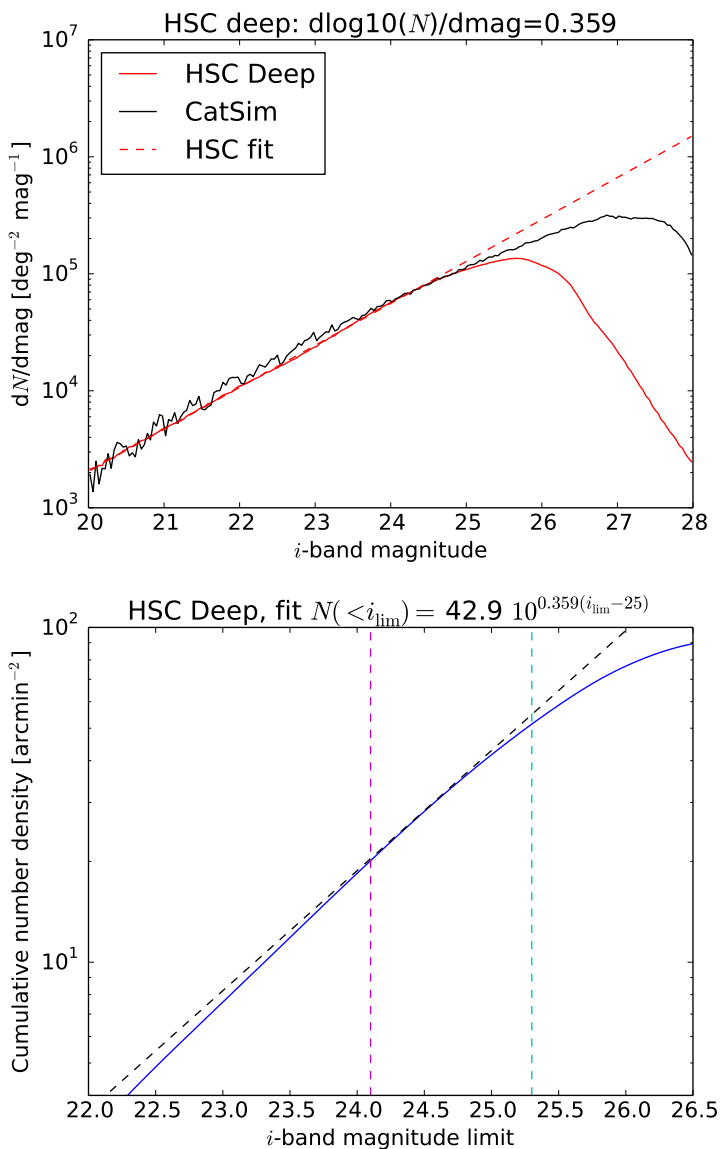


Figure F1: *Top*: The differential distribution of  $i$ -band galaxy magnitudes in the HSC Deep survey. Before the turnover due to incompleteness, the data (red solid curve) were fit to a power-law, shown as a red dotted line, with a slope indicated in the plot title. Finally, the  $dN/dmag$  in the CatSim catalog used for WeakLensingDeblending simulations (described in more detail in [Appendix F2](#)) is shown in black. *Bottom*: The cumulative number density of galaxies as a function of  $i$ -band limiting magnitude  $i_{lim}$ . The power-law fit to the differential counts from the left panel was used to get an extrapolated version of the cumulative counts, shown as a dashed line. Vertical lines show the Y1 and Y10 limits of the photometric sample used for clustering analysis, as described in [Appendix F1](#). The power-law equation is shown in the plot title.

We are interested in different sample definitions using:

- Y10 or Y1, where Y1 is defined as 0.1 of the total exposure time in each band for the purposes of WLD simulations.
- The combined  $i+r$  sample or else  $i$  and  $r$  individually. For the combination, we use only galaxies detected in both bands and define the combined  $\sigma_{m,i+r}^{-2} = \sigma_{m,i}^{-2} + \sigma_{m,r}^{-2}$ .
- A weak-lensing sample selected using  $\sigma_m < k \cdot \sigma_{SN}$  with  $k = 1$  (nominal), 0.5 (conservative) or 2.0 (optimistic). We fix  $\sigma_{SN} = 0.26$  for this cut.
- With or without blending corrections. Blending reduces  $\nu$ , which in turn reduces  $\sigma_m(\nu, R)$ , and thereby the selection fraction and the  $n_{\text{eff}}$  weight. We also remove galaxies with  $\rho < \rho_{\text{min}}$  from the sample, assuming that they are too blended for reliable photo- $z$  and shear estimation.

**Table F1** summarizes the results with  $k = 1$ . Note that our treatment of blending effects is not particularly conservative: we assume that all galaxies below a certain overlap fraction ( $\rho_{\text{min}} = 0.85$ ) are unusable and all other galaxies are optimally deblended.

Epoch	Bands	Blended	$n$	$n_{\text{eff}}$
Y10	$i+r$	Y	34.091	<b>27.737</b>
Y10	$i+r$	N	41.765	34.581
Y10	$i$	Y	25.658	20.732
Y10	$i$	N	32.557	26.562
Y10	$r$	Y	26.594	21.402
Y10	$r$	N	34.319	27.922
Y1	$i+r$	Y	13.969	<b>11.112</b>
Y1	$i+r$	N	16.174	13.052
Y1	$i$	Y	10.230	8.051
Y1	$i$	N	12.317	9.744
Y1	$r$	Y	10.402	8.170
Y1	$r$	N	12.622	10.024

Table F1: Summary of results with  $k = 1$ . The last two columns give the integrated densities  $n(z)$  and  $n_{\text{eff}}(z)$ , respectively, in units of galaxies per square arcminute. These densities are not corrected for any masking effects. The scenarios that we use for forecasts are shown in red.

### F3 Photometric sample redshift distribution

While the photometric sample number density as a function of limiting magnitude can be obtained from HSC, this is not possible for the redshift distributions, due to the lack of redshift information in HSC.



Hence we derive redshift distributions from the CatSim input catalog used for WLD, with a strict  $i$ -band limit as for the photometric samples discussed in [Appendix F1](#). As a sanity check, they were compared against parametric fits to spectroscopic redshift distributions estimated using DEEP2<sup>48</sup> data, correcting for the impact of selection/color cuts using the targeting weighting factors. The data only include redshifts up to  $z \sim 1.4$ , so the redshift distribution beyond that is an extrapolation. In addition, DEEP2 is limited to  $R < 24.1$ , so the distribution is extrapolated to fainter magnitudes as well.

The comparison between the input catalog to WLD, our best-fitting parametric distribution in [Equation 5](#), and the best-fitting DEEP2 distribution<sup>49</sup> is shown for Y1 and Y10 in [Figure F2](#). As shown, the results for  $z \lesssim 1.4$  (where less extrapolation is required) agree quite well between CatSim and DEEP2.

#### F4 Source sample redshift distribution

The jupyter notebook mentioned in [Appendix F2](#) saves the  $n(z)$  and  $n_{\text{eff}}(z)$  distributions for each row of [Table F1](#) to a subdirectory `notebooks/neff/` using plain text format and a file name based on the first three columns. [Figure F3](#) has several panels comparing the resulting  $n_{\text{eff}}$  distributions to show the impact of different choices (Y1 vs. Y10, blending, single band vs. both).

The resulting  $n_{\text{eff}}(z)$  (histograms and parametric fits) are shown for Y1 and Y10 in [Figure F4](#).

## G Forecasting-related plots

In this section, we collect a subset of representative plots from the forecasts:

- [Figure G1](#) illustrates the main steps involved in the error budgeting process described at the start of [Section 5](#).
- [Figure G2](#) shows the  $(w_0, w_a)$  constraints from all five probes individually, and the joint forecast including Stage III priors as well<sup>50</sup>.
- [Figure G3](#) shows how requirements were set for the calibratable systematic uncertainties for the supernova analysis.

<sup>48</sup><http://deep.ps.uci.edu/>

<sup>49</sup>See ‘number\_density/dndz.py’ in the Requirements repository.

<sup>50</sup>[Figure G2](#) was produced using [ChainConsumer](#) ([Hinton 2016](#)), with advice and support provided by the ChainConsumer team.

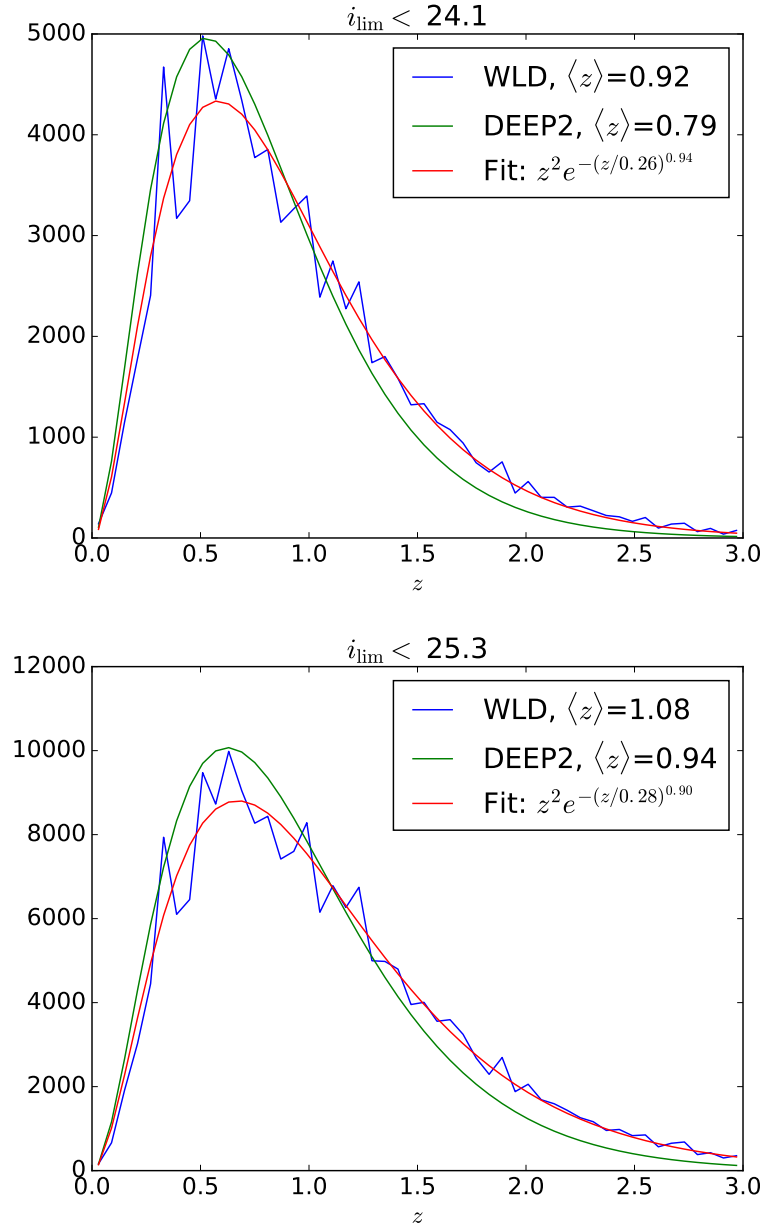


Figure F2: The redshift distribution for the Y1 (top) and Y10 (bottom) photometric sample used for clustering, as predicted based on the CatSim input catalog used by WLD, a parametric fit to that data used in [Appendix D2](#), and DEEP2 (parametric fit based on data to  $z = 1.4$  only).

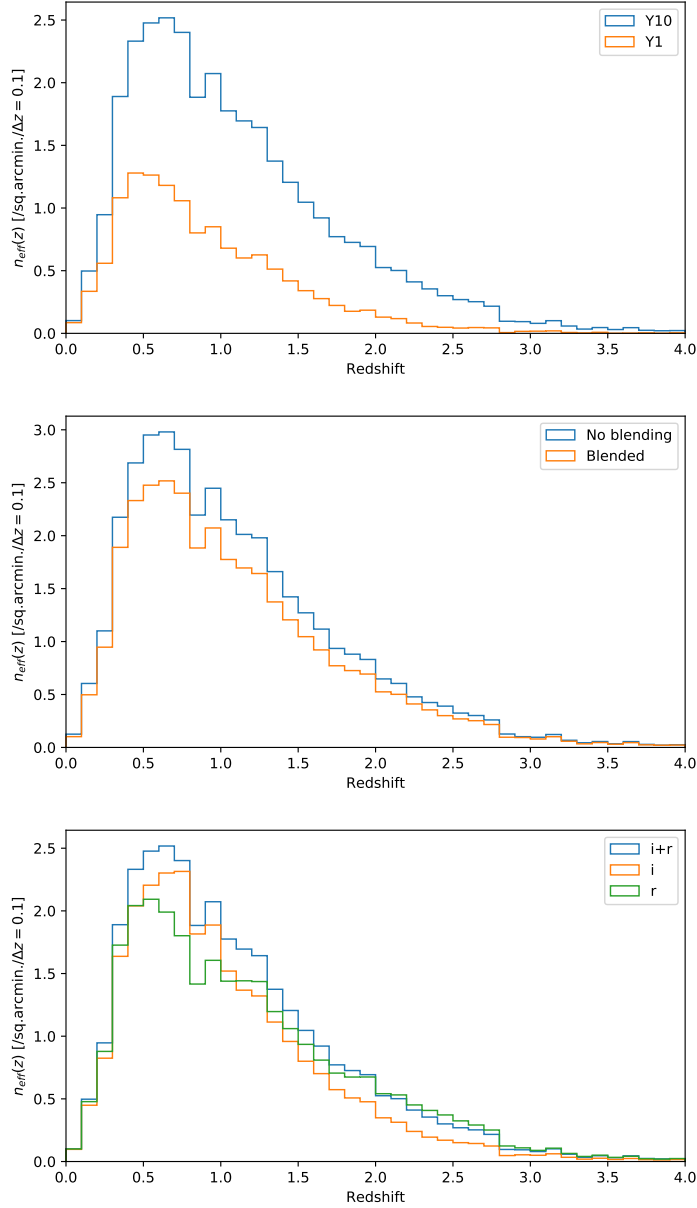


Figure F3: *Top*: The effective  $k = 1$  redshift distribution for the Y10 and Y1 samples of  $i + r$ , including the effects of blending. *Middle*: The effective  $k = 1$  redshift distribution for the Y10  $i + r$  sample, with and without including the effects of blending. *Bottom*: The effective  $k = 1$  redshift distribution for the Y10 samples in  $i + r$ ,  $i$  and  $r$ , including the effects of blending.

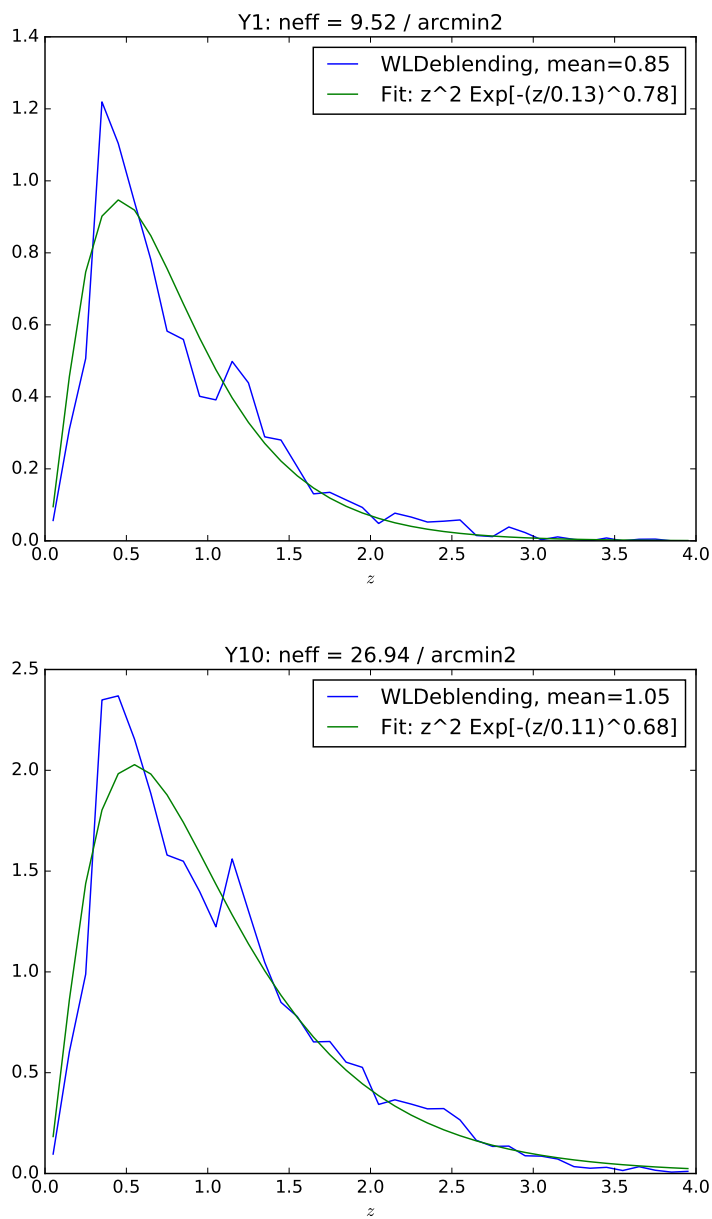


Figure F4: The effective redshift distribution  $n_{\text{eff}}(z)$  for the Y1 (top) and Y10 (bottom) source sample from WLD, and a parametric fit to that data used in [Appendix D2](#).

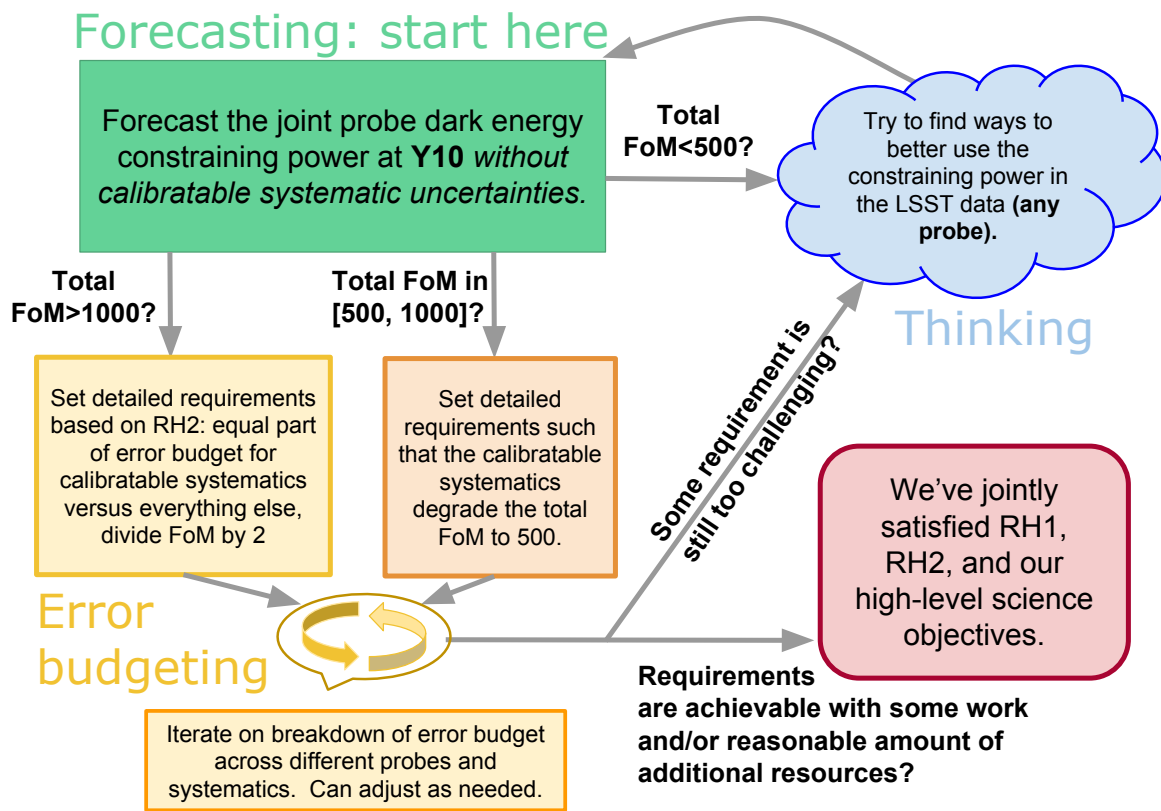


Figure G1: A schematic illustrating the error budgeting process through which the Y10 detailed requirements in Section 5 are derived.

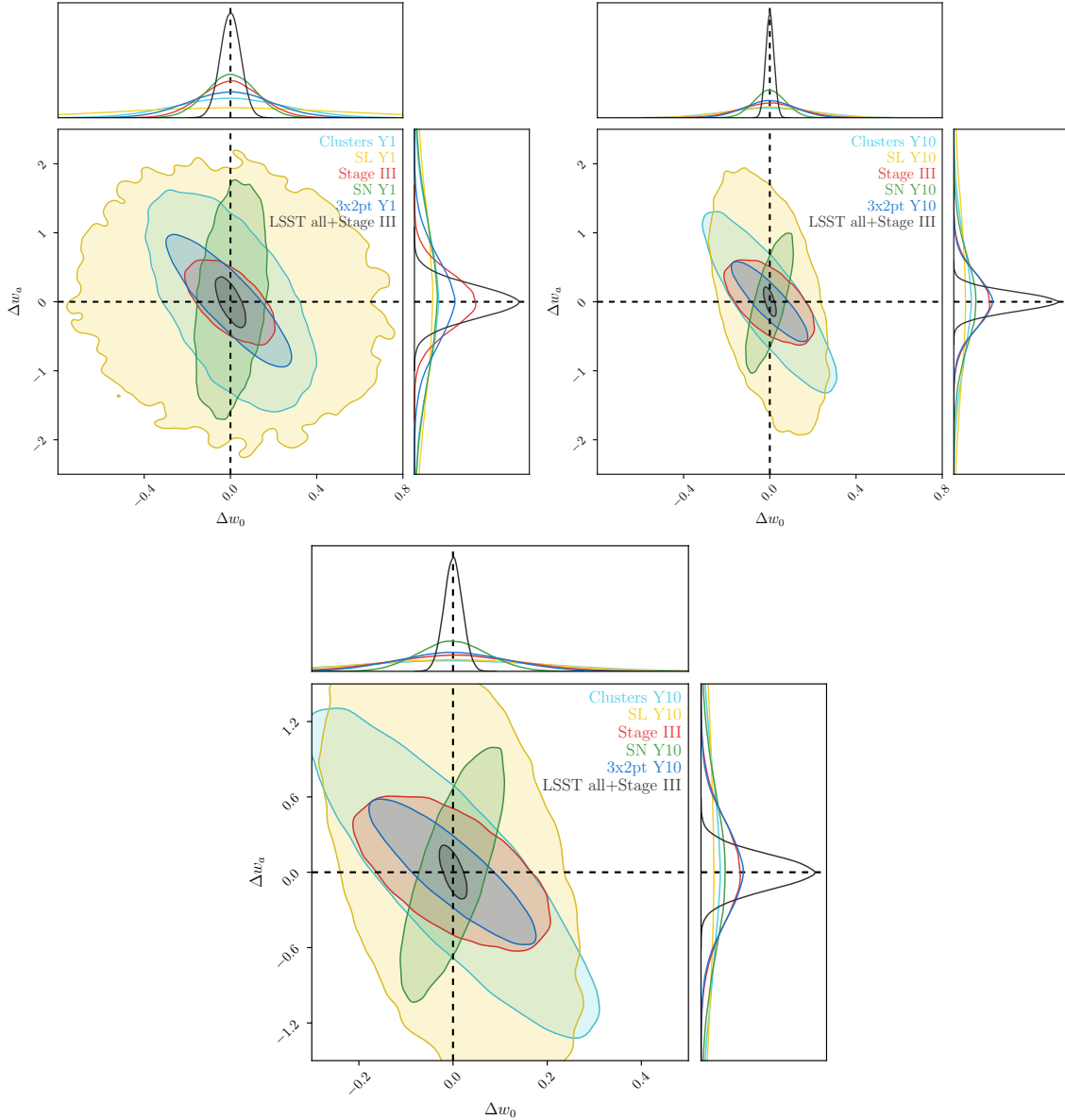


Figure G2: The forecast dark energy constraints at Y1 (top left) and Y10 (top right; bottom) from each probe individually and the joint forecast including Stage III priors. For consistency, the same axes are used on the Y1 and the top Y10 plot, while the bottom Y10 plot is zoomed in further. Note that the supernova contours appear to be tilted clockwise with respect to typical forecasts shown in the literature, because most papers include a Stage III prior when generating the contour for SN. 68% confidence intervals are shown in all cases; the plotted quantities  $\Delta w_0$  and  $\Delta w_a$  are the difference between  $w_0$  and  $w_a$  and their fiducial values of -1 and 0. The contours in this figure for individual probes do not include Stage III priors, so they should only be compared with the individual probe FoM values in [Table 6.1](#) that have no Stage III prior included.

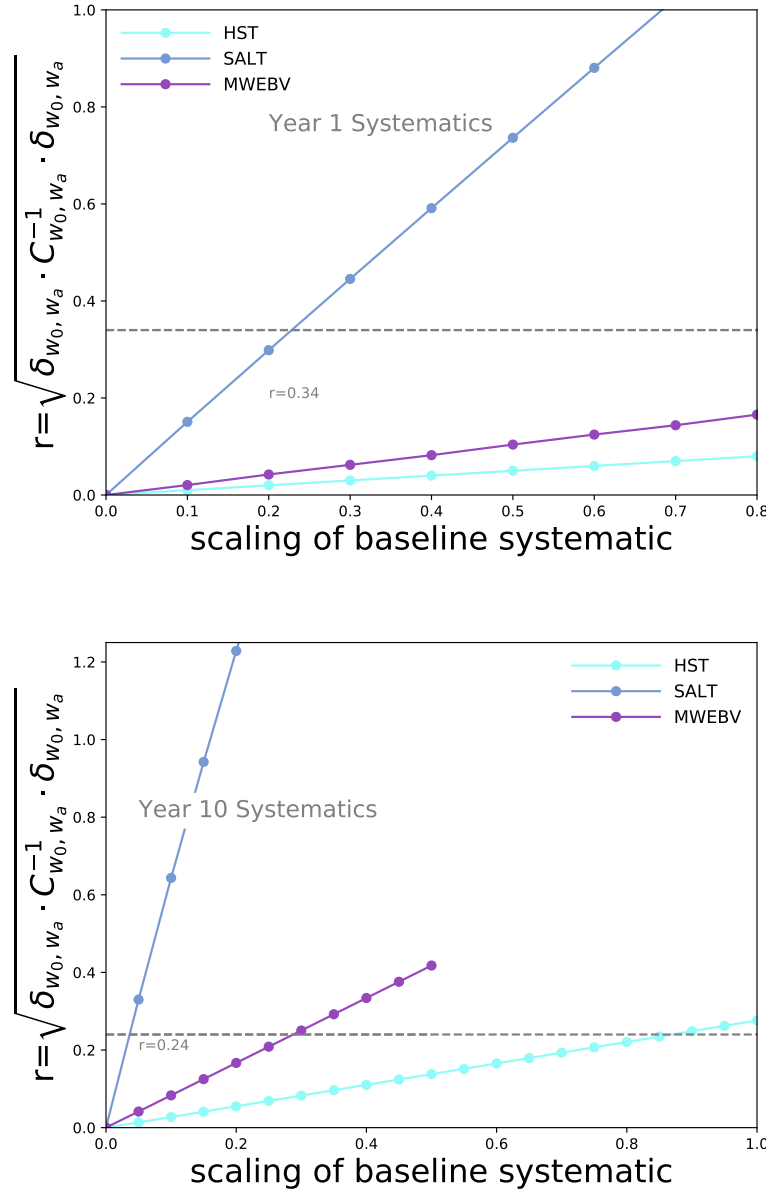


Figure G3: Figures illustrating how requirements are set for supernova, for Y1 (top) and Y10 (bottom), for the systematics that are given the tightest restrictions. The horizontal axis gives the scaling of the systematic uncertainty with respect to the baseline value given in [Table D8](#). The vertical axis shows the bias in cosmological parameters with respect to the statistical plus self-calibrated systematic uncertainties, with the horizontal lines indicating the point at which a given individual source of calibratable systematic uncertainty would take up its allocated fraction of that error budget ( $r = 0.24$  for Y10 and  $r = 0.34$  for Y1, where  $r$  is defined in [Equation 2](#)).